PROCEDURES FOR ESTIMATING GROSS IRRIGATION WATER REQUIREMENT FROM CROP WATER REQUIREMENT

GREGORY WILLIAM ASCOUGH

Submitted in partial fulfilment of the requirements
for the degree of MSc Engineering

School of Bioresources Engineering and Environmental Hydrology
University of Natal
Pietermaritzburg
South Africa
2001

ABSTRACT

The goal of irrigation is to supply sufficient water for crop growth to all areas within a field. Therefore, the uniformity of application of irrigation water is of great importance. The objectives of this study were to quantify the performance of irrigation systems under field conditions using standard evaluation techniques and to investigate the use of spatial statistics to characterise the spatial variability of application. The main objective was to develop techniques to estimate gross irrigation water requirement that incorporates the uniformity of application.

Different practitioners have given different definitions to the criteria used to evaluate the performance of an irrigation system. A literature review was conducted to determine the current definitions used and the factors that affect these performance criteria. The theory and application of spatial statistics was investigated in order to characterise the spatial distribution of irrigation water. The spatial distribution of irrigation water under centre pivots was determined using field measurements. A number of centre pivot, sprinkler, floppy, drip and micro-irrigation systems were evaluated using standard techniques.

The results from the evaluation of spatial data show that this approach is useful to determine a map of the distribution of applied irrigation water. Due to the smoothing characteristic of the spatial statistical method employed, the maps have a uniformity that is greater than in reality. The results from the standard evaluation techniques show that quick and representative results for the performance of an irrigation system can be obtained. The distribution uniformity has an affect on the efficiency of a system and should therefore be included in the calculation of the gross irrigation water requirement. The methods for these calculations are discussed.

Further research needs to be conducted to determine actual distribution uniformities and application efficiencies for irrigation systems under various field conditions. This will provide useful standards to include in the calculation of gross irrigation water requirements.

DISCLAIMER

I wish to certify that the work reported in this dissertation is my own original and unaided work except where specific acknowledgement is made.

Signed: ______________

GW Ascough

ACKNOWLEDGEMENTS

The author wishes to express his sincere appreciation for the assistance given by the following:

Mr CT Crosby, Agricultural Research Council-Institute of Agricultural Engineering (ARC-ILI), for supervision and assistance throughout the project.

Dr GA Kiker, School of Bioresources Engineering and Environmental Hydrology, University of Natal, for supervising this project and for his assistance, guidance and support throughout.

Professor PWL Lyne, School of Bioresources Engineering and Environmental Hydrology, University of Natal, for his advice and encouragement.

The Agricultural Research Council-Institute of Agricultural Engineering, for funding the project. The University of Natal for post graduate scholarship and financial support.

Mr E Schmidt, South African Sugar Association (SASA), for his advice and the use of results from a project conducted on behalf of SASA by the ARC- ILI.

Mr Q Turner, Fort Nottingham, for use of his centre pivot and assistance in gathering the data necessary for the spatial analysis.

Dr SA Lorentz, School of Bioresources Engineering and Environmental Hydrology, University of Natal, for assistance and expertise.

Mr JJ Pretorius and Mr S Thornton-Dibb, School of Bioresources Engineering and Environmental Hydrology, University of Natal, for their assistance with infield instrumentation and data gathering.

The Staff of the School of Bioresources Engineering and Environmental Hydrology, University of Natal, for support and assistance.

TABLE OF CONTENTS

LIST OF TABLES

LIST OF FIGURES

1 INTRODUCTION

Irrigation is the largest user of water in South Africa. This use is estimated at 53.6% of the total water consumption (WRC, 1999). For this reason, the efficient and prudent use of water by irrigators is of paramount importance.

The National Water Act (1998) recognises the need for the equitable use of water as well as the provision of basic water requirements for a "reserve". This reserve includes basic human consumption and the minimum requirements to ensure the protection of the ecology of the water resource. In light of the National Water Act (1998), the water use by irrigators will have to be registered and they will receive a certain allocation of water. Thus to ensure profitability, the irrigators will have to pay particular attention to the performance of their irrigation systems.

Since one of the goals of irrigation is to produce high yielding fields, the uniformity of water application across the entire field is of importance. A field with high uniformity of application will produce higher yields with less variability in the yield within the field (Letey *et al.*, 1984; Solomon, 1984; Letey, 1985; Solomon, 1990). However, under these conditions of higher levels of adequacy, the application efficiency of the system can be much lower. This is caused by deep percolation resulting from excess water being applied to ensure a greater uniformity of infiltrated water in the root zone (Rogers *et al.*, 1997).

The application efficiency of a system is the ratio of the volume of water contributing to the target over the volume of irrigation water applied (Burt *et al.*, 1997). In South Africa, the South African Irrigation Institute (SABI) gives acceptable design norms for the application efficiency for different types of irrigation systems. These design norms range from 95% for drip irrigation to 60% for flood irrigation with earth supply channels (SABI, 2000). These norms are used to obtain gross irrigation water requirements from crop water requirements. Although these are accepted design norms, they are not usually met in practise. Therefore, the estimation of water allocation using the design norms may result in an inadequate amount of irrigation water being allocated. Bos and Nugteren (1990) and Wolters (1992) evaluated irrigation systems from around the world and found that the average application efficiency was less than 70%. An average application efficiency of 53% was observed for furrow irrigation. These averages are well below the design norms used in practice and since the application efficiency is important for the design of irrigation systems, the relationship between uniformity and efficiency needs to be understood to ensure that farmers receive an adequate allocation of water.

The objectives of the study were to:

- Review current principles and procedures for the determination of irrigation performance criteria including distribution uniformity, coefficient of uniformity, sagacity, adequacy and efficiency.
- Quantify irrigation performance measures and spatial variability under existing systems using field observations.
- Quantify irrigation performance using standard irrigation evaluation procedures.
- Investigate the use of spatial statistical methods to evaluate the performance of irrigation systems.
- Propose an initial methodology for assessing the spatial variability for selected irrigation systems.
- Develop procedures for the estimation of the conversion factor to calculate the irrigation water requirement.

To accomplish these objectives, a literature review of current procedures and principles of irrigation performance criteria was conducted. This literature reviewed is presented in Chapter 2. In order to assess the spatial variability, the theory and application of spatial statistics, or geostatistics, was investigated. This is contained in Chapter 3. The methodology used to satisfy the field evaluation objectives of the study is given in Chapter 4. Here the method used for both the spatial evaluation as well as the standard evaluation procedures is detailed. The results obtained for the study are discussed in Chapter 5. The main results of the study and the methodology used to determine gross irrigation water requirement from crop water requirements are discussed in the final Chapter.

2 IRRIGATION PERFORMANCE CRITERIA

In order to estimate the gross amount of irrigation water required, the performance of an irrigation system has to be quantified. This is obtained by using performance criteria to describe the irrigation system. To ensure standardisation of these criteria, the definitions need to be clearly stated and the factors that affect these terms need to be understood. In the past there has been confusion over the definitions of irrigation performance criteria. The terms, such as irrigation efficiency, application efficiency and distribution uniformity, have been given different definitions by various evaluators and thus a comparison between different irrigation systems has not always been possible (Wolters, 1992; Burt *et al.*, 1997; Rogers *et al.*, 1997). Therefore, a standard definition of performance criteria was required to enable comparison of irrigation systems. In an attempt to accomplish this, a Task Committee of the American Society of Civil Engineers (ASCE) set about redefining irrigation performance criteria so that they could be used as industry standards and address any confusion in the definitions previously used. This collaborative effort is contained in Burt *et al.* (1997) and has become the new industry standard on the correct definitions of irrigation performance criteria. The definitions contained in this paper will be used throughout this document.

An irrigation efficiency, defined as the ratio of water beneficially used to water applied less change in storage, of 80% does not imply that 20% of the water used is available for conservation. Therefore, the fate of water from an irrigation event needs to be ascertained in order to determine the amount of water that could be conserved (Burt *et al.*, 1997). Since not all losses from irrigation events are recoverable or unavoidable, the use of irrigation sagacity as a performance measure gives a better representation of the amount of water available for conservation. Irrigation sagacity includes reasonable uses and is defined as the ratio of water beneficially or reasonably used to water applied less change in storage (Solomon and Burt, 1999). Once the performance and variability of an irrigation system have been quantified, they need to be included into the calculation of the gross irrigation water requirement.

In this Chapter the definitions of performance criteria will be investigated. Of these criteria, particular attention will be paid to the distribution uniformity of an irrigation system. This is a measure of the variability of applied irrigation water. Current techniques used to evaluate the distribution uniformity will be discussed.

The partitioning of irrigation water into various categories is required to calculate the performance criteria for an irrigation system. The partitioning of applied water will be discussed in the next section.

2.1 Partitioning of Irrigation Water

The water balance of the irrigation event needs to be clearly understood and the fates of fractions of the water balance need to be determined in order to evaluate an irrigation system. The amount of water distributed to the crop, the amount of recoverable water, the degree of deep percolation, and the amount of surface runoff need to be quantified or estimated for the calculation of irrigation performance criteria. Fractions of the irrigation water balance can be lumped together into categories, such as beneficial, recoverable, reasonable, required, and useful to estimate performance (Burt *et al.*, 1997). The partitioning of irrigation water, which allows one to calculate irrigation performance criteria, will be discussed in the following sections.

2.1.1 Water balance in an irrigation region

The various components of the water balance in an irrigation region, with defined boundaries and for a specific time interval, are described in Figure 2.1. The specification of boundaries plays an important role in the determination of irrigation performance criteria. The region under consideration for the irrigation water balance is in fact a volume and not just surface area. For example, the plant canopy can form the top boundary and the bottom of the root zone can form the lower boundary. In previous definitions of irrigation performance the time scale for establishing the destination or function of some portion of the applied water was often ambiguous. Therefore, to evaluate the performance of an irrigation event, the various fractions entering and leaving the boundaries in a specified time must be estimated. Water not leaving the boundary in the specified time is excluded from the evaluation (Burt *et al.*, 1997).

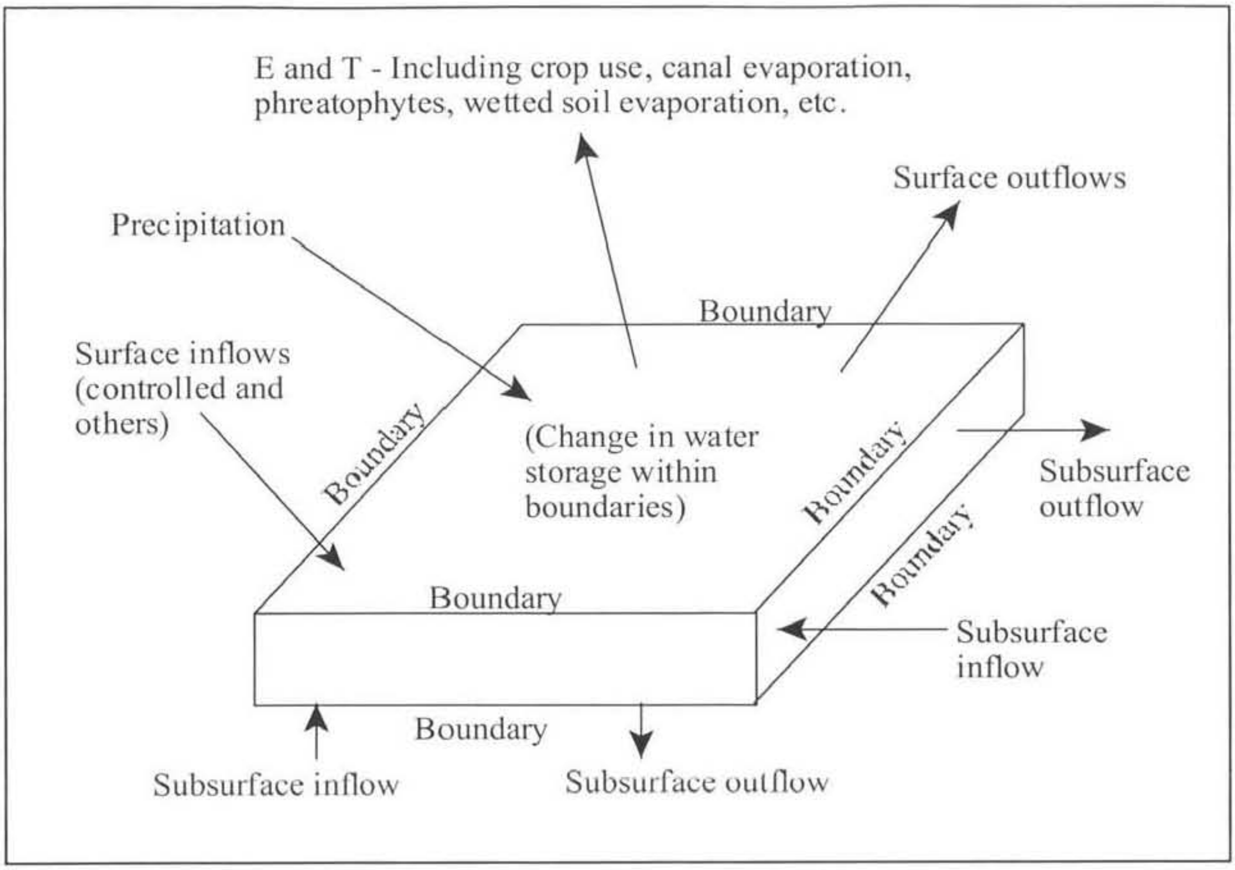

Figure 2.1 Components of a simplified water balance within defined boundaries for specified time interval (after Burt *et al.*, 1997).

The definitions of the components of the water balance, as indicated by Figure 2.1, for use in irrigation system evaluations are evaporation, transpiration, evapotranspiration, crop evapotranspiration, infiltration, deep percolation and runoff.

- Evaporation is the conversion of water from liquid form to vapour form. In the context of this discussion, only evaporation from free surfaces of water in transit, from plant surfaces that have intercepted irrigation water and from the soil surface interface will be considered. Examples of water in transit are sprinkler droplets, surface ponding, puddles and surface runoff. The rate of evaporation is dependant on climatic conditions, water surface area and soil properties. Changing the frequency of application, the irrigation method used, or the amount of mulching and shading can modify the amount of evaporation that takes place. The amount of evaporation can also be influenced by advection; for example, a flowing canal can have higher evaporation per unit area than a large open body of water (Burt *et al.*, 1997).

- Transpiration is water that has passed through the plant's stomata to the atmosphere as vapour. Transpiration and evaporation at the plant surface are closely related, as an increase in evaporation leads to a decrease in transpiration. Factors such as the microclimate formed around the plant and plant physiology, can also influence the rate of transpiration (Burt *et al.*, 1997).
- Evapotranspiration (ET) is the combined process of evaporation from the soil and wet plant surfaces as well as the transpiration from the plant. Soil, crop, irrigation and atmospheric factors influence the ET process. Since evaporation and transpiration are difficult to measure individually, the ET is estimated by soil water balance or aboveground energy balance methods (Burt *et al.*, 1997).
- Crop evapotranspiration (ETc) is the quantitative amount of evaporation and transpiration that occurs within the cropped area of a field, and which is associated with the growing of the crop. The ETc will vary with different irrigation methods and management. Management decisions such as maintaining wet or dry soils, or stressed versus unstressed crops will influence ETc. For most climates the ETc is partly supplied through rainfall and the rest through irrigation water (Burt *et al.*, 1997).
- Infiltration is the process of the movement of water through the soil surface into the soil matrix. All infiltrated water is in transit. Some enters the plant root zone immediately, another fraction is temporarily stored in the root zone that equals or exceeds the field capacity of the soil (Burt *et al.*, 1997).
- Deep percolation (DP) is the fraction of applied water that moves through the soil below the root zone (Burt *et al.*, 1997) and is then unavailable to the crop.
- Runoff (RO) is surface water that leaves the region's boundary in liquid form. Runoff from part of a region that re-infiltrates elsewhere in the region is not considered as runoff. Surface water that is collected from a region's boundary and reapplied within the region does also not contribute to runoff (Burt *et al.*, 1997).

The partitioning of water can also be classified by the availability for recovery.

2.1.2 Partitioning of applied irrigation water by availability for recovery

The amount of applied irrigation water that is available for recovery depends on whether the water was consumed or not. Consumptive and non-consumptive uses of irrigation water can be defined as follows:

- Consumptive uses: Irrigation water that ends up in the atmosphere, through evaporation and transpiration, or in the harvested plant tissue, is considered irrecoverable (Burt *et al.*, 1997).
- Non-consumptive uses: These include any other amounts of water that leave the selected region that can be reapplied elsewhere. Runoff, deep percolation and canal spills are considered non-consumptive uses. However, the movement of this water within the boundaries may degrade the quality of the water (Burt *et al.*, 1997).

The partitioning of applied irrigation water can also be conducted on a judgmental basis.

2.1.3 Judgmental partitioning of applied irrigation water

The judgmental partitioning of irrigation water divides the water into categories that include beneficial uses, non-beneficial uses, reasonable uses and unreasonable uses. This method of classification is very subjective and it will therefore vary between evaluators. The definitions of these categories are:

- Beneficial uses.

A beneficial use of water is one that supports the production of a crop. Water consumed in order to fulfil an agronomic purpose is therefore classed as beneficial. Examples of beneficial uses of water for irrigation events on a field scale are:

  - crop evapotranspiration,
  - improving or maintaining soil productivity, such as "salts" leaching,
  - water for climate control, such as frost protection or plant cooling, or seedbed preparation and seed germination, and
  - evapotranspiration from plants beneficial to crop production, such as windbreaks.

Although the benefits of some of the above can be small, they can make up a considerable portion of the beneficial irrigation water use (Burt *et al.*, 1997). Previously, the only recognised beneficial use of water by a crop was the crop transpiration. Merriam (1999) believes that this should be kept as the only beneficial use of irrigation water and that the other uses should be reclassified. However, Burt *et al.* (1999) hold that the other uses should be included as they do have a beneficial affect on crop production.

- Non-beneficial uses.

Any water use that is not beneficial is by definition non-beneficial. Water uses that fall into this category include (Burt *et al.*, 1997):

  - unnecessary evaporation from a wet soil,
  - excess deep percolation due to non-uniformity of irrigation water application and from excess salt leaching,
  - tail water from irrigations that is not recovered and redistributed,
  - evaporation due to excessively high irrigation frequency, and
  - weed or phreatophyte ET.

- Reasonable uses.

All beneficial uses are reasonable uses in the context of irrigation performance. Non-beneficial uses are reasonable if they are justified under certain circumstances at a particular time and place. Some degree of non-beneficial uses is reasonable if they are due to physical, economic or managerial constraints, or environmental requirements. An example of a non-beneficial, but reasonable water use would be runoff from an irrigated land into a wetland. This use is beneficial for the environment, but not for agricultural production. Reasonable, but non-beneficial deep percolation can result due to the uncertainty of the farmer on how much to irrigate. These uncertainties can be due to estimation of actual soil moisture depletion, crop coefficients, reference evapotranspiration, measurement of the inflow rates, estimates of advance times and infiltration depths for surface irrigation, and necessary leaching requirements for salt control (Burt *et al.*, 1997).

- Unreasonable uses.

For the purpose of measuring irrigation performance, unreasonable uses are non-beneficial uses that are not reasonable. That is, they are without economic, practical, or other justification. For example, excess deep percolation or excess tail water can be considered unreasonable uses as they could be curtailed (Burt *et al.*, 1997).

Once the partitioning of irrigation water has been determined, the next step is to calculate irrigation performance criteria. The definitions of these criteria will be discussed in the next section.

2.2 Definitions of Irrigation Performance Criteria

Performance criteria for evaluating an irrigation system are influenced by the design and management of the irrigation system. Physical properties of a field as well as managerial elements such as scheduling, allowable moisture deficits, and soil moisture deficits at the time of an irrigation event, will have a direct bearing on the calculated performance term for the irrigation system under consideration (Pereira, 1999). For this reason, both design and managerial practices should be taken into consideration when evaluating an irrigation system. This section will address the definition of several irrigation performance indicators including irrigation efficiency, irrigation consumptive use coefficient, irrigation sagacity, distribution uniformity, application efficiency, potential application efficiency, low-quarter adequacy and the coefficient of uniformity.

2.2.1 Irrigation efficiency

Irrigation efficiency (IE) can be defined by the following relationship:

$$\text{IE} = \frac{\text{volume of irrigation water beneficially used}}{\text{volume of irrigation water applied} - \Delta \text{ storage of irrigation water}} \times 100\% \qquad (2.1)$$

The denominator in Equation 2.1 represents the total volume of water that leaves the boundaries. These volumes leave within a specified time, i.e. the interval from just before an irrigation event until just before the next irrigation event. The volume of irrigation water applied includes water that results in crop ET, runoff, deep percolation, evaporation, and so forth. If, at the end of a period, the water contained within the boundaries is the same as at the beginning of the period, then the Δ storage of water = 0 and all the applied water has left the region. Therefore, water that is temporarily stored in the root zone for a subsequent time period is not included in the calculation (Burt *et al.*, 1997).

The term "irrigation water" does not include water obtained from natural sources, such as precipitation or a rise in the natural water table. In Equation 2.1 the depth of water can replace the volume of water without loss in generality (Burt *et al.*, 1997).

The beneficial use term in irrigation efficiency is often improperly defined. Common mistakes are the use of theoretical beneficial uses instead of actual beneficial uses, and the double counting of beneficial uses. An example of double counting is water that is applied for frost protection, which is later available to the crop for evapotranspiration (Burt *et al.*, 1997). Thus care should be exercised when calculating irrigation efficiency. It was noted by Solomon and Burt (1999) that IE is often misinterpreted from the point of view that (100 - IE)% of applied irrigation water can be conserved or reallocated.

2.2.2 Irrigation consumptive use coefficient

Jensen (1993, cited by Burt *et al.*, 1997) introduced the concept of the irrigation consumptive use coefficient (ICUC). It is defined as the ratio of the volume of irrigation water consumptively used to the total volume of water that has left the irrigation boundaries, both in a specified period of time. ICUC expressed as a formula as follows:

$$\text{ICUC} = \frac{\text{volume of irrigation water consumptively used}}{\text{volume of irrigation water applied} - \Delta\ \text{storage of irrigation water}} \times 100\% \quad (2.2)$$

ICUC can be applied at a field, project, district or farm scale. ICUC has sometimes been incorrectly used to estimate IE. Water used for salt removal or drainage water may have quality problems that make them unusable. However, this does not mean that they have been consumed, as they can be reused after treatment (Burt *et al.*, 1997).

2.2.3 Irrigation sagacity

Irrigation efficiency is a useful term for comparison, but from a societal and grower's point of view it can be incomplete. Benefits may accrue to society or to the environment and hence reasonable uses need to be included (Burt *et al.*, 1997). Solomon and Burt (1999) gave the following examples of reasonable losses:

- Losses that cannot be avoided because it would not be economical to prevent them.
- Losses that are the result of technical requirements, such as the evaporation for a reservoir, backwashing of filters for micro irrigation, or spray and evaporation losses from sprinkler systems.
- Losses due to uncertainties, such as soil water capacity, or crop ET since the previous application.
- Losses that contribute to environmental goals and/or requirements.

For this purpose, irrigation sagacity (IS) is defined as (Burt *et al.*, 1997):

$$IS = \frac{\text{volume of irrigation water beneficially and / or reasonably used}}{\text{volume of irrigation water applied} - \Delta \text{ storage of irrigation water}} \times 100\% \quad (2.3)$$

Burt *et al.* (1997) do not suggest that IS be used in place of IE, but that the two should be given with clear definitions so that the appropriateness of the ratio can be judged.

2.2.4 Distribution uniformity

In irrigation, the uniformity with which water is applied is as important as how efficiently the applied water was used. The non-uniform application of irrigation water can lead to areas of over-irrigation in a field which can cause water-logging, plant injury, salinisation, and contamination of groundwater (Solomon, 1983, cited by Burt *et al.*, 1997). Distribution uniformity (DU) is defined as a measure of the uniformity with which irrigation water is distributed within a field (Burt *et al.*, 1997).

Expressing DU solely in terms of post-irrigation infiltrated depths of water ignores water that is intercepted by the canopy and the reduction in crop transpiration due to evaporation from the canopy. These are fractions of the applied water that do not contribute to infiltrated depth. Including the canopy interception and the reduction in transpiration for light sprinkler irrigation applications can greatly improve the true DU as opposed to the calculated DU. Thus in the definition of DU the term accumulated water is used which includes the infiltration, canopy interception and reduction in transpiration during an irrigation event (Burt *et al.*, 1997).

In order for DU to be applied universally to all crops, the concepts of the totality of field elements and elements of scale need to be incorporated. An element is defined as the smallest area in the field that requires water within which the variation in distributed water is not important. The concept of element scale is crucial for universal use of DU. For example, in an orchard a DU = 1.0 does not imply that the whole field receives the same amount of water, but that the elemental areas receive the same amount. Whereas, in a wheat field with a plant at every point would imply that the whole field receives the same application for a DU = 1.0 (Burt *et al.*, 1997).

DU is usually defined as a ratio of the smallest accumulated depths in the distribution to the average depths of the whole distribution. The largest depths could also be used to express DU, but since the low values in irrigation are more critical, the smallest values are used (Burt *et al.*, 1997).

The average of the smallest depths in the field over the portion of the field, in which they occur, is given the notation d_{lowest}. This term is used in the numerator of the DU calculation. The values of DU will thus depend on the choice of the fraction of the total area for which the smallest values will be taken. This area does not have to be contiguous. A commonly used fraction is the lower quarter, which has been used by the United States Department of Agriculture (USDA) since the 1940's. This definition has proven useful in irrigated agriculture (ASCE, 1978) and leads to the definition of the average low-quarter depth, d_{lq}. Thus, the average accumulated depth in the quarter of the field receiving the smallest depths is given by:

$$d_{lq} = \frac{\text{volume accumulated in 25\% of total area of elements with smallest depths}}{\text{25\% of the total area of elements}} \quad (2.4)$$

From this the low-quarter distribution uniformity, DU_{lq}, can be defined as:

$$DU_{lq} = \frac{d_{lq}}{d_{avg}} \quad (2.5)$$

$$DU_{lq} = \frac{\text{average low - quarter depth}}{\text{average depth of water accumulated in all elements}} \quad (2.6)$$

where d_{avg} = total volume accumulated in all elements [mm], divided by the total area of all the elements. These definitions allow the elements to be of different sizes by using area weighting (Burt *et al.*, 1997).

Distribution uniformity is not an efficiency term and to emphasize this it should be quoted as a ratio and not a percentage. An irrigation event can have a high DU, but if excessive water has been applied then the application efficiency (AE), which will be defined next, will be low. However, a high AE with minimal under-irrigation is only possible if the DU is also high (Burt *et al.*, 1997). The above concept of distribution uniformity assumes that a uniform target is desired within the irrigated field.

2.2.5 Application efficiency

The efficiency terms IE, IS and ICUC are difficult to evaluate rapidly and require a detailed quantification of the water balance components. Application efficiency (AE) is based on the concept of meeting a target application depth for an irrigation event. This allows judgmental decisions, such as beneficial or reasonable uses, to be separated from how well the irrigation system is able to meet a target depth of application. The AE term applies only to a single irrigation event. The target depth chosen can be the soil moisture deficit (SMD), or a smaller amount to supplement potential rainfall, or it could contain a desired depth of reclamation water, or it may be a requirement for leaching of salts (Burt *et al.*, 1997). The definition of AE for a single event is thus:

$$AE = \frac{\text{average depth of irrigation water contributing to target}}{\text{average depth of irrigation water applied}} \text{ x } 100\% \quad (2.7)$$

Implicit in the definition of AE is the assumption that the target depth is uniform across the field and that no time period needs to be specified, as it accounts for a single event only. Since there are some unavoidable evaporation losses in an irrigation event, AE will generally be lower than IE. If the target is equal to the sum of beneficial uses, AE can be used as an estimate of IE (Burt *et al.*, 1997).

2.2.6 Potential application efficiency

Potential application efficiency (PAE) is based on the concept that the irrigation event could be terminated when the target depth would just be met by the average of the lowest values in the irrigation infiltration distribution. In this way deep percolation losses would be kept to a minimum, due only to the non-uniformity of application, and the AE would be at a maximum with minimal under-irrigation (Burt *et al.*, 1997).

As with DU, PAE cannot be quantified until the lowest values in the distribution have been characterised over a specified fraction of the field area. Here again the norm is to use the lower quarter and hence the definition for PAE_{lq} follows (Burt *et al.*, 1997):

$$PAE_{lq} = \frac{\text{average depth of irrigation water contributing to target}}{\text{average depth of irrigation water applied such that } d_{lq} = \text{target}} \times 100\% \quad (2.8)$$

Thus, PAE_{lq} can be used to estimate the gross amount of water to apply. The denominators of DUlq and PAE_{lq} differ by the amount of surface losses, such as runoff and evaporation, and therefore PAE_{lq} can be accurately estimated from (Burt *et al.*, 1997):

$$PAE_{lq} \approx DU_{lq} \times (100 - \%\ \text{surface losses}) \quad (2.9)$$

where surface losses include evaporation during an irrigation event, spray drift and surface runoff.

From the above, the gross irrigation water required for an irrigation event can be estimated as (Burt *et al.*, 1997):

$$\text{Gross average depth to apply} = \text{Target depth} \times \frac{100}{PAE_{lq}} \quad (2.10)$$

2.2.7 Low-quarter adequacy

The degree to which the target, or required depth, is met is termed adequacy. In keeping with the definition of AE based on the requirement for all beneficial uses, the low-quarter adequacy (AD_{lq}) is given by (Burt *et al.*, 1997):

$$AD_{lq} = \frac{d_{lq}}{d_{req}} \tag{2.11}$$

where d_{req} = the required depth for all beneficial uses [mm].

With this definition, an $AD_{lq} < 1$ indicates under-irrigation and $AD_{lq} > 1$ indicates over-irrigation. When $AD_{lq} = 1$, then AE = PAE_{lq} and the surface losses match potential values. This definition of adequacy differs from other definitions that are based on the percentage of area adequately irrigated (Burt *et al.*, 1997).

2.2.8 Coefficient of uniformity

One of the first criteria defined to express uniformity was the coefficient of uniformity (CU) as defined by Christiansen (1942). Christiansen's CU is the most widely used and accepted criteria used to define uniformity (Zoldoske *et al.*, 1994). This coefficient is derived from catch can data assuming that the catch cans represent the same area. It is a measure of the absolute difference from the mean divided by the mean. The CU can be expressed by (ASAE, 1993a):

$$CU = 100\left(1 - \left(\sum_{s=1}^{n}\left|D_s - \overline{D}\right| \Big/ \sum_{s=1}^{n} D_s\right)\right) \tag{2.12}$$

where D_s is the catch can depth of application at catch can s [mm], $\overline{D}$ is the mean catch can depth [mm] and n is the number of catch cans.

Christiansen's CU was modified by Heermann and Hein (1968) for use under centre pivot irrigation systems. Equation 2.12 is modified to include a term representing the distance from the centre to the catch can, S_s [m]. The modified Heermann-Hein CU_{HH} equation is given by (ASAE, 1993a):

$$CU_{HH} = 100\left(1 - \left(\sum_{s=1}^{n} S_s \left| D_s - \frac{\sum_{s=1}^{n} D_s S_s}{\sum_{s=1}^{n} S_s} \right| \Bigg/ \sum_{s=1}^{n} D_s S_s \right)\right) \tag{2.13}$$

There are three features of CU, and CU_{HH}, that should be considered when interpreting the uniformity values obtained (Zoldoske *et al.*, 1994). Firstly, the absolute difference between the measured and mean depth of application results in over- and under-irrigation being treated equally. Thus the deviations are represented by magnitude only and not by whether they represent a deficit or excess of irrigation water, one of which may be more critical than the other for the crop. Secondly, the penalty assigned to each deviation is linearly proportional to the magnitude of the deviation. Thirdly, CU is an average measure and as such compares the average absolute deviation to the mean application. Thus CU indicates on average how uniform the application depths are and does not give an indication of how bad a particular area may be, or how large the area may be (Zoldoske *et al.*, 1994).

Of these performance criteria the DU of irrigation systems is of particular importance. The importance and determination of DU will be discussed in the next chapter.

2.3 Distribution Uniformity

In irrigation systems, the desired state is a uniform application of irrigation water. This ensures that the field as a whole receives an adequate amount of water for crop production. The non-uniformity of irrigation water application leads to over- or under-irrigated areas in the field. This can lead to high soil moisture tensions due to insufficient water being applied that may cause plant stress and reduced yields. Poor uniformity may also cause plant stress and increased disease in the case of excess water being applied (Solomon, 1990). For this reason the DU of an irrigation system plays an important role in the profitability of an irrigation system. In a study conducted by Pitts *et al.* (1996) on irrigation systems in the United States of America, they found that the mean DU for sprinkler, micro, furrow and turf irrigation were 0.65, 0.70, 0.70 and 0.49 respectively. These are below the desired DU of

0.80, or better, needed for high yielding fields (Zoldoske *et al.*, 1994). For the evaluation of irrigation systems, the factors that cause non-uniformity need to be determined.

2.3.1 Factors influencing distribution uniformity

The DU of a system is a function of both design and managerial variables that characterise an irrigation event (Pereira, 1999), with the former being more easily characterised. Factors that influence the uniformity of water application during an irrigation event for hand-move, furrow, micro, moving sprinkler, under-tree sprinkler and high-volume gun sprinkler irrigation are summarised in Tables 2.1 to 2.4. The components that affect uniformity will differ between various irrigation types and the factors causing non-uniformity will depend on the characteristics of the irrigation system. The components that affect the uniformity of an irrigation event need to be known for the application of statistical methods to determine a global uniformity of an irrigation system. These methods will be discussed later in this Chapter.

The design and management of an irrigation system are not the only factors that influence uniformity. Perrens (1984) and Li (1998) found that the uniformity of soil moisture from a non-uniform application of irrigation water at the soil surface improves over time. This is due to lateral flow within the soil matrix and a redistribution of soil moisture.

Table 2.1 Examples of components that affect uniformity for hand-move and under-tree sprinkler irrigation systems (after Burt *et al.*, 1997).

Uniformity component	Factors causing non-uniformity
Hand-move sprinkler irrigation systems	
Flow rate differences between sprinklers.	Pressure differences. Different nozzle sizes. Nozzle wear. Nozzle plugging.
Sprinkler pattern (catch can) non-uniformity.	Spacing. Sprinkler design (angle of trajectory, impact-arm interception characteristics). Nozzle size and pressure. Wind. Vertical orientation of sprinkler head. Plant interference around a sprinkler.
Unequal application during start-up and shutdown.	Pipe diameter and length. Duration of set.
Edge effects.	Inadequate overlap on edges.
Under-tree irrigation systems	
Same as hand-move sprinkler systems, except that the sprinkler overlap non-uniformity around each sprinkler is usually not considered if there is one sprinkler for every two trees.	Tree interference can cause large, non-irrigated areas or segments in some cases.

Table 2.2 Examples of components that affect uniformity for furrow irrigation systems (Burt *et al.*, 1997).

Uniformity component	Factors causing non-uniformity
Furrow irrigation systems	
Opportunity-time differences down a furrow.	Extent of ponding. Flow rate and duration. Slope and roughness. Furrow cross-sectional shape. Furrow length.
Opportunity-time differences between furrows.	Different day/night irrigation set times. Wheel row compaction/no wheel compaction. Different furrow flow rates.
Different infiltration characteristics for individual furrows.	Different degree of compaction due to tractor tyres and tillage.
Different infiltration characteristics across the field.	Different soil types. Soil chemical differences. Texture differences of soil.

Table 2.2 Examples of components that affect uniformity for furrow irrigation systems (Burt *et al.*, 1997).

Uniformity component	Factors causing non-uniformity
Furrow irrigation systems	
Other opportunity time differences throughout a field.	Non-uniform land preparation.
Differences in day and night intake rates.	Viscosity changes due to temperature changes.
Infiltration rate differences due to differences in wetted perimeter.	Slope changes or restriction to flow along the furrow.

Table 2.3 Examples of components that affect uniformity for drip/micro irrigation and big gun sprinkler irrigation systems (Burt *et al.*, 1997).

Uniformity component	Factors causing non-uniformity
Drip/ micro irrigation systems	
Differences in discharge between emitters.	Pressure differences. Plugging of emitters. Manufacturing variation. Soil differences for buried emitters. Temperature differences along a lateral.
Volumes applied not proportional to plant area assuming the same plant age.	Variations in plant spacing are not matched by emitter spacing or irrigation scheduling. Unequal discharge during start-up and drainage.
High-volume big gun sprinkler systems	
Flow rate differences between sprinkler locations.	Pressure differences. Length of supply pipeline. Hose on reel rather than on ground. Elevation differences.
Sprinkler overlap non-uniformity.	Plant interference around ground mounted sprinklers. Wind. Lane and/or sprinkler spacing, nozzle and pressure. Gun travel speed.
Edge effects.	Lane spacing. Wind driven changes. Wind velocity changes.
System flow variations.	Engine performance. Pump response to elevation changes. Pressure variations at the source.
Speed variation with continuously moving systems.	Wheel slippage. Fluctuation of water turbine power output. Cable or hose depth on reel.

Table 2.4 Examples of components that affect uniformity for centre pivot irrigation systems (after Burt *et al.*, 1997).

Uniformity component	Factors causing non-uniformity
Centre pivot and lateral move irrigation systems	
Sprinkler (spray head) flow rates not proportional to area served.	Poorly controlled sprinkler pressures. Elevation changes. Pressure regulator differences. Nozzle plugging and wear.
Sprinkler overlap non-uniformity between adjacent sprinklers.	Wind. System travel speed variations. Elevation of sprinkler (spray head). Crop interference. Worn spray plates. Spacing.
Edge effects.	Wind direction changes. Soil texture. Distance from pivot point. Surface conditions (surface ponding, residues). Nozzle angle changes due to topography.
Radial arc effects.	Activation of end guns and corner swing lateral sections or towers without proper control of flow rates along the pivot length.
System flow variation.	Engine performance. Pump response to different pressure requirements. Pressure variations from the source.

Since the non-uniformity of irrigation water results in areas of over and under irrigation, the relationship between DU and AE needs to be understood.

2.3.2 Relationship between distribution uniformity and application efficiency

The relationship between distribution uniformity and application efficiency is best summarised using an example. Figure 2.2 illustrates an example of DU and AE for surface irrigation and sprinkler irrigation. For the calculation of DU and AE in Figure 2.2, the authors defined AE and DU as follows:

$$AE = \frac{\text{water available for use by crop}}{\text{water delivered to field}} \times 100\% \qquad (2.14)$$

$$DU = 100\left[1 - \frac{y}{d}\right] \qquad (2.15)$$

where y is the average absolute numerical deviation in depth of water stored [mm] from average depth of water stored, d [mm], during the irrigation event (Rogers *et al.*, 1997).

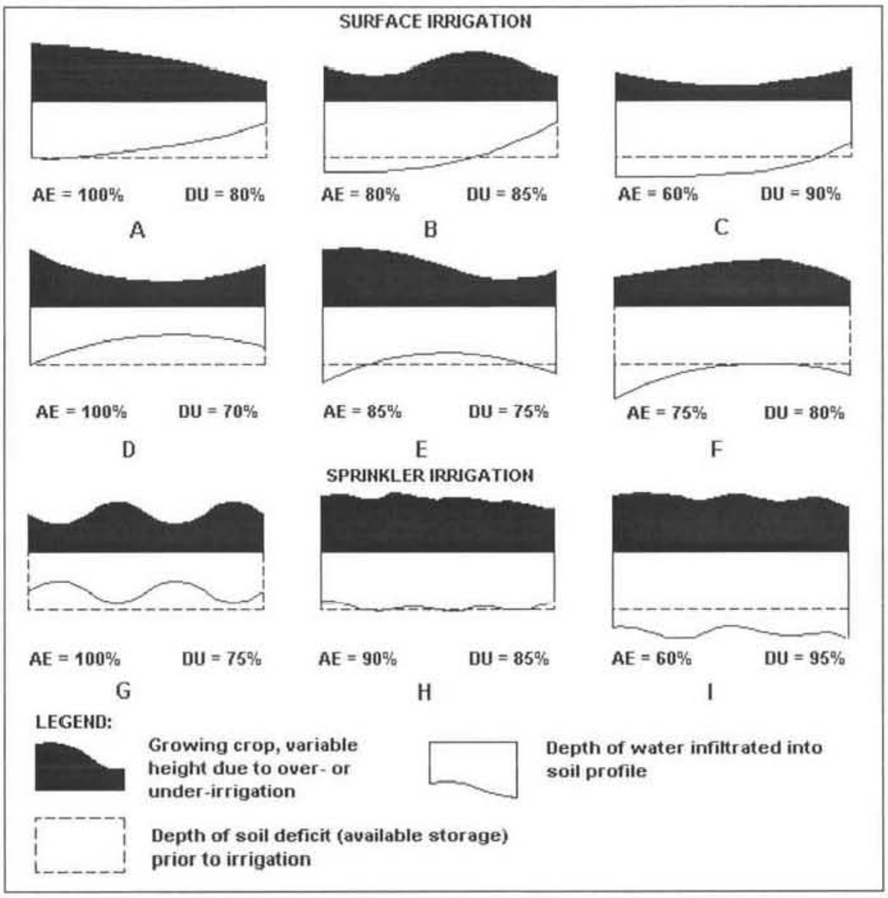

Figure 2.2 Effect of AE and DU on crop production assuming no runoff (after Hansen, 1960, cited by Rogers *et al.*, 1997).

Examples A, B and C in Figure 2.2 show the effect of increasing depth of application on crop production, AE and DU where the heaviest application occurs at the head of the furrow. The dashed rectangle shows the soil moisture deficit prior to the irrigation event. In example A it can be seen that there is no deep percolation so the AE is 100%. However, the amount of water that infiltrates decreases as the flow of water moves down the furrow such that the DU is 80%. The effect on the crop production of the non-uniform application can be seen. Examples B and C show the effect of increasing the water supply to produce a more uniform application of infiltrated water. It can be seen that as the DU increases the AE decreases and that a small change in DU can result in a large change in AE. Examples D, E and F are for a field with blocked-end or dyke surface irrigation. Again the same principles apply (Rogers *et al.*, 1997).

Examples G, H and I are for a sprinkler irrigation system where the distribution pattern results in non-uniform application of water. Here again it can be seen that as the DU increases the AE decreases. Figure 2.2 also illustrates that the gain in uniformity can be at the expense of vast amounts of water. Therefore, a compromise between uniformity and efficiency needs to be reached (Rogers *et al.*, 1997).

2.3.3 Components of global distribution uniformity

The common practice is to focus the uniformity studies on particular components that cause non-uniformity. Examples of components of uniformity and the factors causing non-uniformity are shown in Tables 2.1 to 2.4. For example, soil infiltration depth variation and advance and recession curves have been studied for surface irrigation. Catch-can tests to determine sprinkler spray patterns have been investigated. However, as far as the crop is concerned, it is the field-wide uniformity of the distribution of equal amounts of water to the crops that is important. Although it is impractical to measure field-wide uniformity of distribution, it is feasible to study the uniformity of individual components of the system. However, the components must be investigated in such a manner that an accurate estimate of the global distribution uniformity can be determined (Burt *et al.*, 1997).

At present, the only theoretically defensible method of combining component uniformities is through proper statistical methods. The lack of a statistical basis for the Christiansen Uniformity Coefficient, CU, precludes the combining of sprinkler overlap with some description of pressure uniformity in the lateral (Burt *et al.*, 1997).

Techniques for combining component DU will be discussed in the next section.

2.3.4 Estimation of global irrigation distribution uniformity

The estimation of a global value for distribution uniformity is difficult and often impractical to determine on a field scale (Burt *et al.*, 1997). Thus methods of determining this global value from the components that cause non-uniformity (detailed in Tables 2.1 to 2.4) are briefly discussed in the next section. The full details of the methods are beyond the scope of this review.

- Combination of uniformity components.

Various methods exist for combining uniformity components. These include multiplicative and additive techniques (Clemmens and Solomon, 1997). Traditionally the individual component distribution uniformities have been combined through multiplication (Burt *et al.*, 1992, cited by Clemmens and Solomon, 1997) as follows:

$$DU_{a0} = DU_{a1}\,DU_{a2} \tag{2.16}$$

where a = subscript that denotes the relevant fraction of the population,

1,2 = subscript that denotes the individual DU components 1 and 2 respectively,

DU_{a0} = combined DU.

Equation 2.16 can be expanded to include as many terms as desired on the right-hand side. If all the different components are included, then DU_{a0} is an estimation of the overall or global distribution uniformity. An example of this approach is the emission uniformity (EU) for micro-irrigation given by Karmeli and Keller (1974; cited by Clemmens and Solomon, 1997):

$$EU = \left(1 - 1.27\frac{CV_M}{\sqrt{n}}\right)\left(\frac{Q_{lq}}{Q_{avg}}\right) \text{ x } 100\% \tag{2.17}$$

where CV_M = manufacturers' coefficient of variation for emitters,

n = number of emitters per plant,

Q_{lq} = average low-quarter emitter discharge [l/h] and

Q_{avg} = overall average of emitter discharges [l/h] assuming the same pressure-discharge relationship for all emitters.

In Equation 2.17 the first term on the right-hand side accounts for emitter variation and the second accounts for system pressure variation.

The advantage of this approach is the simplicity of calculation. However, low-quarter averages do not always combine in predictable ways, and the proper method of combination does not always follow the simplicity of the above equations (Clemmens and Solomon, 1997). Clemmens and Solomon (1997) believe that a more statistically based approach produces answers that are more consistent and defensible.

- Statistical expressions of uniformity.

An alternative method to express uniformity of irrigation is to perform a statistical analysis on the depths in the distribution. A standard statistical measure, the coefficient of variation (CV) can be used to evaluate uniformity. The ratio for CV is given by:

$$CV = \frac{\text{standard deviation of accumulated water depths (weighted by area)}}{\text{mean water depth}} \qquad (2.18)$$

The type of statistical distribution, indicated by the shape, determines the relationship between CV and other uniformity criteria, DU_{lq} say. If the distribution pattern is known or can be estimated, then the DU can be determined from:

$$SDU_a = 1 - K_a\, CV \qquad (2.19)$$

where SDU = statistically derived estimate for DU,

a = subscript to denote fraction of area having smallest depths,

K_a = parameter related both to distribution type and area fraction,

= 1.27 for a normal distribution for the low-quarter average (Burt *et al.*, 1997; Clemmens and Solomon, 1997).

The statistical distribution uniformity for several combined components, SDU_{a0}, is given by:

$$SDU_{a0} = 1 - K_{a0}\frac{s_0}{m_0} = 1 - K_{a0}\, CV_0 \qquad (2.20)$$

where 0 = subscript denoting global uniformity,

m, s = mean and standard deviation, respectively (Clemmens and Solomon, 1997).

The approach that is followed is by expressing the right-hand side in terms of its component parts:

$$SDU_{a0} = 1 - K_{a0} f[(K_{a1}, m_1, s_1),(K_{a2},m_2,s_2), \ldots] \quad (2.21)$$

where 1,2 = subscripts that denote components 1 and 2, and so on (Clemmens and Solomon, 1997).

The concept of DU is the same for all irrigation methods. However, the spatial distribution of non-uniformity will be different for each method (Clemmens and Solomon, 1997). Thus, the K_a factor will have to be estimated for each irrigation system. For a normal distribution K_{lq} = 1.27, for a uniform distribution K_{lq} = 1.30 and for a parabolic distribution K_{lq} = 1.68 (Solomon, 1983, cited by Clemmens and Solomon, 1997). Studies conducted by Clemmens and Solomon (1997) showed that component K_{lq} values vary between 1.0 and 1.5. For pressure differences along a lateral line, the distribution is positively skewed and K_{lq} is in the range 1.1 - 1.2, whereas the opportunity time distributions in surface irrigation are negatively skewed with K_{lq} values often above 1.4. Thus, the selection of the proper value for K_{lq} will affect the final estimate of DU_a. If K_a is correctly chosen to match the shape of the distribution pattern, then SDU_a is equal to DU_a.

Merriam (1999) questioned using a statistical approach where there is a dominant aspect such as catch-can patterns or the use of a single furrow. These are then used to estimate the mean value where the mean may not be known, and from which the deviations are taken caused by the other components to find the correct low quarter average in an unspecified global area.

- Errors in distribution uniformity estimation

Errors can result when trying to estimate global distribution uniformities from component DU due to:

  - not including all components that effect global DU,
  - errors associated with the measurement of various components, and
  - errors in the application of the equations used to combine these components (Clemmens and Solomon, 1997).

2.3.5 Alternative methods for distribution uniformity estimation

An alternative method to determine DU for an irrigation system is the sliding window approach (Zoldoske and Solomon, 1988; Zoldoske *et al.*, 1994). The data are collected in a grid pattern to represent the distribution of application depths. The sliding window method consists of moving a window over these data. Typically the window size is 2, 5 or 10% of the area and can be square or rectangular in shape. The data that fall inside this window are averaged and the result stored. The window is systematically moved over the entire data set and the average calculated for each new window position. After the whole data set has been evaluated, the results are sorted and the minimum average is found. This is divided by the mean of the whole data set and multiplied by 100 to be expressed as a percentage. For a window size, as denoted by the subscript a, this can be expressed mathematically by:

$$DU_a = 100 \frac{M^*}{M} = 100 \frac{\text{low critical window value}}{\text{mean value}} \qquad (2.22)$$

This measure for DU addresses the size and magnitude of the critical area. Since the window size can be configured to any size, a sensitivity analysis of the problem area can be determined (Zoldoske and Solomon, 1988).

Another method to estimate the uniformity of an irrigation system involves the fitting of probability distribution functions to measured depth data. Distribution functions that have been investigated are the normal, lognormal, uniform, beta, gamma and specialised power functions (Warrick, 1983; Warrick *et al.*, 1989; Clemmens, 1991; Heermann *et al.*, 1992). In these investigations the mean, standard deviation and coefficient of variation (CV) are used as input values for the distribution functions. These distribution functions can also be used to determine application efficiency and the area of the field adequately irrigated.

Heermann *et al.* (1992) found that the normal distribution could be used to estimate uniformity under a centre pivot system with varying sprinkler patterns and wind conditions. However, they caution against the use of the normal distribution when the CV is greater than 0.5. In these circumstances a truncated normal distribution may have to be used. A truncated distribution is used when the theoretical distribution results in negative infiltration or application depths. The theoretical distribution is then truncated to exclude these negative values (Jaynes, 1991). Warrick *et al.* (1989) found that the specialised power function could be used to estimate uniformity for furrow irrigation systems and that the normal distribution function could be used for sprinkler irrigation systems.

The use of theoretical distribution functions to represent the uniformity of irrigation water application may provide a better estimation of performance parameters than using just the measured data. The methods are relatively simple to use as they involve solving algebraic equations, except in the case of the normal and lognormal distribution where probabilities have to be determined. However, it is not guaranteed that a theoretical distribution function will fit the measured data (Warrick *et al.*, 1989).

2.4 A Yield Model that Incorporates Irrigation Uniformity into Yield Predictions

A yield model proposed by de Juan *et al.* (1996) incorporates the uniformity of irrigation in the calculation of the gross amount of water that needs to be applied and the potential yield reduction due to the non-uniformity. In the method used by de Juan *et al.* (1996), a normal distribution is used to characterise the distribution of applied water depths. It has been found that the normal distribution can be used to describe the application of sprinkler and centre pivot irrigation systems (Warrick *et al.*, 1989; Heermann *et al.*, 1992; de Juan *et al.*, 1996). The applied depth profile, indicated in Figure 2.3, is the distribution obtained at the soil surface after evaporation losses have been taken into consideration. In Figure 2.3, d_{req}, d_m and d_{def} are the required, mean and deficit depths respectively. The deficit depth is the area of the field that is under-irrigated. AD is the adequacy of the irrigation, i.e. the portion of the field that receives the required depth. This is assumed to be the soil water deficit or crop water needs. The gross amount of irrigation water applied is $d_{gross} = d_m/(1\text{-}\%\text{ spray losses})$. The application efficiency (AE) of the system is the depth of water that contributes to the target (d_{req}) divided by the mean depth applied (d_m). Here the target is the root zone storage.

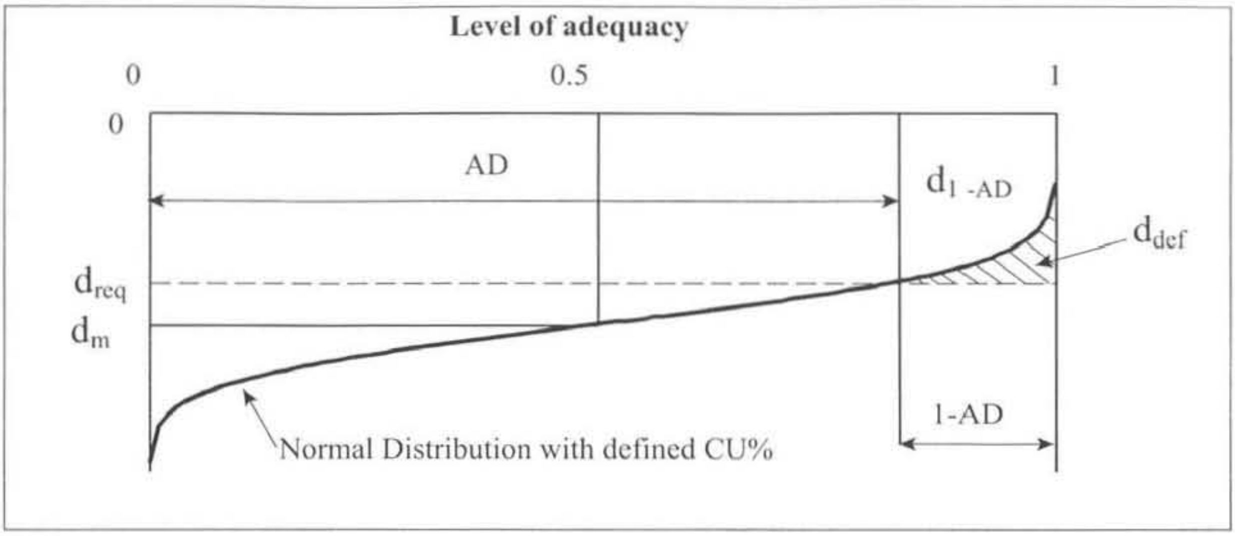

Figure 2.3 A normal distribution for applied irrigation depths with a certain coefficient of uniformity (CU) value (after de Juan *et al.*, 1996).

For a normal distribution, the coefficient of uniformity (CU) and the low-quarter distribution uniformity (DU_{lq}) are related to the coefficient of variation (CV), and to each other, by the following relationships (Warrick *et al.*, 1989):

$$CU = 100 - 0.798\ CV, \text{ where } CV\ [\%] \tag{2.23}$$

$$DU_{lq} = 100 - 1.27\ CV \tag{2.24}$$

$$DU_{lq} = 1.5915\ CU - 59.15 \tag{2.25}$$

To calculate the potential reduction in yield, the deficit coefficient is used as a measure of the effect of the non-uniform application of water. The deficit coefficient (Cd) is given by (de Juan *et al.*, 1996):

$$Cd = \frac{d_{def}}{d_{req}} \tag{2.26}$$

The relative yield (y/y_m) is given by (de Juan *et al.*, 1996):

$$1 - \frac{y}{y_m} = k_y\ Cd\ (1 - p) \tag{2.27}$$

where y, y_m are the actual and maximum yields [kg],

k_y is a yield response factor, which can be determined using values for crops reported by Doorenbos and Kassam (1979), and

p is the proportion of the water balance that represents contributions from sources other than irrigation during the irrigation season.

The water balance for the maximum evapotranspiration (ET_m) [mm] is given by (de Juan *et al.*, 1996):

$$ET_m = W_i - W_f + P_{eff} + GW + IRR_{gross} - RO - DP - E_{losses} \quad (2.28)$$

where W_i, W_f are the initial and final soil water content in the root zone [mm],

P_{eff} is the effective rainfall [mm],

GW is the contribution from the ground water [mm],

IRR_{gross} is the gross amount of water supplied [mm],

RO, DP and E_{losses} are the runoff, deep percolation and evaporation and spray losses [mm], respectively.

Therefore, p can be given by (de Juan *et al.*, 1996):

$$p = (W_i - W_f + P_{eff} + GW)/ET_m \quad (2.29)$$

The required depth, d_{req} [mm], is represented by the following relationship (de Juan *et al.*, 1996):

$$d_{req} = d_m + \alpha\sigma \quad (2.30)$$

where α is a number in the range [-3,3] and σ is the standard deviation of the applied depths. The range for α is chosen such that the value of d_{req} is part of the distribution with a 99.9% certainty for a normal distribution. The value chosen for α will determine the adequacy of the system. In the same way, a value for α can be calculated from a desired adequacy. The values of α are the values of the standard normal cumulative distribution, i.e. with zero mean and a standard deviation of 1. Therefore, for a given probability (adequacy) the values of α can be determined.

Rearranging the above equation for d_{req}, the ratio of required depth to mean depth can be represented by (de Juan *et al.*, 1996):

$$d_{req}/d_m = 1 + \alpha\, \sigma/d_m \tag{2.31}$$

$$d_{req}/d_m = 1 + \alpha\ CV \tag{2.32}$$

The remaining coefficient, Cd, is determined as follows. The deficit depth, d_{def}, is the area indicated in Figure 2.3. This is the difference in area between the rectangle, d_{req} (1-AD), and $d_{(1-AD)}$, which is the area under the normal distribution curve over the distance (1-AD). Thus, d_{def}, Cd and AE can be calculated by (refer to Figure 2.3) (de Juan *et al.*, 1996; Heermann *et al.*, 1992):

$$d_{def} = d_{req} \cdot (1 - AD) - d_{(1\text{-}AD)}$$

$$d_{(1\text{-}AD)} = \frac{-\sigma}{\sqrt{2\pi}} e^{-0.5u^2} + d_m \frac{1}{\sqrt{2\pi}} \int_{-\infty}^{u} e^{-0.5w^2} dw, \text{ where } u = (d_{req} - d_m)/\sigma = \alpha$$

$$= \frac{-\sigma}{\sqrt{2\pi}} e^{-0.5\alpha^2} + d_m \cdot \text{cumulative distribution}$$

$$= \frac{-\sigma}{\sqrt{2\pi}} e^{-0.5\alpha^2} + d_m \cdot (1 - AD) \tag{2.34}$$

$$\therefore d_{def} = d_{req} \cdot (1 - AD) + \frac{\sigma}{\sqrt{2\pi}} e^{-0.5\alpha^2} - d_m \cdot (1 - AD)$$

$$= (1 - AD) \cdot (d_{req} - d_m) + \frac{\sigma}{\sqrt{2\pi}} e^{-0.5\alpha^2} \tag{2.35}$$

$$\therefore Cd = \frac{(1 - AD) \cdot (d_{req} - d_m) + \frac{\sigma}{\sqrt{2\pi}} e^{-0.5\alpha^2}}{d_{req}} \tag{2.36}$$

$$\therefore AE = \frac{d_{(1\text{-}AD)} + d_{req} \cdot AD}{d_m}$$

$$= \frac{\frac{-\sigma}{\sqrt{2\pi}} e^{-0.5\alpha^2} + d_m \cdot (1 - AD) + d_{req} \cdot AD}{d_m} \tag{2.37}$$

These equations provide the framework for determining the effect of irrigation uniformity on potential yield. The steps in determining the potential reduction in yield are (de Juan *et al.*, 1996):

1. An estimate is made for ET_m.

2. The contribution to the water balance of the crop other than from irrigation is determined. Hence, p can be calculated.
3. The total irrigation depth for the season is calculated from:

$$d_{req} \quad = \quad ET_m - (W_i - W_f + P_{eff} + GW) \tag{2.38}$$

4. The value of k_y is determined from tables for the crop concerned.
5. The maximum yield (y_m) is determined from tables or local knowledge.
6. A value for CU is fixed for the irrigation system. The CV and DU_{lq} can be determined from the relationships stated earlier. Now, either AD or α can be selected and the one that is not fixed can be calculated off the other. Since CV and α are known, the ratio of d_{req}/d_m can be calculated and hence the d_m that needs to be applied. Next Cd and AE are calculated.
7. Finally, the relative yield (y/y_m) and hence y can be calculated.

An example for a maize crop, given by de Juan *et al.* (1996), with ET_m = 881.1 mm, p = 266.8/881.1, CU = 85%, k_y = 1.25 and y_m = 15000 $kg.ha^{-1}$ is shown in Table 2.5. In this example, the DU_{lq} = 0.761. In the scenario where the average depth applied is equal to the required depth the adequacy is 50%, which means that half the field is under-irrigated and half the field is over-irrigated. Under these conditions the application efficiency is 92.5% (this excludes spray and evaporation losses) and the reduction in yield is calculated at 6.54%. If the adequacy is decreased to say 23% then the mean depth that is applied is less than ET_m for the season. Here, the application efficiency increases to 97.5%, but the yield is reduced by 12.55%. Thus, for an increase in efficiency of 5%, a reduction in yield of an extra 6% is seen. If the adequacy is increased, to 84% say, a greater amount of water needs to be applied. In this case 23% extra water has to be applied during the season. The application efficiency drops to 79.7%, but the potential yield is only reduced by 1.7%. The required degree of adequacy will determine the total amount of water that needs to be supplied to the irrigation field. A compromise will have to be reached between increased efficiency and the reduction in yields. In this paper by de Juan *et al.* (1996), they use an optimisation program to determine the optimum cost efficiency depending on the cost of water and other production costs.

Table 2.5 Example calculation for the reduction in maize yield for an irrigation system with a CU = 85% (after de Juan *et al.*, 1996).

AD	d_{req}/d_m	d_m/d_{req}	d_m mm	Cd	AE %	y/ym %	Y $kg.ha^{-1}$
0.00	1.56	0.64	393	0.36	100.0	68.56	10284
0.04	1.33	0.75	462	0.25	99.7	78.22	11733
0.23	1.14	0.88	539	0.14	97.5	87.45	13117
0.40	1.05	0.95	586	0.10	94.6	91.58	13737
0.50	1.00	1.00	614	0.07	92.5	93.46	14020
0.60	0.95	1.05	645	0.06	89.9	95.10	14265
0.69	0.91	1.10	677	0.04	86.9	96.40	14461
0.84	0.81	1.23	756	0.02	79.7	98.30	14746
0.93	0.73	1.37	842	0.01	72.3	99.25	14887
1.00	0.48	2.08	1280	0.00	47.9	100.00	15000

This method allows the mean depth of application to be determined for any CU, DU_{lq} or CV value. Thus, the relative effect of irrigation non-uniformity on yield and irrigation water requirement can be estimated.

The effect of DU_{lq} and AD on d_m/d_{req}, AE and y/y_m is shown in Table 2.6 to Table 2.8, respectively. The same inputs for ET_m, p and Y_{max} as used in the previous example are used here. A normal distribution is assumed. The tables can be used to determine what the ratio of d_m/d_{req}, application efficiency and relative yield for a given level of adequacy and DU_{lq}.

Table 2.6 d_m/d_{req} for different DU_{lq} and AD values.

	d_m/d_{req}							
	DU_{lq}							
AD	0.5	0.6	0.7	0.75	0.8	0.875	0.9	0.95
0.001	0.451	0.507	0.578	0.622	0.673	0.767	0.804	0.892
0.125	0.688	0.734	0.786	0.815	0.847	0.898	0.917	0.957
0.250	0.790	0.825	0.863	0.883	0.904	0.938	0.950	0.974
0.375	0.889	0.909	0.930	0.941	0.952	0.970	0.976	0.988
0.500	1.000	1.000	1.000	1.000	1.000	1.000	1.000	1.000
0.625	1.143	1.112	1.081	1.067	1.053	1.032	1.026	1.013
0.750	1.362	1.270	1.190	1.153	1.119	1.071	1.056	1.027
0.875	1.828	1.568	1.373	1.293	1.221	1.128	1.100	1.047
0.950	2.837	2.075	1.635	1.479	1.350	1.193	1.149	1.069
0.999			3.703	2.553	1.948	1.437	1.322	1.139

For example, for an adequacy of 75% and a DU_{lq} of 75%, the ratio d_m/d_{req} would be 1.153, and the application efficiency and relative yield would be 83.8% and 97.0%, respectively.

Table 2.7. Application efficiency for different DU_{lq} and AD values.

	Application Efficiency [%]							
	DU_{lq}							
AD	0.5	0.6	0.7	0.75	0.8	0.875	0.9	0.95
0.125	97.6	98.0	98.5	98.8	99.0	99.4	99.5	99.8
0.250	94.1	95.3	96.5	97.1	97.7	98.5	98.8	99.4
0.375	89.8	91.8	93.9	94.9	95.9	97.4	98.0	99.0
0.500	84.3	87.4	90.6	92.1	93.7	96.1	96.9	98.4
0.625	77.2	81.8	86.3	88.6	90.9	94.3	95.4	97.7
0.750	67.6	74.1	80.5	83.8	87.0	91.9	93.5	96.8
0.875	52.3	61.8	71.4	76.1	80.9	88.1	90.5	95.2
0.950	34.4	47.5	60.7	67.2	73.8	83.6	86.9	93.4
0.999		2.7	27.0	39.2	51.3	69.6	75.7	87.8

Table 2.8 Relative yield for different DU_{lq} and AD values.

	Relative Yield (y/y_m) [%]							
	DU_{lq}							
AD	0.5	0.6	0.7	0.75	0.8	0.875	0.9	0.95
0.125	71.4	75.6	80.4	83.0	85.9	90.7	92.4	96.0
0.250	77.7	81.4	85.4	87.5	89.8	93.4	94.6	97.2
0.375	82.4	85.6	88.9	90.7	92.4	95.2	96.1	98.0
0.500	86.3	89.0	91.8	93.2	94.5	96.6	97.3	98.6
0.625	89.8	92.1	94.2	95.2	96.2	97.7	98.2	99.1
0.750	93.0	94.8	96.3	97.0	97.7	98.6	98.9	99.5
0.875	96.1	97.3	98.2	98.6	99.0	99.4	99.5	99.8
0.950	98.0	98.8	99.3	99.5	99.6	99.8	99.8	99.9
0.999	100.0	99.7	100.0	100.0	100.0	100.0	100.0	100.0

The above method can also be applied to other distribution types. The specialised power function can be used to describe the water distribution of furrow and basin irrigation systems (Warrick, 1983). The distribution can be described by the following relationship:

$$\frac{d_u - d}{d_u - d_l} = \frac{d_u - d}{\Delta d} = AD^b \tag{2.39}$$

where d_u, d_l are the upper and lower depths in the distribution,

d is the depth at an adequacy AD and $\Delta d = d_u - d_l$.

The mean, variance, coefficient of variation (CV), coefficient of uniformity (CU) and DU_{lq} can be calculated from the above equation and are given by (Warrick, 1983):

$$d_{mean} = d_u - \Delta d / (b+1) \tag{2.40}$$

$$\sigma^2 = \frac{\Delta d^2 b^2}{(1+2b)(b+1)^2} \tag{2.41}$$

$$CV = \frac{b\Delta d}{d_{mean}\,(b+1)(1+2b)^{0.5}} \tag{2.42}$$

$$CU = 1 - \left[\frac{2\,(1+2b)^{0.5}}{(b+1)^{(1/b)-1}}\right] CV, \quad CV < (1+2b)^{-0.5} \tag{2.43}$$

$$DU_{lq} = 1 - (3/b)(1-0.75^b)(1+2b)^{0.5}\,CV, \quad CV < (1+2b)^{-0.5} \tag{2.44}$$

For a given b, CV, AD and required depth (d_{req}), the upper and lower depths of the distribution can be solved for using the following equations:

$$d_{req} = d_u - AD^b d_u + AD^b d_l$$

$$\therefore d_l = \frac{d_{req}}{AD^b} + d_u\left(1 - 1/AD^b\right) \tag{2.45}$$

$$d_{mean} = \frac{b\Delta d}{CV(b+1)(1+2b)^{0.5}} = d_u - \frac{\Delta d}{(b+1)}$$

$$\therefore \quad d_u - \frac{d_u - d_l}{(b+1)} = \frac{bd_u - bd_l}{CV(b+1)(1+2b)^{0.5}} \tag{2.46}$$

Substitute (2.45) into (2.46) and solve for d_u :

$$d_u = \frac{-d_{req} / AD^b\left(b + CV\sqrt{1+2b}\right)}{CV(1+2b)^{0.5}(b+1-1/AD^b) - b/AD^b} \tag{2.47}$$

These equations allow one to solve for d_{mean}, deficit coefficient (Cd), application efficiency (AE), yield and relative yield, and system efficiency (SE). The deficit depth (d_{def}), Cd, AE and SE can be calculated from:

$$d_{def} = d_{req}(1 - AD) - \sum_{AD}^{1}(d_u - x^b \Delta d)dx$$

$$\therefore d_{def} = (d_{req} - d_u)(1 - AD) + \frac{\Delta d}{(b+1)}\left(1 - AD^{b+1}\right) \quad (2.48)$$

$$Cd = \frac{d_{def}}{d_{req}} \quad (2.49)$$

$$AE = \frac{\text{depth stored}}{\text{average depth applied}} = \frac{d_{req} - d_{def}}{d_{mean}} \quad (2.50)$$

$$SE = AE * (100 - \%\text{spray losses}) \quad (2.51)$$

The uniform distribution is a specialised power distribution where b = 1.The methods described above rely on certain assumptions. These are (de Juan *et al.*, 1996):

1. The scheduling of the irrigation is correctly managed to prevent runoff and excess deep percolation. The deep percolation that occurs will be a result of the non-uniformity only.
2. The CV (or DU_{lq} or CU) is constant for the irrigation system irrespective of the depth applied.
3. The actual distribution of water can be accurately described by one of the theoretical distribution types discussed.
4. There is no allocation of water for deep percolation.

2.5 Conclusions

Dwindling water resources require that water use be more efficiently managed. Since irrigated agriculture is the largest user of water, it is important that the concepts and principles of irrigation performance criteria are understood to avoid misconceptions and incorrect policy decisions.

The first step in determining irrigation performance criteria is the correct categorisation of the portions of the water balance. This ensures that accurate estimates are made for the components of the water balance for use in the various performance parameters. However, when it comes to the judgmental partitioning of irrigation water, the process can be more subjective. What constitutes a reasonable use to one evaluator may not be the same as another evaluator. Therefore, a general understanding of what constitutes a reasonable, beneficial, unreasonable, or non-beneficial use is needed.

In the past there have been many different definitions for various performance criteria that have resulted in an inability to compare systems evaluated at different times and places. This has hampered the selection of an optimal irrigation system due to the lack of quantitative comparison. By standardising the definitions and concepts for irrigation performance criteria, appropriate decisions regarding the design and management of irrigation systems can be made. In this way the farmers and policy makers can reach equitable solutions that are practical and agronomically and economically viable.

An important performance measure is the uniformity of application of irrigation water. The uniformity has a direct effect on the yield and efficiency of a system. To strive for high yields, the application of irrigation water needs to be uniform across the field. This will reduce the areas in the field that are under- or over-irrigated. By striving for higher uniformity, the amount of water lost to surface runoff and deep percolation will be reduced. This will improve the application efficiency of the system. The uniformity of a particular system can be improved by addressing shortcomings in the components of the system that cause poor uniformity. These may be related to the design or operation of the system.

The performance of an irrigation system needs to be judged in context of the suitability and economic viability of the systems. Physical constraints, such as topography or environmental factors, should also be considered when deciding on an optimal irrigation system. The decision to improve the efficiency or distribution uniformity of a system has to be made by considering the costs and availability of water resources and the cost of improving the system. Therefore, it may not be practical or economically viable to replace an existing system with a system that has a better uniformity of application. For this reason, the relationship between the uniformity and the efficiency of the system needs to be determined. This is required so that an adequate allocation of water is given to the farmer.

The distribution of applied depths needs to be accurately estimated. Since it may be impractical or uneconomical to determine this on a field scale, methods that have been developed to estimate the distribution need to be understood and evaluated. The current practices use the combination of variance method or fitting the measured depths to a theoretical distribution function. These methods require an understanding of statistics and distribution theory. Although they can be used to approximate the actual distribution, it is not guaranteed that a theoretical distribution will fit the measured data. These methods may provide reliable answers but they do not describe the location and extent of the non-uniformity effectively. They are also prone to errors when all the components that contribute to non-uniformity are not included. Further errors can occur due to the compounding effect of measurement errors of the individual components. The combination of variance method requires assumptions to be made about the type of distribution that fits the measured data in order to estimate the K factor. Since the measured data may not fit a distribution type, using this method may be of limited use.

In this Chapter, the importance of the various criteria was discussed. In particular, the distribution uniformity plays an important role in determining the gross amount of water that needs to be applied. Since the distribution of water across a field varies, a method of describing the spatial variation is required. To assess the spatial variability of a variable a suite of spatial statistical methods called geostatistics is used. The theory and application of geostatistics will be discussed in the next Chapter.

3 GEOSTATISTICS

Geostatistics is a set of tools that can be used to describe the spatial continuity of a continuous random variable. Classical statistics does not take the location of data into consideration. Geostatistics takes advantage of the spatial continuity to make inferences about the variable being studied (Journel and Huijbregts, 1978; Isaaks and Srivastava, 1989; ASCE, 1990a). Geostatistics is a useful tool to give an alternative description of spatial data when the limited data available cannot be used to describe the variable explicitly (ASCE, 1990a). Geostatistical methods have been applied in many areas such as mining resource estimation (Journel and Huijbregts, 1978), groundwater depth estimation (ASCE, 1990a) and in estimation in soil science (Goovaerts, 1999). Fonteh and Podmore (1994) used geostatistics to characterise the spatial variability of infiltration in furrow irrigation and to investigate the effect of the spatial variability on the performance criteria of an irrigation event.

The theory of geostatistics is a vast and sometimes complicated subject. This chapter will focus on the theory used to conduct this study. A few basic assumptions used in the theory of regionalised variables will be discussed. The method used to describe the spatial behaviour of the data and the spatial prediction techniques will be given. The sampling patterns used for spatial evaluations will be discussed. An example is given to illustrate how the spatial continuity is described and how predictions are made at unmeasured locations.

3.1 Random Functions

A random function $Z(\mathbf{x})$ can be interpreted as the set of random variables $Z(\mathbf{x}_i)$ defined on a point $\mathbf{x}_i$ in a region D: $Z(\mathbf{x}) = \{Z(\mathbf{x}_i), \forall\ \mathbf{x}_i \in D\}$. The random variables $Z(\mathbf{x}_i)$ and $Z(\mathbf{x}_i + \mathbf{h})$ are correlated and this correlation depends on the separation vector $\mathbf{h}$ and the nature of the variable being considered. At any point $\mathbf{x}_i$, the true measured value $z(\mathbf{x}_i)$ can be interpreted as a particular realisation of the random variable $Z(\mathbf{x}_i)$. Therefore, the set of measured values $\{z(\mathbf{x}_i), \forall\ \mathbf{x}_i \in D\}$ is interpreted as one particular realisation of the random function $\{Z(\mathbf{x}_i), \forall\ \mathbf{x}_i \in D\}$ (Journel and Huijbregts, 1978).

In geostatistics, it is necessary to assume some form of a stationarity for the regionalised variable in order to estimate the mean and covariance of the population from measured data

(ASCE, 1990a). This is to ensure that all the measured data in the region of interest are part of the same population of the regionalised variable. The various hypotheses of stationarity are as follows:

- *Strict stationarity.* A random function is stationary when its spatial law does not change under translation. For example, two k-component vectoral random variables $\{Z(\mathbf{x}_1), Z(\mathbf{x}_2), ..., Z(\mathbf{x}_k)\}$ and $\{Z(\mathbf{x}_1+\mathbf{h}), Z(\mathbf{x}_2+\mathbf{h}), ..., Z(\mathbf{x}_k+\mathbf{h})\}$ have the same k-variable law whatever the translation vector **h** (Journel and Huijbregts, 1978).

- *Stationarity of order 2.* In geostatistics a random function has stationarity of order 2 if:
  a) the mean exists and does not depend on the support point **x** such that:
     $E\{Z(\mathbf{x})\} = m, \forall \mathbf{x}$ (Journel and Huijbregts, 1978), therefore, the mean is the same everywhere (ASCE, 1990a);
  b) for each pair of random variables $\{Z(\mathbf{x}),Z(\mathbf{x}+\mathbf{h})\}$ the covariance exists and depends only on the separation vector **h** such that:

$$C(\mathbf{h}) = E\{Z(\mathbf{x} + \mathbf{h}).Z(\mathbf{x})\} - m^2 = C(0), \forall \mathbf{x} \text{ (Journel and Huijbregts, 1978).}$$

- *Intrinsic hypothesis.* A random function is said to be intrinsic when:
  a) the mathematical expectation exists and does not depend on the support point **x** such that: $E\{Z(\mathbf{x})\} = m, \forall \mathbf{x}$;
  b) for all vectors **h** the increment $[Z(\mathbf{x}+\mathbf{h})-Z(\mathbf{x})]$ has a finite variance that does not depend on **x**:

$$Var\{Z(\mathbf{x}+\mathbf{h})-Z(\mathbf{x})\} = E\{[Z(\mathbf{x}+\mathbf{h})-Z(\mathbf{x})]^2\} = 2\,\gamma(\mathbf{h}), \forall \mathbf{x} \text{ (Journel and Huijbregts, 1978).}$$

  That is, the variance of $Z(\mathbf{x}+\mathbf{h})-Z(\mathbf{x})$ is defined and can be expressed as a unique function of the separation vector **h** (ASCE, 1990a).

A variable that has stationarity of order 2 also satisfies the intrinsic hypothesis. However, the converse is not true. Assuming the intrinsic hypothesis is useful because it allows the statistical structure of a regionalised variable to be determined without requiring a prior estimation of the mean (ASCE, 1990a). This then allows the spatial continuity of the variable to be determined.

3.2 Description of Spatial Continuity

A continuous variable z at n locations $\mathbf{u}_\alpha$ is usually denoted by $z(\mathbf{u}_\alpha)$, $\alpha = 1, 2, ..., n$. Spatial patterns are described using the experimental semivariogram $\hat{\gamma}(\mathbf{h})$ which is a measure of the average dissimilarity between data separated by vector **h**. The semivariogram is calculated as half the average squared difference between data pairs separated by **h**:

$$\hat{\gamma}(\mathbf{h}) = \frac{1}{2\,N(\mathbf{h})} \sum_{\alpha=1}^{N(\mathbf{h})} \left[z(\mathbf{u}_\alpha) - z(\mathbf{u}_\alpha + \mathbf{h}) \right]^2 \tag{3.1}$$

where $N(\mathbf{h})$ is the number of data pairs within a given class and direction (Goovaerts, 1999).

The spatial continuity can also be expressed in terms of the correlation function $\rho(\mathbf{h})$ or the covariance function $C(\mathbf{h})$:

$$C(\mathbf{h}) = \frac{1}{N(\mathbf{h}) - 1} \sum_{\alpha=1}^{N(\mathbf{h})} \left[z(\mathbf{u}_\alpha + \mathbf{h}) - m \right] \left[z(\mathbf{u}_\alpha) - m \right] \tag{3.2}$$

$$\rho(\mathbf{h}) = \frac{C(\mathbf{h})}{\sigma^2} \tag{3.3}$$

where σ^2 is the sample variance and m is the sample mean (ASCE, 1990b).

In geostatistical modelling, usually the semivariogram is used to describe spatial continuity. For this discussion of the variogram, the point vector **x**, is replaced by a point x, and the separation vector **h** is replaced by the magnitude h. The continuity and regularity of a random function and of the regionalised variables, z(x), that it represents, are related to the behaviour of the semivariogram near the origin. There are four main types of behaviour at the origin and are shown in Figure 3.1. In order of decreasing regularity they are (Journel and Huijbregts, 1978):

a) Parabolic: $\gamma(h) \sim A|h|^2$ when $h \to 0$, where A is a constant. $\gamma(h)$ is twice differentiable at the origin and the random function itself is differentiable. This type of behaviour is characteristic of high spatial continuity.

b) Linear: $\gamma(h) \sim A|h|$ when $h \to 0$. $\gamma(h)$ is not differentiable at the origin, but it remains continuous at h=0 and therefore, for all |h|. The random function Z(x) is mean square continuous ($\lim E\{[Z(x+h)-Z(x)]^2\}=0$, when $h \to 0$), but not differentiable.

c) Discontinuity at the origin: $\gamma(h)$ does not tend towards 0 as $h \to 0$. However, by definition $\gamma(0)=0$. The random function is no longer mean square continuous. Hence, the variability between two close values z(x+h) and z(x) can be high and it can increase as the size of discontinuity increases at the origin. The discontinuity at the origin is referred to as the nugget effect and can be due to measurement errors and micro-variability of the variable at small separation distances. At distances h>0, the variability is often more continuous due to the continuity of $\gamma(h)$ for h>0.

d) Pure nugget effect. This is when $\gamma(h)$ appears simply as a discontinuity at the origin where $\gamma(0)=0$ and $\gamma(h)=C_0$. The value of C_0 is the sill. The pure nugget effect represents a total lack of correlation.

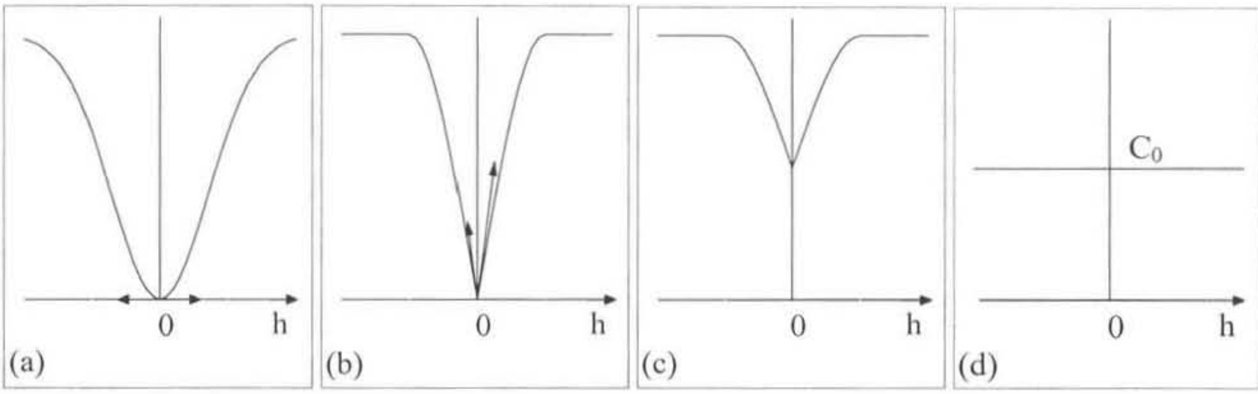

Figure 3.1 Behaviour near the origin of the variogram. (a) Parabolic, (b) linear, (c) nugget effect, and (d) pure nugget effect (after Journel and Huijbregts, 1978).

Some common variogram models are:

a) Spherical model. This is one of the most common models used and its standardised equation is:

$$\gamma(h) = \begin{cases} 1.5\dfrac{h}{a} - 0.5\left(\dfrac{h}{a}\right)^3, & \text{if } h \le a \\ 1, & \text{otherwise} \end{cases} \tag{3.4}$$

where a is the range. The spherical model has a linear behaviour near the origin and reaches its sill value at a (Isaaks and Srivastava, 1989).

b) Exponential model. This is another commonly used model whose standardised equation is:

$$\gamma(h) = 1 - \exp\left(-\frac{3h}{a}\right) \tag{3.5}$$

This model reaches its sill value asymptotically and the practical range is assumed to be the distance where the variogram value is 95% of its sill. It too has a linear behaviour near the origin, but rises more steeply than the spherical model (Isaaks and Srivastava, 1989).

c) Gaussian model. This model is usually used to represent highly continuous phenomena. Its standardised equation is:

$$\gamma(h) = 1 - \exp\left(-3\left(\frac{h}{a}\right)^2\right) \tag{3.6}$$

The Gaussian model also reaches it sill asymptotically and the range is taken as the distance where the variogram equals 95% of the sill value. These three models are shown in Figure 3.2.

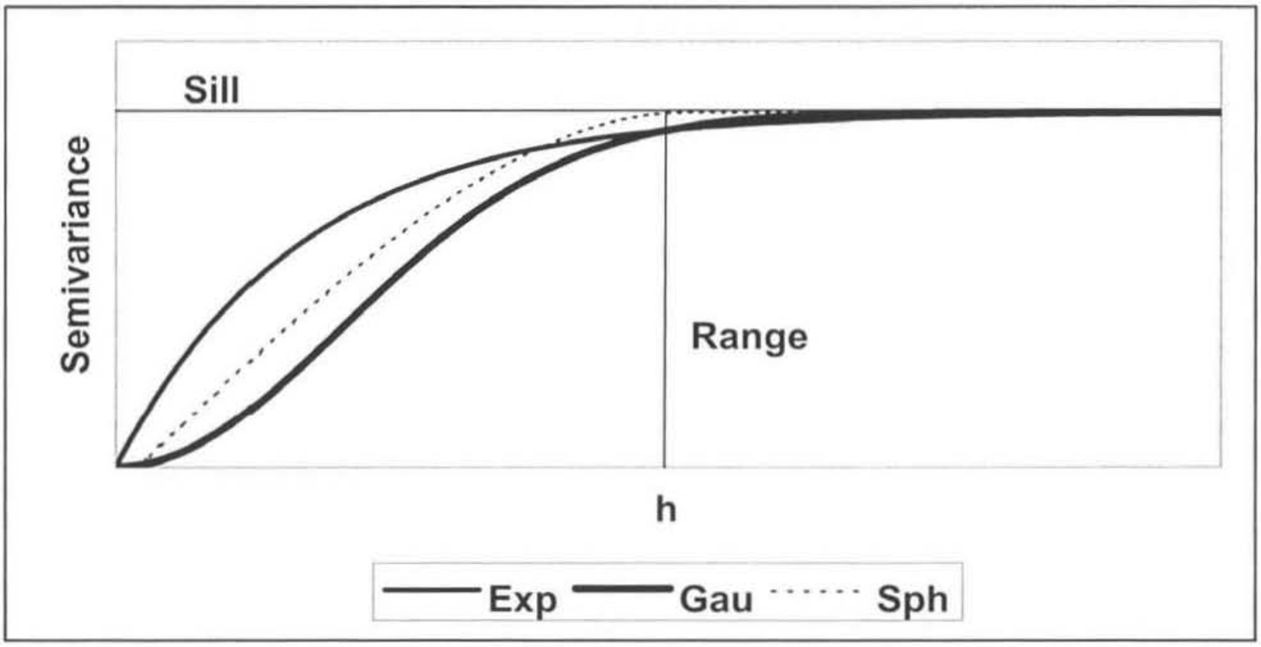

Figure 3.2 The three most commonly used variograms: the Gaussian (Gau), spherical (Sph) and exponential (Exp) models shown with the same range and sill (after Isaaks and Srivastava, 1989).

Geostatistical modelling is often started with an omni-directional variogram, which is based on the magnitude of the separation vector **h** and not the direction. This provides an initial representation of the spatial structure. The omni-directional variogram does not imply that the spatial structure is the same in all directions. A well-behaved omni-directional variogram may suggest well-behaved directional variograms. In many data sets the data is more continuous in certain directions than in others. These directional variograms fall along anisotropic axes. There are various methods to determine the axes of maximal and minimal continuity (Isaaks and Srivastava, 1989).

Once the variogram has been determined, spatial interpolation can be done using the measured data available.

3.3 Spatial Prediction

Geostatistics uses a set of prediction methods that are given the name kriging. Kriging is a local estimation technique that provides the best linear unbiased estimate (BLUE) of the unknown characteristic being studied (Journel and Huijbregts, 1978).

Let Z(x) be a random function which is defined on a point support and is second order stationary with: expectation, $E\{Z(x)\} = m$, a constant m which is generally unknown; centred covariance, $E\{Z(x+h)Z(x)\} - m^2 = C(h)$; and variogram $E\{[Z(x+h)-Z(x)]^2\} = 2\gamma(h)$. Either of these two second-order moments is assumed known. When only the variogram is known the random function Z(x) is intrinsic only (Journel and Huijbregts, 1978).

The linear estimator Z^*_K is a linear combination of n data values such that:

$$Z^*_K = \sum_{\alpha=1}^{n} \lambda_\alpha Z_\alpha \tag{3.7}$$

The n weights λ_α are calculated to ensure that the estimator is unbiased and that the estimation variance is a minimum. To ensure the unbiasedness of the estimator the sum of the weights λ_α are set equal to 1. This is to obtain a zero error expectation, i.e. $E\ \{[Z_V - Z^*_K]\} = 0$ (Journel and Huijbregts, 1978).

The estimation variance is given by:

$$E\{[Z_V - Z_K^*]^2\} = \overline{C}(V,V) - 2\sum_{\alpha} \lambda_\alpha \overline{C}(V,v_\alpha) + \sum_{\alpha}\sum_{\beta} \lambda_\alpha \lambda_\beta \overline{C}(v_\alpha, v_\beta) \quad (3.8)$$

where $\overline{C}(V, v_\alpha)$ is the mean value of the covariance function $C(\mathbf{h})$ when the two extremities of vector **h** independently describe the domains of V and v_α respectively (Journel and Huijbregts, 1978).

The 'kriging system' is obtained by setting the n partial derivatives of:

$$\frac{\partial\left[E\{[Z_V - Z_K^*]^2\} - 2\mu \sum_{\alpha} \lambda_\alpha \right]}{\partial \lambda_\alpha} \quad (3.9)$$

to zero. Where μ is a Lagrange Multiplier to make the constrained linear system unconstrained. This results in the kriging system:

$$\left.\begin{aligned} \sum_{\beta=1}^{n} \lambda_\beta \overline{C}(v_\alpha, v_\beta) - \mu &= \overline{C}(v_\alpha, V), \qquad \forall \alpha = 1 \text{ to } n \\ \sum_{\beta=1}^{n} \lambda_\beta &= 1 \end{aligned}\right\} \quad (3.10)$$

The minimum estimation variance is given by:

$$\sigma_K^2 = E\{[Z_V - Z_K^*]^2\} = \overline{C}(V,V) + \mu - \sum_{\alpha=1}^{n} \lambda_\alpha \overline{C}(v_\alpha, V) \quad (3.11)$$

When the random function is intrinsic only, the covariance function C can be replaced by the semivariogram function γ (Journel and Huijbregts, 1978).

To ensure that the kriging system produces one and only one solution, the covariance function C(h) needs to be positive definite. The positive definite character of C(h) has the following properties (Journel and Huijbregts, 1978):

a) $C(0) = Var\{Z(x)\} \geq 0$, an *a priori* variance must be greater or equal to zero,
b) $C(h) = C(-h)$, the covariance is an even function,
c) |C(h)| #C(0), Schwarz's inequality.

A way to ensure positive definiteness is to model the variogram using functions that are known to be positive definite. The Gaussian, spherical and exponential models already discussed are example of positive definite functions (Isaaks and Srivastava, 1989). Also, models in $|h|^{\theta}$, with $\theta \in]0,2[$, and the logarithmic model are further examples. These last two models do not reach a sill value and the random function is intrinsic only and has neither an *a priori* variance nor covariance (Journel and Huijbregts, 1978).

A linear combination of positive definite functions with positive coefficients is also positive definite. Therefore, nested models comprising of a linear combination are often used to describe the shape of the variogram. However, forming complex nested models do not usually result in more accurate estimates than using simpler models. For example, if an exponential model fits the variogram as well as two nested spherical models, then using the principle of parsimony, the exponential model should be used (Isaaks and Srivastava, 1989).

Once the nested model has been chosen, the determination of the coefficients and range parameters is an exercise in model fitting. Often the method of weighted least squares (WLS) is used to fit the variogram model. The weights are either chosen to be proportional to N_i or $(\gamma(h_i))^{-2}N_i$, where N_i is the number of data pairs in interval, i, and $\gamma(h_i)$ is the variogram model value at the average interval, i, distance h_i (Pebesma and Wesseling, 1998).

3.4 Spatial Sampling Patterns

The collection of data for spatial analysis over a domain of interest, D, is costly and time consuming. For this reason an optimal sampling design strategy needs to be decided on to reach some optimality criterion (Cressie, 1991). There are various sampling plans to select, n sites within a region, D. The most commonly used are the; simple random sampling, stratified random sampling, cluster random sampling, regular (or systematic) random sampling, and regular non-random sampling (Cressie, 1991).

- In simple random sampling, the sites are chosen independently, each with a uniform distribution over the region, D (Cressie, 1991; Brus and de Gruijter, 1997).
- In stratified random sampling, the region, D, is divided into non-overlapping strata. In each stratum a simple random sample is chosen (Cressie, 1991; Brus and de Gruijter, 1997).

- In systematic random sampling, an initial site is chosen at random and the remaining (n - 1) sites are specified so that all n sample sites follow some regular pattern. If the initial site is not chosen at random, then the resulting sampling plan is called deterministic or regular. The most common regular plans are the equilateral triangular grid, the rectangular or square grid, and the hexagonal grid (Cressie, 1991).
- Cluster random sampling consists of the random selection of groups of sites. These sites are spatially "close" within the groups. This sampling plan has not received much attention, as it is often poorly adapted (Cressie, 1991).

Cressie (1991) gives the following discussion on the comparison of the different types of sampling plans. The easier implementation of regular random sampling is an advantage over simple or stratified random sampling. It also provides a means of determining variograms for different directional classes. The equilateral triangular grid provides three basic directions along which to determine spatial dependence with more replication at spatial lags than the hexagonal plan. The use of regular plans could also reduce the amount of computation required over randomised plans. Regular sampling patterns allow variograms to be estimated at a small number of lags than compared to random sampling where many irregular lags have to be analysed. In practise, these irregular lags are placed into distances classes, which may not be a satisfactory solution and could lead to imprecision in the estimation of the variogram. In general, the use of a regular sampling pattern is more efficient than simple and stratified sampling (Olea, 1984; cited Cressie, 1991). Here the average and maximum kriging variances are used as a measure of efficiency.

The choice of the "best" sampling strategy will be determined by the optimality criterion or objective function to be minimised (Cressie, 1991). In a statistical context this usually applies to some measure of closeness of an estimator (or predictor) to an unknown parameter (or datum). To arrive at an optimal statistical design is the choice of; i) what is to be estimated or predicted, ii) the estimator or predictor, and iii) the measure of closeness that is to be minimised. The second choice usually consists of a standard statistical procedure, such as best linear unbiased estimator (or predictor), or generalised least squares estimator. Generally, the mean square error, the variance, the generalised variance, or the mean square prediction error is used as the minimising criterion (Cressie, 1991). The optimisation of the sampling strategy is beyond the scope of this review. Readers are referred to Olea (1984), Warrick and Myers

(1987), Cressie (1991), Wopereis *et al.* (1992), Chen *et al.* (1995), Brus and de Gruijter (1997), Bogaert and Russo (1999), and Warrick *et al.* (1999) for optimisation strategies of sampling designs.

3.5 An Example of Spatial Continuity and Spatial Prediction

To illustrate how the spatial continuity of measured data can be determined and how it can be used in the prediction of values at unmeasured points, the following example extracted from ASCE (1990a) will be discussed. In an area of 2500 sq mi, the specific yield from 20 groundwater wells was measured. The co-ordinates and specific yield of the 20 measured locations are shown in Table 3.2. The sample locations are shown in Figure 3.3 together with the 3 locations at which an estimate was made using ordinary kriging. The measured data was separated into four lag distances of 10 miles with a maximum distance of 40 miles. The experimental semivariogram obtained from these four points is shown in Figure 3.4. An exponential model was fitted to these four points. The equation of the fitted model was as follows:

$$\gamma(\mathrm{h}) = 0.7424\,(1 - \delta(\mathrm{h})) + 14.01\left(1 - \exp\left(\frac{-3\mathrm{h}}{50}\right)\right) \tag{3.12}$$

where h is the magnitude of the lag separation and δ(h) is the Kronecker delta (δ = 1 if h = 0, else δ = 0). The Kronecker delta is used to ensure that the value of γ(0) = 0, since it is zero at the origin by definition. In this example the nugget effect is 0.7424 and could be due to measurement error or small-scale variability. The range is 50 miles and the sill variance is 14.7524.

Table 3.1 Specific yield (S_y) at measured locations and kriging weights used to estimate the specific yield at unmeasured locations A, B and C (after ASCE, 1990a).

Observation point	X	Y	Sy	Kriging weights		
Number	[miles]	[miles]	[%]	A	B	C
1	55	0	11	-0.004162	0.002271	-0.001685
2	53.1	6.3	10	-0.006089	-0.012301	-0.004246
3	44.1	4.5	14	-0.002411	0.122721	-0.004161
4	41.3	12.1	14	0.309991	0.028920	-0.003627
5	34	13	17	0.211914	0.219263	-0.002265
6	28.9	14	12	0.038277	0.558959	-0.002437
7	64	4	7	-0.003888	0.008405	-0.005745
8	58.3	8.1	8	-0.003296	-0.008985	-0.001042
9	49.1	9.2	11	0.016028	-0.013501	-0.000414
10	49.4	14.8	11	0.086932	-0.018898	0.023740
11	38.9	24	12	0.220565	-0.028925	0.001042
12	34.9	25.1	13	0.092924	-0.015618	-0.002780
13	27.8	28	12	-0.004859	0.085424	-0.001740
14	66	16	6	-0.006323	0.009650	0.042046
15	59	17	8	-0.007620	-0.004219	0.120859
16	51.3	21.4	11	0.046977	-0.012613	0.353794
17	43.6	26.6	14	0.058919	-0.011993	0.050559
18	37.1	30.3	14	-0.023220	0.000817	0.004403
19	53	28	8	-0.011000	0.005210	0.435553
20	51	-4.2	17	-0.009659	0.085413	-0.001854
Sum of weights				1.000000	1.000000	1.000000

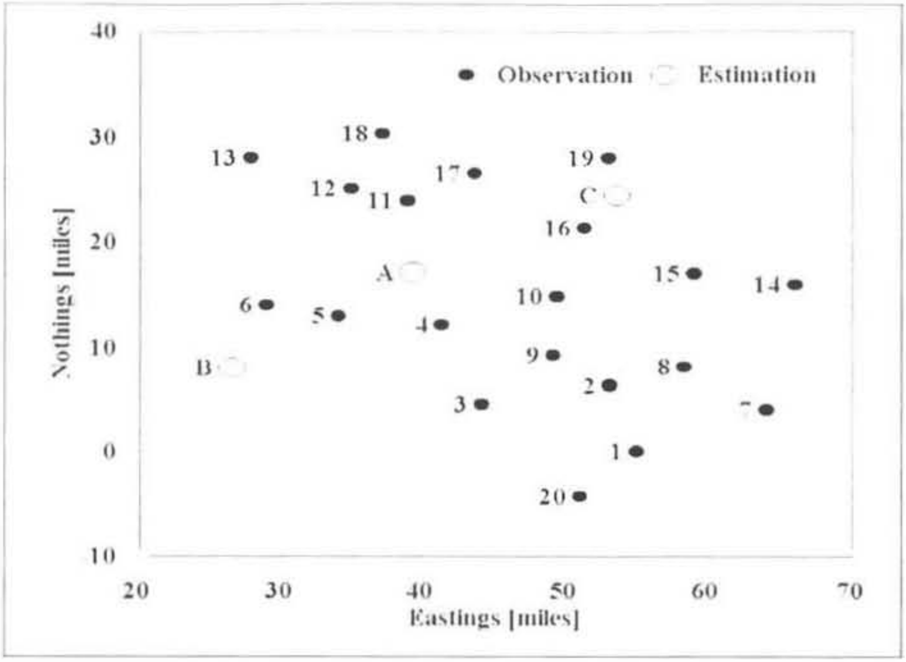

Figure 3.3 Location of 20 measured sites of specific yield (1–20) and position of the estimation sites (A-C) (after ASCE, 1990a).

In this example, all 20 data points and the exponential semivariogram in Equation 3.12 were used to set up the kriging system. The estimate at each of the unknown points was made using Equation 3.7 and the weights were obtained by solving the kriging system shown in Equation 3.10. The function C was replaced by the semivariogram function γ in this example. The weights obtained from the kriging system for each of the three locations for each data point is shown in Table 3.1. Points that are closest to the point being estimated have a higher weighting than points further away. The weights and data values are substituted into Equation 3.7 to obtain the estimate at the unmeasured location. The estimation variance was calculated according to Equation 3.8. These results are given in Table 3.2 together with the average estimate and the co-ordinates of the unmeasured locations.

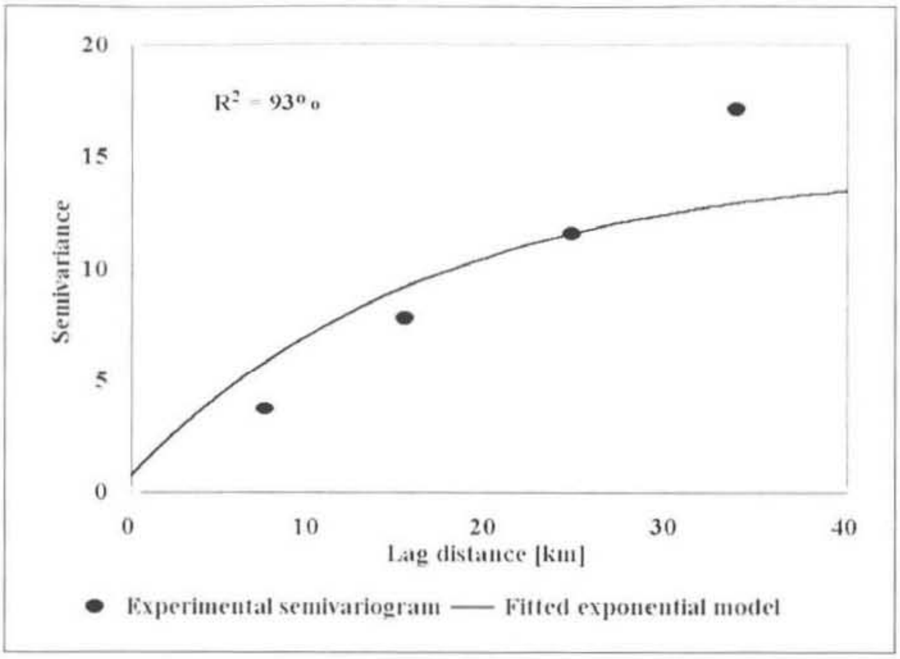

Figure 3.4 Experimental semivariogram and fitted exponential model (after ASCE, 1990a).

Table 3.2 Estimated specific yields (%) and estimation variance (after ASCE, 1990a).

		Point	
Estimator	A	B	C
$Z^* = \Sigma_i \lambda_i z_i$	13.8	13.79	9.23
Estimation variance	0.93	2.54	0.59
$\overline{Z} = (1/n)\, \Sigma_i z_i$	11.5	11.5	11.5
Estimation variance	2.38	5.83	3.18
X co-ordinate [miles]	39.3	26.5	53.6
Y co-ordinate [miles]	17.1	8	24.5

The estimates obtained using kriging are substantially different from the mean estimate and amongst themselves. This fits in with the observed spatial variability. At all three locations the estimation variance for the kriged estimate is lower than that of the average estimate. This indicates that the kriged estimate is more accurate than the arithmetic mean estimate (ASCE, 1990a).

3.6 Summary

Geostatistics provides a useful tool to represent the spatial dependence of a regionalised variable. Once an assumption about the stationarity of the variable has been made, the semivariogram is used to model the spatial continuity of the variable being studied. If the semivariogram can be modelled, then it can be used for spatial prediction to estimate values at unmeasured locations. The most common models used for the semivariogram are the spherical, exponential and Gaussian models. These, or any linear combination thereof with positive coefficients, ensure that the semivariogram is positive definite so that it can be used for spatial interpolation. The sampling plan used for a spatial investigation of a variable can be optimised to an optimality criterion. In most random sampling regimes, the use of a regular sampling pattern on a grid will make the modelling of the semivariogram computationally easier. An equilateral sampling grid allows the semivariogram to be modelled in three main directions. In this way the omni-directional and directional semivariograms can be determined with more data pairs at each lag compared with a rectangular or hexagonal sampling patterns. The theory in this Chapter forms the basis of the methodology used to evaluate the spatial distribution of applied irrigation water and soil properties. This methodology is discussed in the next Chapter.

4 METHODOLOGY

The sites that were evaluated as well as the methodology followed at each site will be discussed in this Chapter. This Chapter contains a description of each of the sites where an evaluation took place, the data that was acquired and the how these data were analysed. The different methodologies for the spatial evaluations and for the standard evaluations are described.

4.1 Site Description

The sites that were evaluated in this study can be separated into two categories. These were the sites where a spatial analysis was conducted and the sites where a standard uniformity evaluation took place. These two types of sites were chosen to investigate the usefulness of the information derived from the different types of evaluations.

4.1.1 Spatial sites

There were two sites that were used to analyse the spatial distribution of water under a centre pivot irrigation system. One was situated in Mpumalanga (named the Major site) and one was situated in the Kwazulu Natal Midlands (named the Turner site). The location of these two sites is indicated in Table 4.1. The make and characteristics of the centre pivots are detailed in Table 4.2.

Table 4.1 Site locations of the centre pivots evaluated.

Site Name	Location	Co-ordinates	Height above MSL [m]
Major	Witbank, Mpumalanga	25°59'04" S 29°14'24" E	1559
Turner	Fort Nottingham, Kwazulu Natal	25°26'16" S 29°53'48" E	1472

Table 4.2 Centre pivot description.

Site name	Manufacturer	Number of towers	Radius [m]	Nozzle type
Major	Agrico	6	320	Wobbler
Turner	Valley	5 + overhang	320	Wobbler

The delivery rate of the Major centre pivot was designed to vary along the length of the centre pivot radius. This was so that water could be applied to an experimental field with three different target depths. These were: greater than field capacity, at field capacity and deficit irrigation. These correspond to an application rate of 12 mm/ 24 h, 10 mm/ 24 h and 8 mm/ 24 h for the first two, second two and last two spans respectively. However, it was found that the crop stress was far too great in the last span. Therefore, the application rate was increased to 10 mm/ 24 h before this study began.

The Turner centre pivot was designed to give a uniform application of water along the length of the centre pivot. However, the design application rate was not known, as the irrigator did not have the design details available. Maize and wheat are grown under the centre pivot at the Major site and rye grass is grown under the centre pivot at the Turner site. At the time of measurement, there were no crops under the Major centre pivot and short grass under the Turner centre pivot.

4.1.2 Standard uniformity evaluations

The sites that were evaluated using standard uniformity tests, which will be discussed later in this Chapter (Section 4.2.3), formed part of a project that was undertaken by the Agricultural Research Council- Institute for Agricultural Engineering (ARC-ILI) on behalf of the South African Sugar Association (SASA). The author participated in the collection and analysis of data within this project. These sites were situated in five major sugar cane growing areas in southern Mpumalanga and northern Kwazulu Natal. In each of these regions a sample of different irrigation systems were evaluated. The number and type of irrigation systems that were evaluated are shown in Table 4.3. A total of 38 irrigation systems were evaluated.

Table 4.3 Number and type of systems evaluated in each region.

Region	Type of system					
	Dragline	Semi-	Centre	Drip	Micro	Floppy
1	1	2	1	1	2	1
2	1	1	1	2		
3	3		2	1		1
4	5	1		3		
5	3	3	1	1		1
Total	13	7	5	8	2	3

All evaluations were conducted in sugar cane fields where the sugar cane was just emerging, or in the case of micro spray systems, in citrus orchards. The slope of the sites tested varied from flat flood plains to relatively steep slopes and undulating lands. The soils at these sites also varied from sandy soils to soils that were rocky with high clay content. An analysis of the affect of the soil on the performance of these irrigation systems was not considered, as it was not an objective of that study. The time and funding available for the evaluations precluded an in-depth investigation of the soils.

4.2 Data Acquisition at Each Site

The measurements that were conducted at each site will be described separately. The description of testing procedure will be separated into the Major centre pivot site, the Turner centre pivot site, and the standard uniformity evaluations.

4.2.1 Major centre pivot

The tests that were conducted at this site were as follows: a catch can uniformity analysis, tension infiltrometer measurements, and the monitoring of the soil moisture tension using tensiometers.

For the spatial distribution under a centre pivot, 150 catch cans were placed to measure the surface delivery at different points in the field. To measure the spatial distribution, a grid spacing based on an equilateral triangle with the side lengths approximately equal to 55 m was used. This sampling pattern was chosen to enable directional variograms to be determined in at least three main directions (Cressie, 1991). A total of 126 catch cans were used for this purpose. The remaining catch cans were placed at approximately 11 m intervals along one radius to simulate the standard centre pivot distribution test. The positions of the catch cans were determined using a Trimble® PRO XRS GPS system. The details of the GPS system are given in Appendix A. The positions were corrected using base station data obtained from the Telkom Pretoria base station. The position of the catch cans can be seen in Figure 4.1. A 500 ml oilcan that was supported on a steel rod was used as a catch can. The volume of water collected in the catch can was measured using a 50 ml measuring cylinder with 1 ml graduations. The depth was then calculated from this volume. The depth delivered was measured for two revolutions of the centre pivot.

Soil samples and tension infiltrometer measurements were taken to investigate the spatial variation in soil properties. Undisturbed soil samples were taken at the surface and at a depth of 500 mm using a core sampler. These samples were analysed for bulk density, porosity, final water holding capacity, and water retention characteristics at different matric heads. These samples were analysed by technicians in the School of Bioresources Engineering and Environmental Hydrology. The samples were taken at five points along two radii separated by 120 degrees. The position of each sampling location coincided with a catch can position. The location of these sampling positions is shown in Figure 4.2.

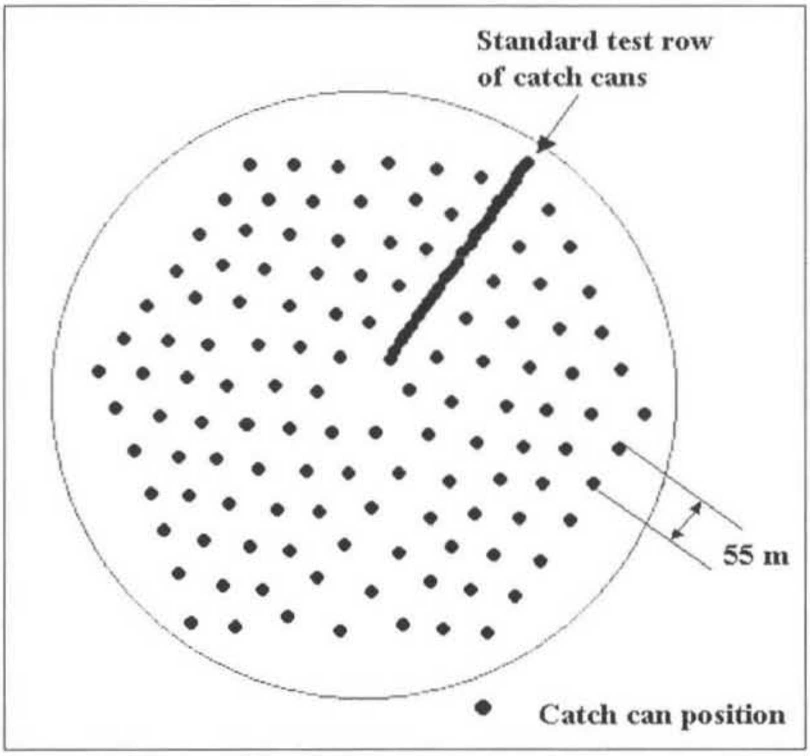

Figure 4.1 Sampling pattern for the Major centre pivot.

Tension infiltrometer readings were taken at 35 locations in the field. The locations of these measurement points are indicated in Figure 4.2. The rate of infiltration was measured at tensions of 5, 30, and 60 mm. A description of the tension infiltrometer used appears in Appendix B.

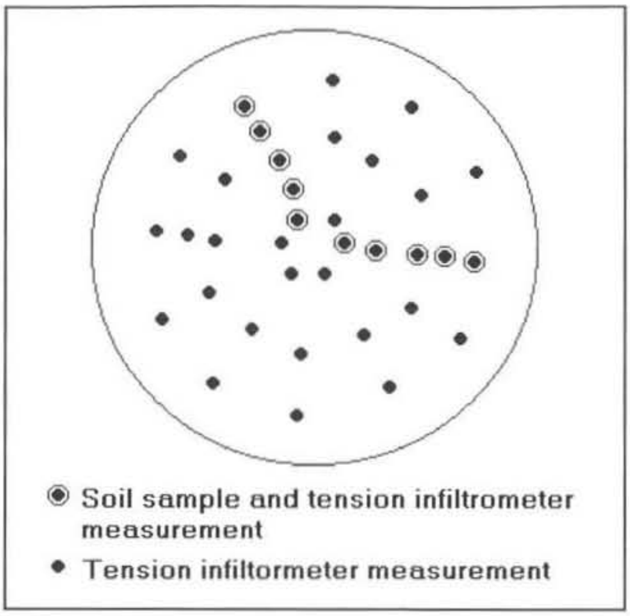

Figure 4.2 Soil sample and tension infiltrometer measurement location for the Major centre pivot.

Tensiometers were used to investigate the movement of water through the soil. The tensiometers, which are described in Appendix C, were installed in the ten locations where soil samples were taken (see Figure 4.2). The tensiometer nests consisted of three tensiometers placed at different depths. The three desired depths were 250 mm, 500 mm and 1000 mm. However, in some locations the maximum depth that could be bored to was less than 1000 mm due to hard layers in the soil. The depth to which the ten nests of tensiometers were installed is given in Table 4.4. The tensiometer nests remained in the field for a period of five days and were then removed.

Table 4.4 Depth of tensiometers below soil surface at each nest.

Nest	Tensiometer 1 [mm]	Tensiometer 2 [mm]	Tensiometer 3 [mm]
Major1	250	500	930
Major2	250	500	630
Major3	250	500	1000
Major4	250	500	1000
Major5	250	500	1000
Major6	250	500	530
Major7	250	500	355
Major8	250	500	855
Major9	250	500	1000
Major10	250	500	1000

4.2.2 Turner centre pivot

To evaluate the spatial distribution of applied water, the same equilateral grid of approximately 55 m spacing was used. At the Turner site a portion of the field under irrigation was occupied by grazing cattle. Therefore the catch cans that were supposed to be put in this segment of the field were randomly distributed in the area being evaluated. A total of 141 catch cans were placed in the accessible portion of the field. The sampling layout can be seen in Figure 4.3. The Trimble® GPS Pathfinder Pro XRS system was used to determine the position of the catch cans. The initial positions were post corrected using Telkom SA Kloof base station data.

To attempt to gauge the influence of the wind, a recording anemometer and wind vane was placed at the site. The instruments were installed 3 m above the ground within 30 m from the edge of the centre pivot field.

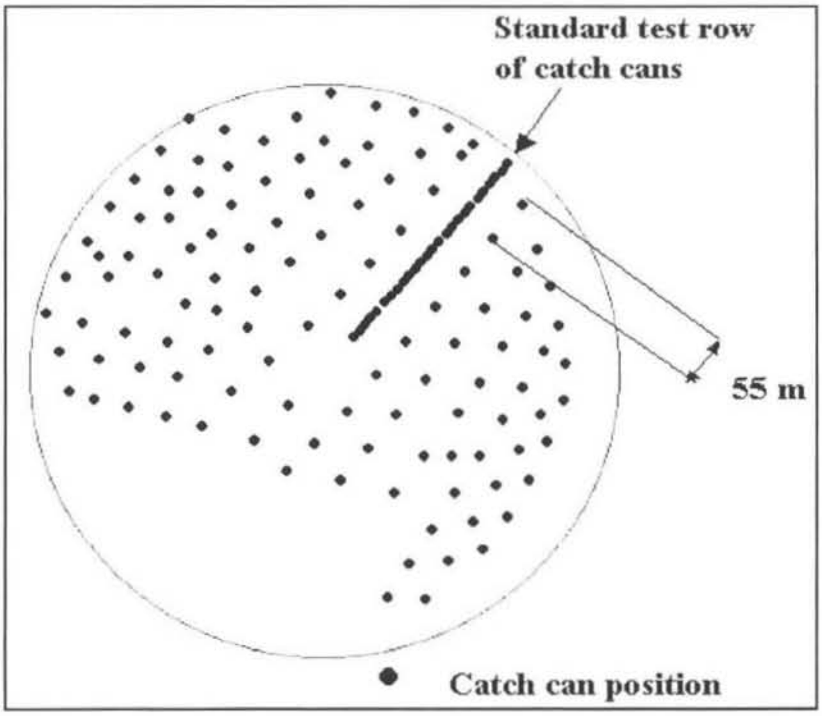

Figure 4.3 Sampling pattern for the Turner centre pivot.

4.2.3 Test procedures for the standard evaluations

For these tests, the uniformity of application, system pressure variation, water delivery, wind speed, and sprinkler spacing were measured. The evaluation method for determining the distribution of water under the various irrigation systems were based on the following American Society of Agricultural Engineers (ASAE) Standards:

- Centre Pivot – ASAE S436 (ASAE, 1993a).
- Micro irrigation systems – ASAE EP458 (ASAE, 1993b),
- Overhead sprinklers – ASAE S398.1 (ASAE, 1993c).

The number of catch cans placed in the test block depended on the system being tested and the spacing of the emitters. For dragline and semi-permanent systems 36 catch cans were placed between four sprinkler positions. A spacing of 3 m was used between catch cans. This configuration can be seen in Figure 4.4.

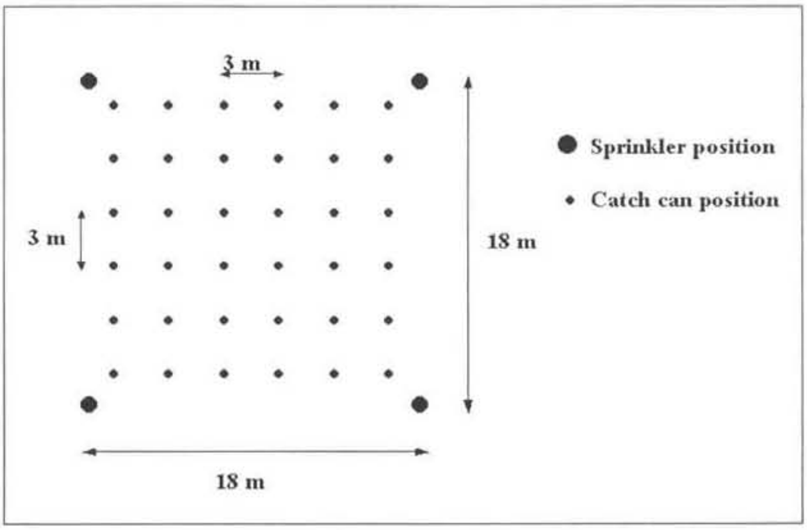

Figure 4.4 Sampling pattern for overhead sprinkler assuming an 18 m x 18 m spacing.

The sampling used for floppy sprinklers is shown in Figure 4.5. The typical spacing for these sprinklers is 15 m x 12 m. For these systems, 20 catch cans were used to determine the uniformity. For these tests a standard rain gauge was used as the collection device. The depth was recorded from the rain gauge.

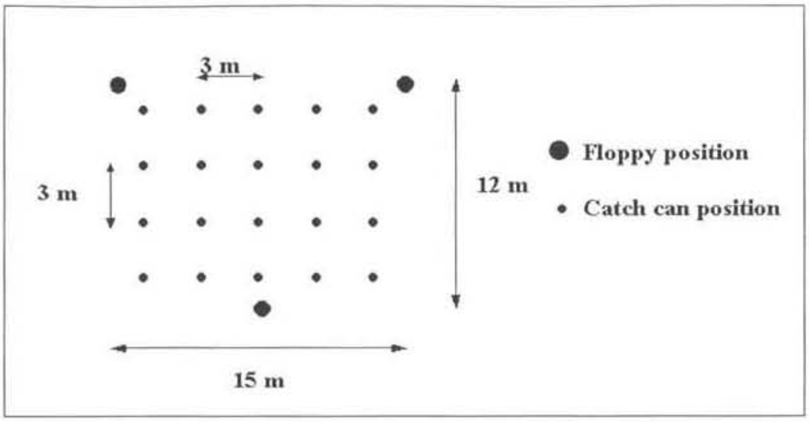

Figure 4.5 Sampling pattern for Floppy sprinkler assuming a 15m x 12 m spacing.

Figure 4.6 shows the sampling pattern for micro irrigation systems. The water delivery was measured at 25 points in a block. The lines in a block that were selected for the evaluation were the second line, the lines at a quarter, half and three quarter distances, and the second to last line of the block. On each line the delivery of five emitters were measured. These were situated at the start of the line, at a quarter, half and three quarter length and at the end of the line. The delivery of the emitters was measured using a container placed under the emitter and a graduated measuring cylinder with 1 mm graduations.

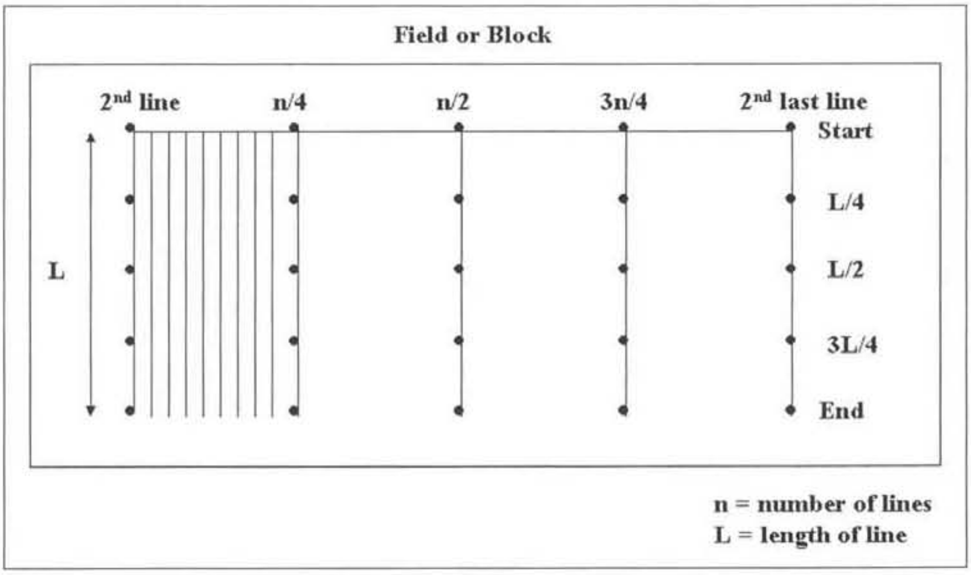

Figure 4.6 Sampling pattern for drip and micro spray irrigation blocks.

The length of the centre pivot and the number of catch cans available determined the spacing of the catch cans. Table 4.5 shows the number of catch cans used, the spacing of the catch cans, and the length of the centre pivot tested.

Table 4.5 Number of catch cans and catch can spacing for centre pivot evaluations.

Centre pivot number	Number of catch cans	Catch can spacing [m]	Centre pivot length [m]
1	74	5	373
2	71	5	393
3	63	5	355
4	75	7	574
5	72	5	363

The pressure variation in the overhead sprinkler irrigation fields was measured using a pressure gauge fitted with a pitot tube. The tube was placed in the vena contracta of the stream at a distance of 2 mm from the nozzle. The number of sprinklers that were measured depended on the number of sprinklers that were operating in the irrigation field being tested.

The flow rate and delivery of the sprinkler and Floppy irrigation nozzles were determined by measuring the time to fill a 21.1 l bucket using a stop watch. The spacing of the sprinkler and Floppy stand positions were measured using a 50 m measuring tape.

4.3 Data Analysis

The data analysis can be separated into two categories, namely spatial and standard uniformity evaluations. The spatial analysis uses the theory as detailed in Chapter 3. The standard uniformity evaluations use the equations contained in Chapter 2.

4.3.1 Spatial analysis

The location and depth data were processed using the *Trimble® Pathfinder Office 2.51* software. The positions were differentially corrected to remove the selective availability error using the utility contained in the software. The positions and data were exported into a dBase file for use in other programs. The data was screened for position or input errors. Depth data that were extreme outliers were discarded from the data set used in the analyses. This was done to remove depth data that were unrealistically high due to a catch can being placed directly below a drain plug or dribbling sprayer.

The data was analysed for uniformity using the Heermann-Hein coefficient of uniformity (CU_{HH}) (ASAE, 1993a) for centre pivots. Since the Major centre pivot had four application rates, the CU_{HH} was calculated for each zone as well as for the whole field. The coefficients of uniformity were calculated using all the spatial data and using just the standard line of data. This was done so that comparisons could be made between the spatial determination of uniformity and the standard techniques used to calculate uniformity. Statistics such as the mean, standard deviation and coefficient of variation were calculated for the data measured. The distribution of the data was compared to a normal distribution with the same mean and standard deviation of the measured data. This was done to determine how closely the normal distribution approximation for uniformity matched the calculated uniformity.

To analyse the spatial dependence of the data, the *GSTAT 2.1.0* software was used (Pebesma and Wesseling, 1998). The software is available as freeware under the GNU licence from the Department of Geography, Utrecht University, Netherlands. The *GSTAT* software has a suite of functions to characterise the spatial dependence, to fit a model to the sample variogram, and to perform kriging or inverse distance weighting interpolations. An example of the program main screen is shown in Figure 4.7.

Figure 4.7 *GSTAT* main screen.

The modelling of the spatial dependence of the data is done using the interactive main menu. The data for the variable being analysed is contained in a specially formatted data file. An example of the correct format is given in Appendix D. The user has the option of calculating the semivariogram or the covariogram. For two variables the cross variogram or the cross covariogram can be calculated. The user needs to set the maximum lag separation as well as the lag interval distance. Usually the maximum lag is chosen as half the maximum distance between two points. The lag interval is set at not less than the closest distance between two points. The lag interval is usually set to the spacing of a regular grid if it was used in the sampling. The cutoff distance and lag width where chosen such that the semivariogram produced was not too erratic and so that there were a sufficient number of pairs at each lag separation. The semivariogram was edited by removing pairs of data that had a large leverage on the semivariance at a particular lag interval. The method suggested by Isaaks and Srivastava (1989) was used. They further stated that the upper 10% of data pairs that have high leverage could be removed to improve an erratic semivariogram. The selection of the cutoff distance and the cutoff width will be discussed in Chapter 5 with the results.

A suitable experimental semivariogram was fitted to the sample semivariogram using weighted least squares (WLS) estimation. The weights chosen were the number of pairs at each lag. The shape of the sample semivariogram and the apparent behaviour at the origin was used to select the type of model to fit to the sample semivariogram. To ensure that the fitted model was positive definite, only the nugget, spherical, exponential, and Gaussian models were used. This was to ensure that no errors would occur in the kriging matrices. Initial values for the parameters were fitted visually to provide a starting point for the WLS estimation process. Once a suitable model had been fitted to the sample semivariogram, a jack knifing procedure was used to test the model. A single data point was omitted from the data set and estimated from the remaining data. This process was repeated for each data point and the measured and estimated values compared.

The spatial dependence was modelled for the application depth data and the tension infiltrometer data for the Major centre pivot. The spatial dependence of the application depth data was modelled for the Turner centre pivot. The elevation was also modelled so that contour maps could be interpolated for the fields instead of using inverse distance weighting. The spatial dependence of the position data of the standard tests was evaluated to see if any spatial structure could be seen over the distance between sprinklers.

The final step in the spatial analyses was to use the model fitted to the sample semivariogram to make predictions at unmeasured locations. Predictions were performed using ordinary kriging and conditional Gaussian simulation on a 10 m by 10 m grid, a 5 m by 5 m grid, and a

3 m by 3 m grid. The conditional simulations were performed for 25, 50, 100 and 200 simulations. The average and standard deviation of the simulated maps were calculated for each of the different number of simulations. This enabled the calculation of confidence intervals for each of the grid cells. The maps where represented graphically using *ESRI ARCVIEW 3.1* software.

4.3.2 Standard evaluation analyses

The analyses performed depended on the type of irrigation system being evaluated. The statistics calculated for overhead sprinkler systems were:

- mean application rate,
- coefficient of variation of the application rate (CV),
- mean system pressure at the nozzle,
- coefficient of variation of the system pressure ($CV_{pressure}$),
- coefficient of uniformity (CU),
- low-quarter distribution uniformity (DU_{lq}), and
- application efficiency.

For Floppy systems, the following were determined:

- mean application rate,
- coefficient of variation of the application rate (CV),
- coefficient of uniformity (CU),
- low-quarter distribution uniformity (DU_{lq}), and
- application efficiency.

For the centre pivot systems tested, the following statistics were calculated:

- mean application rate,
- coefficient of variation of the application rate (CV),
- Heermann-Hein coefficient of uniformity (CU_{HH}), and
- low-quarter distribution uniformity (DU_{lq}).

The statistics that were calculated for the micro irrigation systems were:

- mean delivery from the emitters,

- coefficient of variation of delivery,
- coefficient of uniformity (CU),
- low-quarter distribution uniformity (DU_{lq}),
- statistical uniformity (SU),
- emission uniformity (EU),
- mean block pressure, and
- coefficient of variation of pressure within a block.

The results obtained by applying the methodology of this Chapter will be detailed and discussed in the next Chapter.

5 RESULTS

The results of the analysis of the data obtained by following the methodology given in Chapter 4 will be discussed in this Chapter. The presentation of the results will be divided into four sections. The results from the two spatial sites as well as the spatial analysis of the standard evaluation sites will be presented first. The results from the soil properties measured at the Major centre pivot site will be discussed second. The analysis of the wind data recorded at the Turner centre pivot will be presented third. Finally the results of the performance of the irrigation systems evaluated using the standard evaluation techniques will be given.

5.1 Results of the Spatial Analyses of Depth Data

The results from the analysis of the spatial data measured will be discussed in this section. The spatial continuity of the data as well as the results from using ordinary kriging and conditional simulation will be given. The Major centre pivot site will be presented first, followed by the Turner centre pivot site and finally the standard evaluation sites.

5.1.1 Major centre pivot

The two data sets measured were named Major1 and Major2. The two data sets combined were called Major12. The depths at each location were added together to get a fourth data set called MajorSum. The mean, standard deviation, CV and uniformity criteria of the measured data are summarised in Table 5.1. The data were analysed using: all the data, just the standard row of catch cans, and by separating the data into the different application rate regions.

The standard row of catch cans exhibited a higher uniformity than all the spatial data. This could be due to the single row experiencing the same conditions at the same time. Since the centre pivot took 12 hours to complete a revolution, the conditions experienced by the spatially distributed catch cans were different. This could account for the difference between the uniformity calculated for the spatial data and the standard data. These uniformity results are misleading, as the centre pivot was not designed to give a uniform application along the centre pivot radius. For this reason, the data were analysed by separating the data into regions where the spans had the same design application rate.

Table 5.1 Performance criteria of the four data sets for the Major site.

Data Set	Mean	Std Dev	CV	CU_{HH}	DU_{lq}	DU_{norm}
	mm	mm		%		
Major1 Std	3.585	0.955	0.266	79.927	0.645	0.662
Major2 Std	4.348	1.303	0.300	80.446	0.644	0.619
Major1 All	3.613	1.170	0.324	73.224	0.609	0.589
Major2 All	3.905	1.288	0.330	75.830	0.648	0.581
Major12 Std	3.974	1.198	0.301	76.183	0.651	0.617
Major12 All	3.759	1.237	0.329	76.156	0.627	0.582
MajorSum	7.545	2.164	0.287	79.872	0.682	0.636
Major1 All						
Span 1&2	4.812	1.502	0.312	72.937	0.625	0.604
Span 3&4	3.775	0.891	0.236	80.624	0.723	0.700
Span 5	3.005	0.911	0.303	73.667	0.610	0.615
Span 6	2.984	0.910	0.305	75.253	0.616	0.613
Major2 All						
Span 1&2	5.909	1.463	0.248	79.988	0.698	0.685
Span 3&4	4.772	1.489	0.312	78.087	0.689	0.604
Span 5	3.671	0.956	0.260	79.655	0.715	0.669
Span 6	3.928	1.007	0.256	79.056	0.669	0.674
Major12 All						
Span 1&2	5.036	1.308	0.260	77.329	0.679	0.670
Span 3&4	3.951	1.116	0.283	78.940	0.701	0.641
Span 5	3.089	0.870	0.282	75.767	0.660	0.642
Span 6	3.197	0.903	0.282	75.813	0.613	0.641
MajorSum						
Span 1&2	10.196	2.452	0.241	81.617	0.734	0.695
Span 3&4	7.870	1.732	0.220	84.469	0.759	0.720
Span 5	6.182	1.374	0.222	82.003	0.755	0.718
Span 6	6.339	1.258	0.198	84.429	0.765	0.748

The uniformity calculated for each region was generally higher than the uniformity calculated for all the data. The exceptions were Span 1&2 for the Major1 data set, and Span 5 and Span 6 for the Major12 data set. The DU_{lq} calculated for each region is low with a maximum of 0.715 in Span 5 of the Major2 data set. The low uniformity is confirmed by the high coefficient of variation in each region. The average application in each region was higher, by almost 1 mm, for the Major2 data set than for the Major1 data set. The regions: Span 1&2, Span 3&4, Span 5, and Span 6, were designed to apply 6, 5, 4, and 5 mm respectively. Table

5.1 shows that the average recorded in each of the regions for the Major1 and Major2 data sets follows this trend. The difference between the design application and the average recorded on the ground could be used as an estimate of the losses between the nozzle and the ground. Since the delivery of the nozzle was not directly measured, this difference can only serve as a rough estimate of the losses.

The uniformity in each region was better for the MajorSum data set. The DU_{lq} was higher by around 0.1 and the CU_{HH} was higher by up to 9%. Therefore, it seems that the greater the depth of application, the higher the uniformity will be. The DU_{norm} approximation of DU_{lq} is within a few percent of the calculated DU_{lq}. The average depth applied during the evaluations was low because the centre pivot was run at a speed setting of 100% in order to obtain as much data in the time available. The uniformity determined may have been greater if the centre pivot had been run at a lower speed setting to deliver a greater application depth.

The spatial dependence of data for the four data sets is shown in Figure 5.1 to Figure 5.4. A cutoff distance of 300 m was used to model the semivariogram. This is approximately half the diameter of the centre pivot and half the maximum distance between measured points. The lag interval was determined through trial and error and was fixed at 15 m for the Major1 and Major2 data sets. The lag interval for the Major12 data set was 30 m and the lag interval for the MajorSum data set was 25 m. The choice of these lag intervals produced semivariograms that were not too erratic and that had sufficient data pairs at each lag. The hollow circular (O) data points in Figure 5.1 to Figure 5.4 are the semivariograms produced by the data as measured. The solid circular data points are the semivariogram produced when some pairs of data that had high leverage on the semi-variance were removed. At each of the lags fewer than 4% of the data pairs were removed. The resulting semivariogram is less erratic than the unedited one. The models fitted to the edited depth data sample semivariogram in Figure 5.1 to Figure 5.3 were spherical models (Equation 5.1) with nugget, range and sill values as shown in Table 5.2.

The model fitted to the sum of depth data in Figure 5.4 was a Gaussian model (Equation 5.2) with a nugget value of 2.44 mm^2, a range of 123.4 m and a sill value of 4.62 mm^2. These two models can be described mathematically by the following equations:

$$\text{Depths: } \gamma\ (h) = \begin{cases} \text{Nug} + \text{sill}\left(\dfrac{3h}{2 \cdot \text{range}} - \dfrac{1}{2}\left(\dfrac{h}{\text{range}}\right)^3\right), \text{ for } 0 < h \le \text{range} \\ \text{Nug} + \text{sill, for } h > \text{range} \end{cases} \quad (5.1)$$

$$\text{SumDepths: } \gamma\ (h) = 2.44 + 2.18\left(1 - \exp\left(-\left(\dfrac{h}{123.4}\right)^2\right)\right), \text{ for } h > 0 \quad (5.2)$$

Table 5.2 Nugget, sill and range values for the Spherical model fitted to the sample semivariogram.

Data set	R^2 [%]	Nugget [mm^2]	Sill [mm^2]	Range [m]
Major1	97.6	0.46	0.91	200
Major2	96.2	0.55	1.1	200
Major12	98.4	0.51	1.06	200

The R^2 value, indicating how well the model chosen fitted the sample semivariogram, is also shown in Table 5.2. A Gaussian model approaches its sill asymptotically and has an effective range $\sqrt{3}$ times the range shown in the model, i.e. 213.7 m. The model fitted to the sum of depths data had an R^2 value of 97.5%. The high R^2 values indicate that the models chosen show a good fit. The nugget values from Table 5.2 are a third of the sill semivariances. The nugget value of the MajorSum semivariogram is 52.8% of the sill semivariance. This shows that at short distances the variation is high. However, since there are insufficient data at small lags (less than 15m for example), a better estimate of the nugget could not be determined. The Gaussian model fitted to the MajorSum data increases less rapidly near the origin than a spherical model indicating that the MajorSum data have less variance at close distances. In Figure 5.4 the Gaussian model increases slowly over the first 50 m and then increases more rapidly.

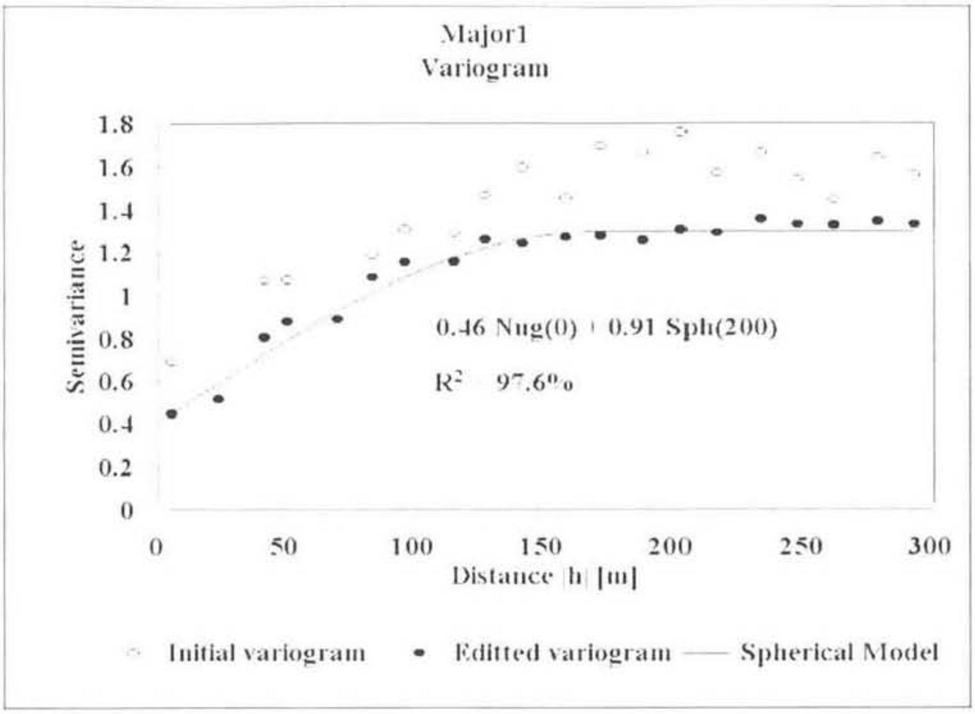

Figure 5.1 Semivariogram for the Major1 depth data with experimental variogram fitted to the sample semivariogram.

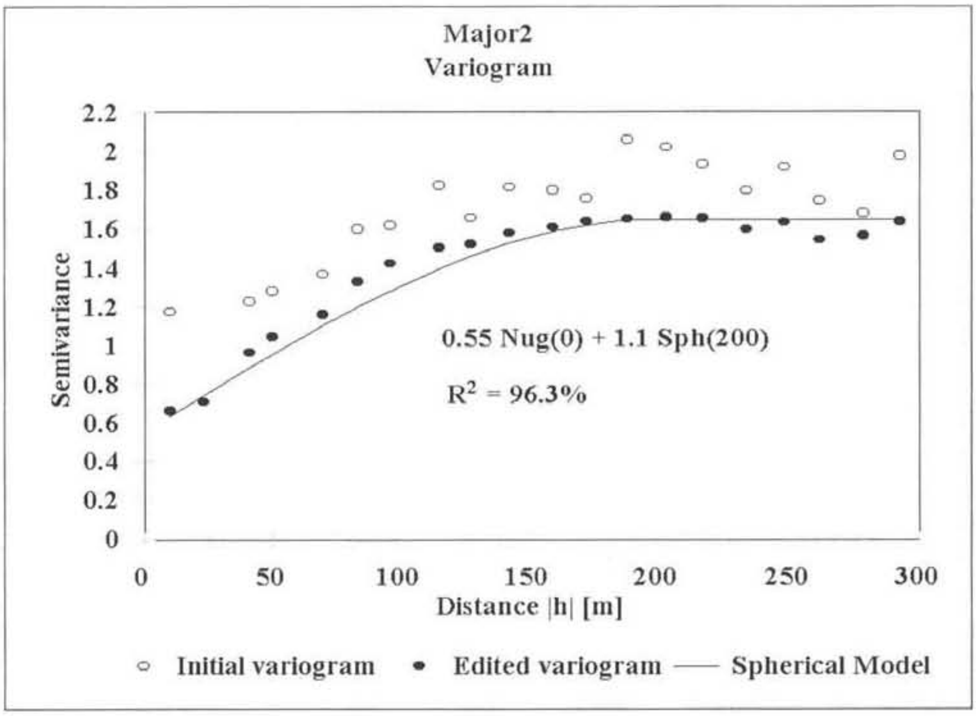

Figure 5.2 Semivariogram for the Major2 depth data with experimental variogram fitted to the sample semivariogram.

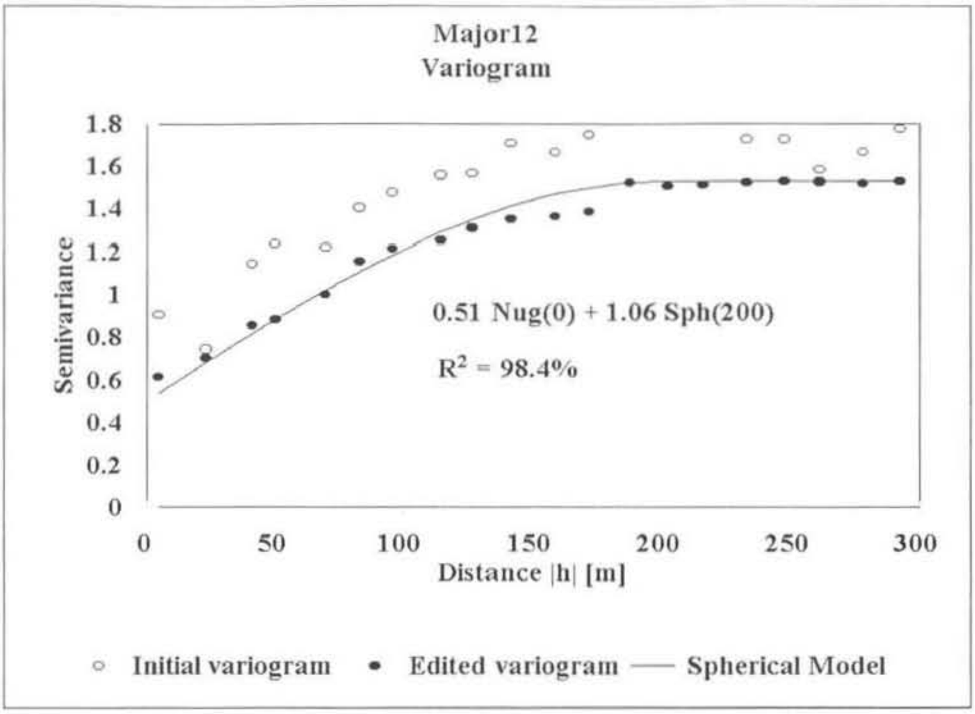

Figure 5.3 Semivariogram for the Major12 depth data with experimental variogram fitted to the sample semivariogram.

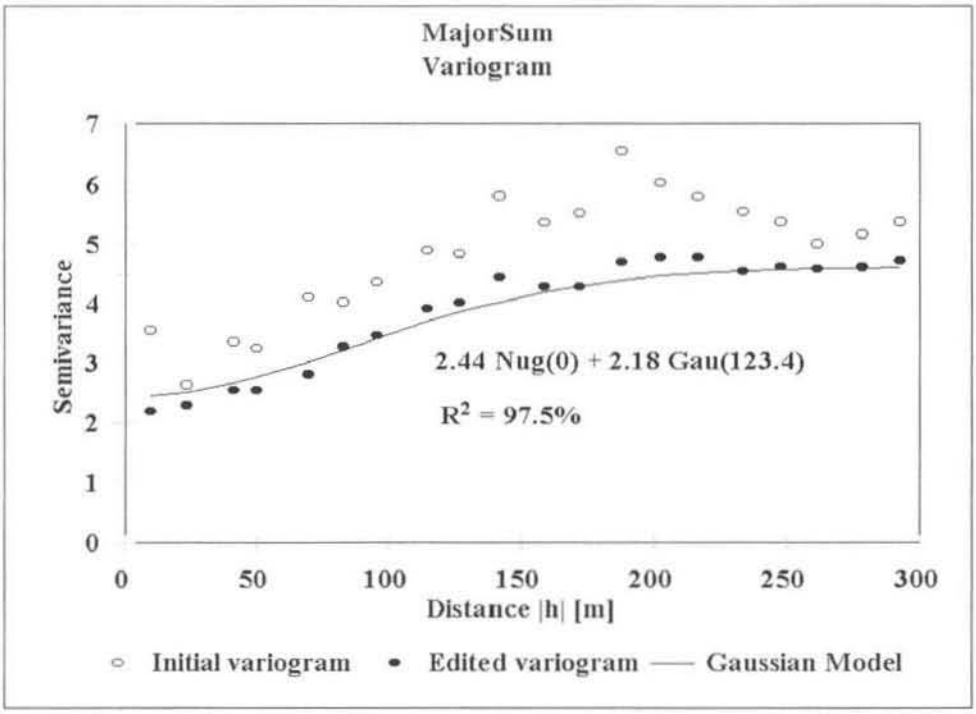

Figure 5.4 Semivariogram for the MajorSum depth data with experimental variogram fitted to the sample semivariogram.

The models that were fitted to the sample semivariograms were used for making ordinary kriging predictions and conditional simulations at unmeasured locations. The maps produced by performing ordinary kriging for the four data sets are shown in Figure 5.5 and Figure 5.6. The maps produced using inverse distance square interpolation are shown in Figure 5.7. The maps produced by ordinary kriging (Figure 5.5 and Figure 5.6) are smoother than the maps produced by inverse distance square interpolation (Figure 5.7). All four data sets show similar areas of high and low depths of irrigation. There is a visible difference between the Major1 and Major 2 maps. The map for the Major2 data set shows additional areas of higher application depths. The Major1 map shows larger areas of low irrigation depths. The estimation variance maps show that this variance is lower nearer measured points and increases with distance. The maps shown in Figure 5.6 for the Major12 and MajorSum data sets exhibit the same pattern, with the MajorSum map being smoother than the Major12 map. An example of a map produced from the average of 200 conditional simulations for the Major12 data set is shown in Figure 5.8. The maps produced using condition simulation for the other data sets, for the different number of simulations, are given in Appendix E. The map in Figure 5.8 closely resembles the ordinary kriging map for the Major12 data set in Figure 5.6. The variance calculated from the simulated maps could be used to determine confidence intervals for the average depth predicted.

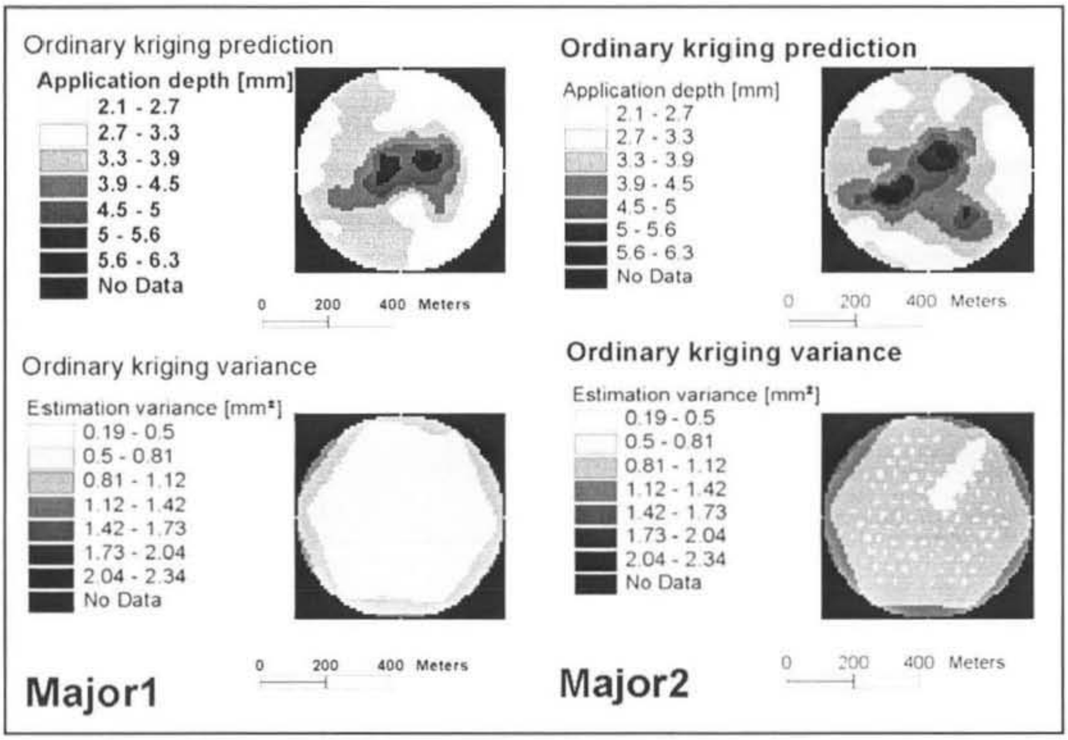

Figure 5.5 Map of depth and estimation variance produced from ordinary kriging on a 10 m grid for the Major1 data set and the Major2 data set.

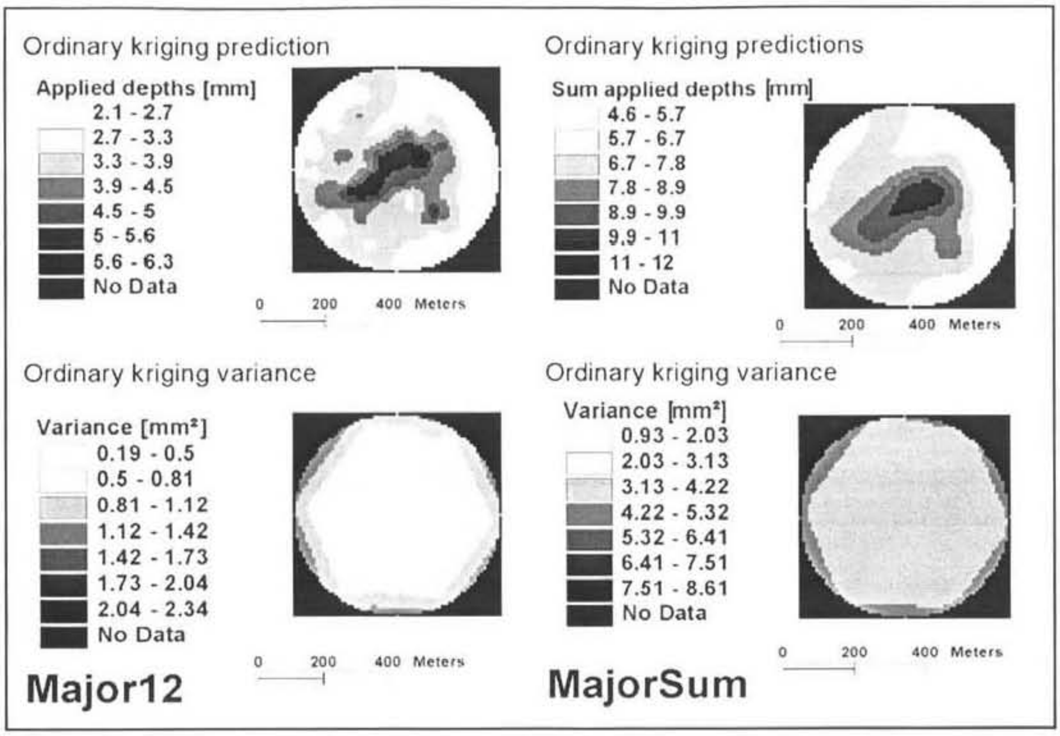

Figure 5.6 Map of depth and estimation variance produced from ordinary kriging on a 10 m grid for the Major12 data set and the MajorSum data set.

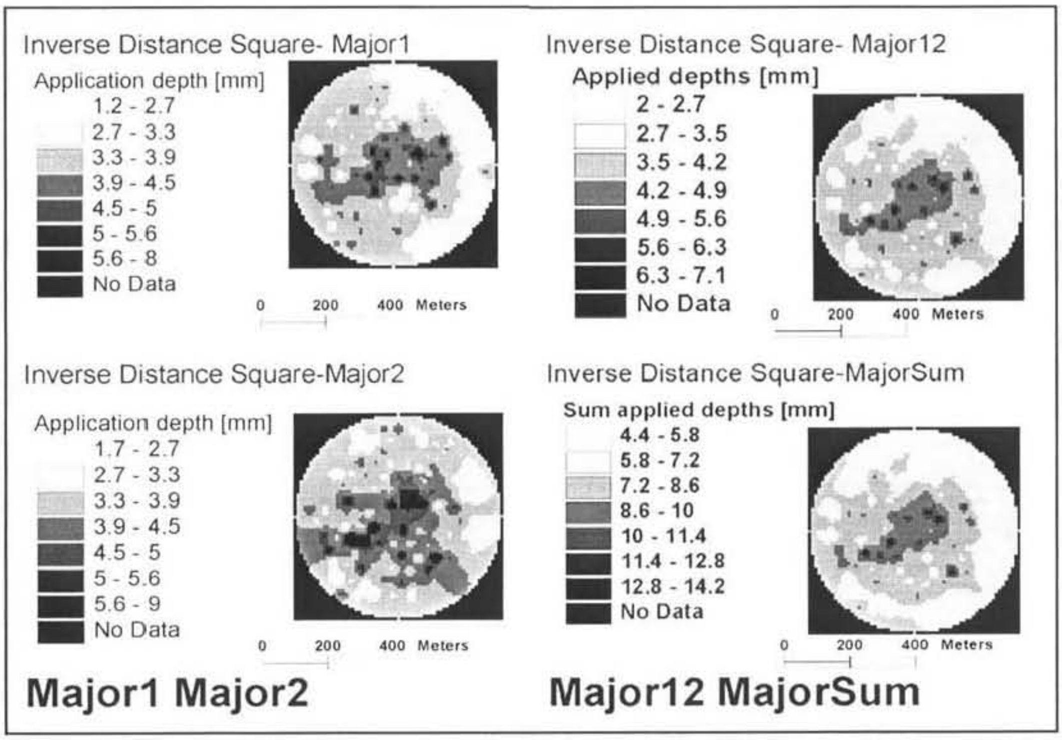

Figure 5.7 Map of depth of application produced from inverse distance square interpolation on a 10 m grid for the Major1, Major2, Major12 and MajorSum data sets.

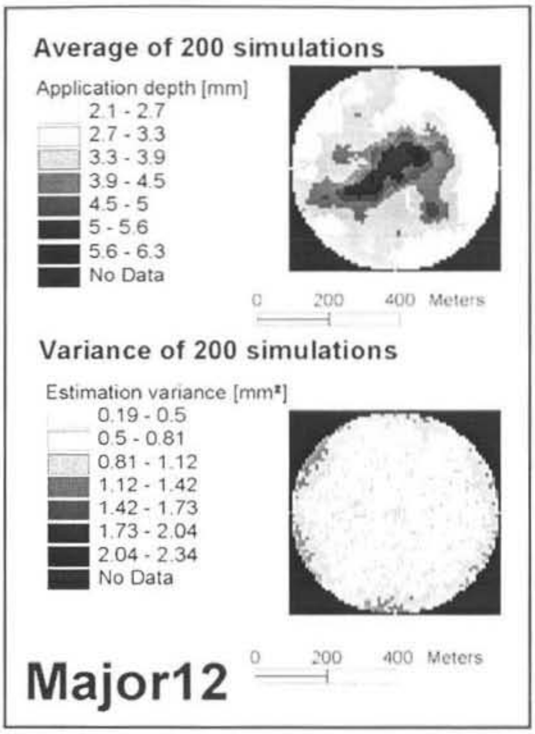

Figure 5.8 Map of depth and variance produced from the average and variance of 200 conditional simulations on a 10 m grid for the Major12 data set.

The results of uniformity determined for the predicted maps are shown in Table 5.3. The uniformity parameters calculated from the maps produced from ordinary kriging and the average of the condition simulation are greater than the measured data. This is due to the smoothing effect of the kriging techniques. The CU_{HH} and DU_{lq} were noticeably greater for the maps than for the measured data.

Table 5.3 Average, CV, CU_{HH}, and DU_{lq} calculated from maps produced (Figures 5.5 to 5.8).

Map (Figure)	Parameter			
	Average [mm]	CV [%]	CU_{HH} [%]	DU_{lq} [%]
Major1 (5.5)	3.507	19.8	86.1	77.2
Major2 (5.5)	3.734	18.3	87.8	80.1
Major12 (5.6)	3.604	19.1	87.8	79.7
MajorSum (5.6)	7.263	16.5	90.2	82.8
Average of 200 simulations Major12 (5.8)	3.632	18.7	88.3	80.4
Major1 IDW (5.7)	3.588	16.0	89.1	81.4
Major2 IDW (5.7)	3.853	15.7	90.4	83.4
Major12 IDW (5.7)	3.720	14.1	91.3	84.8
MajorSum IDW (5.7)	7.461	14.2	91.3	84.8
1 realisation from Major12 simulation (-)	3.608	30.7	76.0	62.8

The uniformity parameters of the inverse distance square interpolation were slightly greater than those from ordinary kriging and the average of the conditional simulations. The average, CV, CU_{HH}, and DU_{lq} of a single simulated realisation of the Major12 data set from Table 5.3, were very similar to that of the measured data from Table 5.1. This illustrates the preservation of variance characteristic of the conditional simulation technique.

5.1.2 Turner centre pivot

A single set of data was collected from the Turner centre pivot. A total of 141 catch can depths were recorded. No data were removed from the data set, as there were no apparent outliers in the data. The statistical summary of the data from the standard line of catch cans and from the all the spatial data is shown in Table 5.4. The weighted averages were similar, differing by 0.08mm. The DU_{lq} and the CU_{HH} were higher for the standard row of catch cans than for all the catch cans measured. This could be due to the same climatic conditions being experienced by the standard row of catch cans as compared to the variable conditions experienced by the spatially distributed catch cans.

Table 5.4 Summary statistics and uniformity of the Turner data set.

	Minimum	Maximum	Weighted average	Average	CV	DU_{lq}	CU_{HH}
	mm	mm	mm	mm	%	%	%
All data	4.0	13.4	7.16	7.09	18.8	79.0	87.2
Standard	5.7	13.4	7.24	7.46	18.5	85.3	91.9

The semivariogram produced is shown in Figure 5.9 and the spherical model fitted to the edited variogram is given by:

$$\text{Depth}: \gamma = \begin{cases} 0.24 + 0.98 \cdot \left(\dfrac{3\,h}{2 \cdot 118} - \dfrac{1}{2}\left(\dfrac{h}{118}\right)^3 \right), h \leq 118\,\text{m} \\ 1.22, h > 118\,\text{m} \end{cases}$$

A cutoff value of 300 m and a lag separation of 50 m were used to determine the semivariogram. The variogram produced from all the data was edited to remove the pairs that had high leverage on the semivariance. The maximum percentage of pairs removed was 6.9%. At most of the lags less than 4% were edited out. The variogram that was produced was less erratic at the smaller lag distances. The model fitted to the edited variogram using weighted least squares estimation had a good fit with a R^2 of 95.3%. This model was used for the spatial prediction and conditional simulation. The map produced using inverse distance square interpolation is shown in Figure 5.10. The predicted map is not circular, as in the case of the Major centre pivot, since the area that was occupied by the cattle was ignored. The maps produced using ordinary kriging on a 10 m and 2.5 m grid are shown in Figure 5.11. The two maps in Figure 5.11 show the same areas of high and low application depth. The summary statistics for the maps in Figure 5.11 are shown in Table 5.5 below. A t-test of the means of the two samples summarised in Table 5.4 showed that the two means were not significantly different. Since the 10 m map had fewer data points, it was used for conditional simulation to reduce processing time. The inverse distance square map and the maps produced using ordinary kriging have a similar pattern with the kriged map being smoother.

Table 5.5 Summary statistics of the maps produced on a 2.5 m and 10 m grid using ordinary kriging (Figure 5.11).

	Minimum	Maximum	Mean	Standard Deviation	CV	DU_{lq}	CU_{HH}
Grid	mm	mm	mm	mm	%	%	%
2.5 m	4.719	10.229	6.970	0.794	11.367	86.06	91.05
10 m	4.723	9.899	6.970	0.794	11.391	86.09	91.03

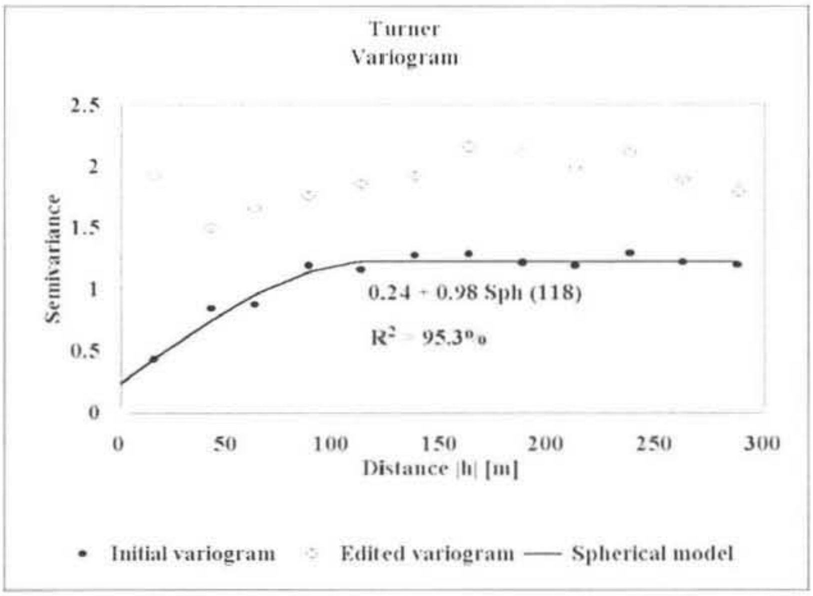

Figure 5.9 Semivariogram for the Turner depth data with experimental variogram fitted to the edited sample semivariogram.

The difference between the DU_{lq} of the all the measured data in Table 5.4 and the DU_{lq} of the 10 m grid map in Table 5.5 is 7.09%. This is to be expected since the averaging effect of ordinary kriging produces data that are more uniform. The average of the two sets of data differ by 0.12 mm and a t-test indicated that the means were not significantly different. This is to be expected, as ordinary kriging is an interpolator that preserves the mean. The estimation variance maps again show that the variance is lower closer to measured points and increases with distance from the point.

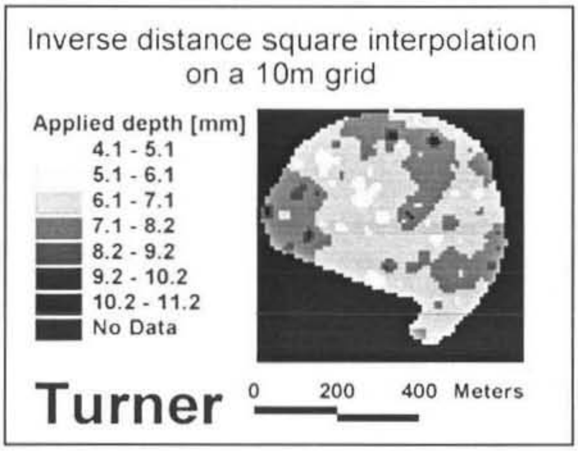

Figure 5.10 Map of applied depths calculated using inverse distance square interpolation for the Turner centre pivot.

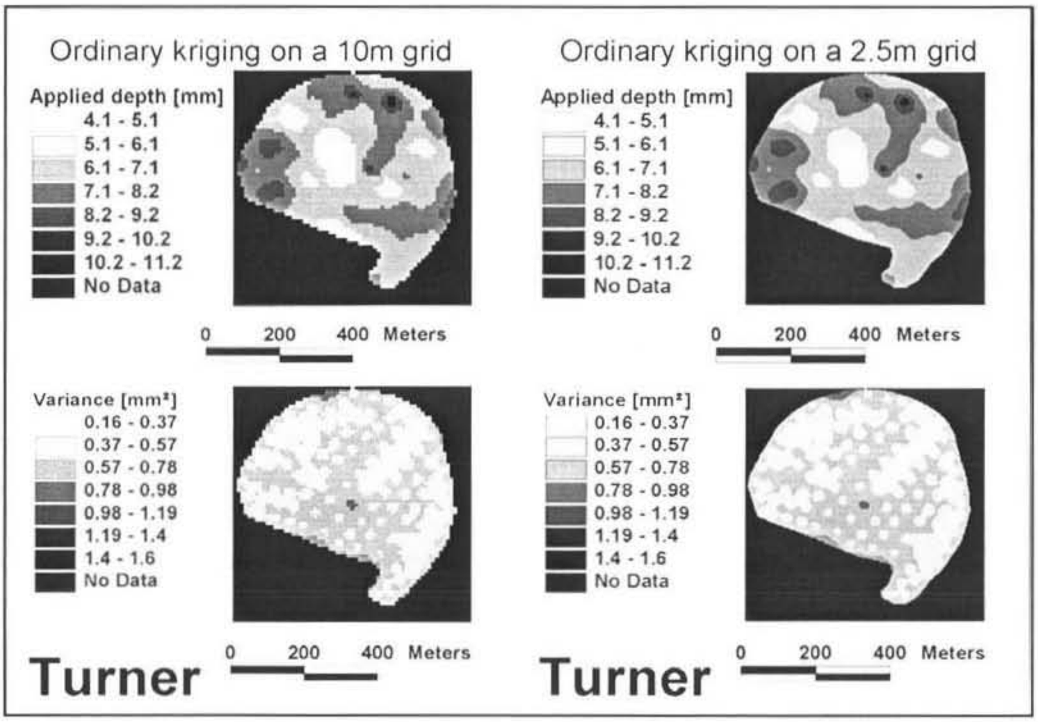

Figure 5.11 Map of depth and estimation variance produced from ordinary kriging on a 10 m grid and a 2.5 m for the Turner centre pivot.

Figure 5.12 and Figure 5.13 show the maps produced from the average of 200 and 100 conditional simulations and from the average of 50 and 25 conditional simulations, respectively. The variance map shows the cell variance of the data from each simulation. These variances could be used to determine confidence intervals for the cell average calculated. The maps produced from the average of the conditional simulations closely resemble the map produced using ordinary kriging. The summary statistics of the data from the average of the conditional simulations are shown in Table 5.6. These results and the results for the ordinary kriging on a 10 m grid in Table 5.5 are very similar. The mean, standard deviation, CV, DU_{lq}, weighted average, and CU_{HH} differ by very small amounts. The uniformity criteria are again higher than the measured data due to the average having been taken, which smoothes the data and decreases the non-uniformity.

Table 5.6 Summary statistics of the maps produced on a 10 m grid using the average of the conditional simulations performed (Figures 5.12 and 5.13).

	Number of simulations performed				
Statistic	1	25	50	100	200
Minimum [mm]	3.398	4.847	4.789	4.758	4.779
Mean [mm]	6.856	6.995	6.992	6.976	6.983
Maximum [mm]	10.542	9.927	10.113	9.941	10.019
Standard deviation [mm]	1.147	0.805	0.798	0.792	0.789
CV [%]	16.730	11.504	11.416	11.358	11.299
DU_{lq} [%]	79.280	85.974	85.994	86.133	86.281
Weighted average [mm]	7.001	7.123	7.116	7.102	7.105
CU_{HH} [%]	86.996	90.938	90.994	91.038	91.086

The statistics for the single conditional simulation in Table 5.6 are again similar to the statistics from all of the measured data. The DU_{lq}s are within 0.29% of each other and the CU_{HH}s are within 1.7% of each other. This confirms that the retention of variance property of conditional simulations. Since there is very little difference between the statistics of Table 5.6 for 25, 50, 100 and 200 simulations, the computation time can be reduced by performing fewer simulations. However, the greater the number of simulations, the better the average of the simulated maps resemble the ordinary kriging map.

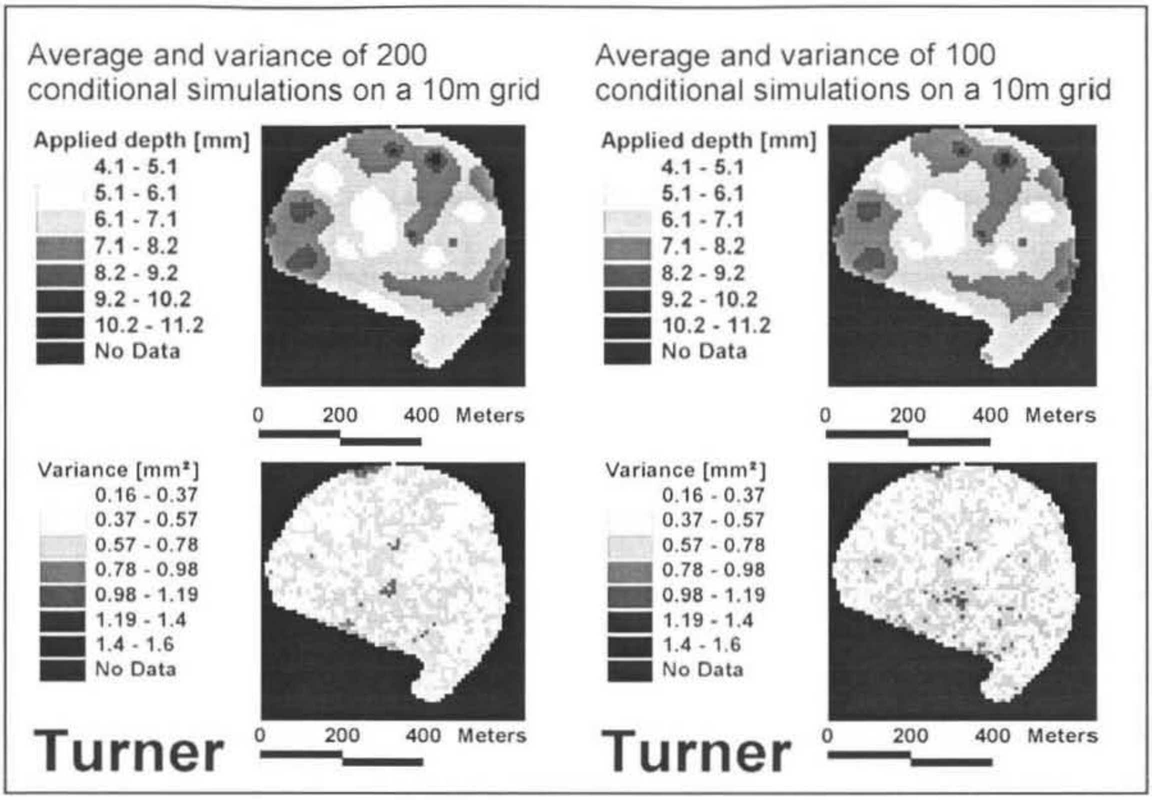

Figure 5.12 Maps produced using 200 and 100 conditional simulations for the Turner centre pivot.

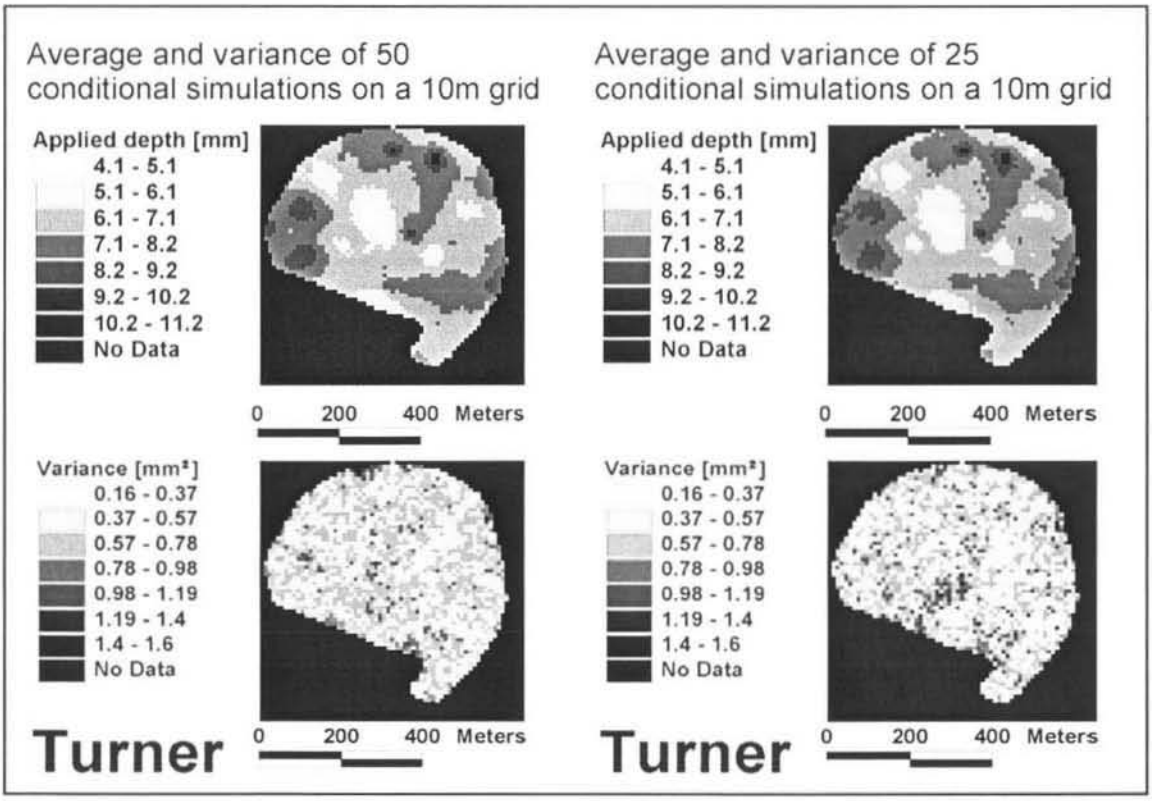

Figure 5.13 Maps produced using 50 and 25 conditional simulations for the Turner centre pivot.

5.1.3 Spatial analysis of data from Standard tests

The data collected from the standard tests were analysed for spatial continuity to determine spatial relationship of the applied depth of irrigation water. The spatial relationship was investigated for 28 of the 38 systems. The drip and micro spray systems were not analysed due to the lack of accurate position data. The centre pivot data was analysed using the distance from the centre as the location parameter. The data from the other systems were analysed using an x and a y coordinate. An example of the semivariogram produced for centre pivot system number 2 is shown in Figure 5.14. This shows the semivariance versus the separation distance along the radius of the pivot. The semivariogram shows a periodic behaviour in the semivariance, which makes it difficult to use an experimental model to represent the spatial variation. This shows that the semivariance of the depth delivered along the radius of the centre pivot has a periodic behaviour. This periodic pattern was not seen in the semivariograms for the Major or Turner centre pivots. This could be due to the higher number and the closer spacing of the data points measured for the standard evaluations. This higher resolution shows more detail in the semivariogram for the single row of data points. An example of a semivariogram produced for dragline system number 10 is shown in Figure 5.15. The shape of the semivariogram is similar to an inverse parabola. This indicates that the variation increases with distance as points get further apart and them decreases as points get even further apart. This could be attributed to the sprinkler pattern produced between four sprinklers with the depth applied nearer the sprinklers being similar. The semivariogram for floppy system number 29 and semi-permanent sprinkler system number 36 are shown in Figure 5.16 and Figure 5.17. These two semivariograms also exhibit the same pattern as the dragline system in Figure 5.15. The semivariograms for the other 24 systems are shown in Appendix F. The majority of the centre pivot systems showed a periodic pattern similar to Figure 5.14. Most of the dragline, floppy and semi-permanent sprinklers exhibited the semivariogram shape shown in Figure 5.15.

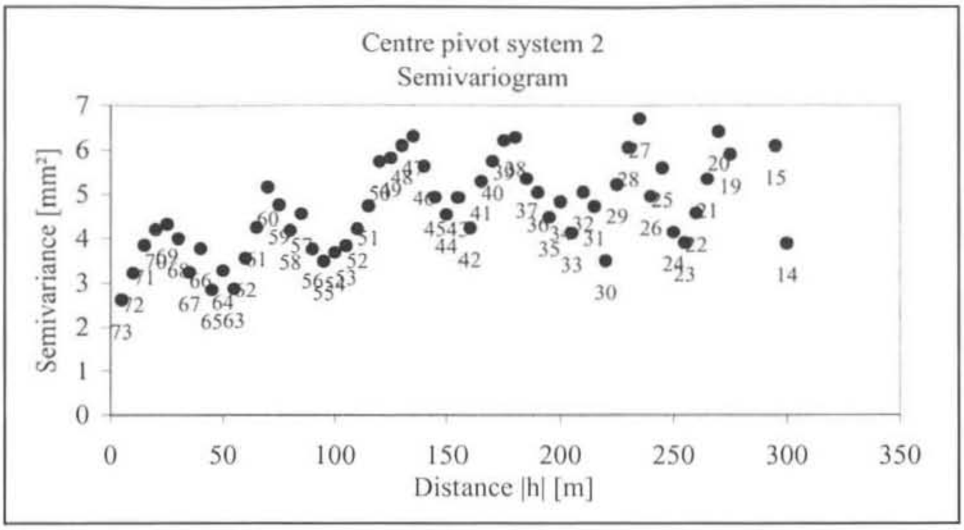

Figure 5.14 Semivariogram for centre pivot system 2.

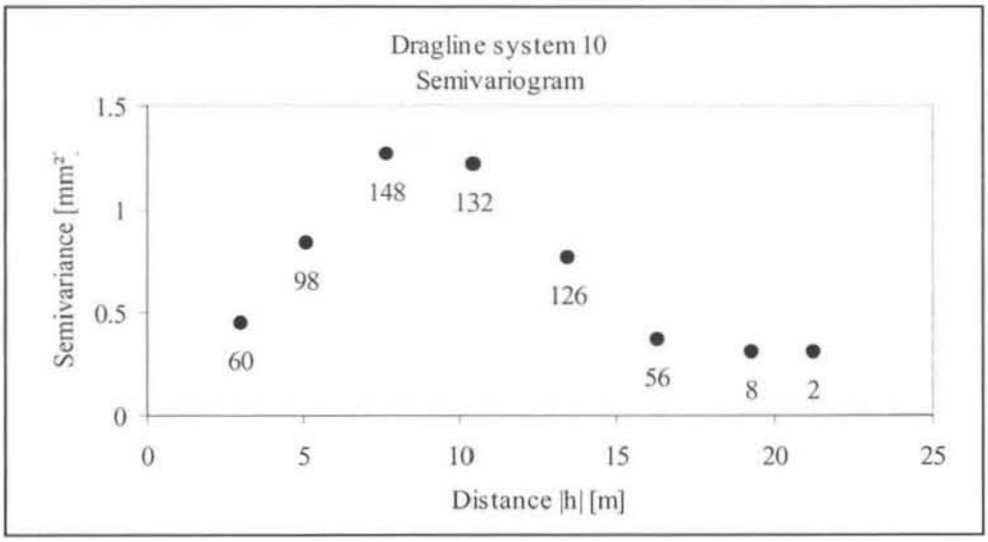

Figure 5.15 Semivariogram for dragline system 10.

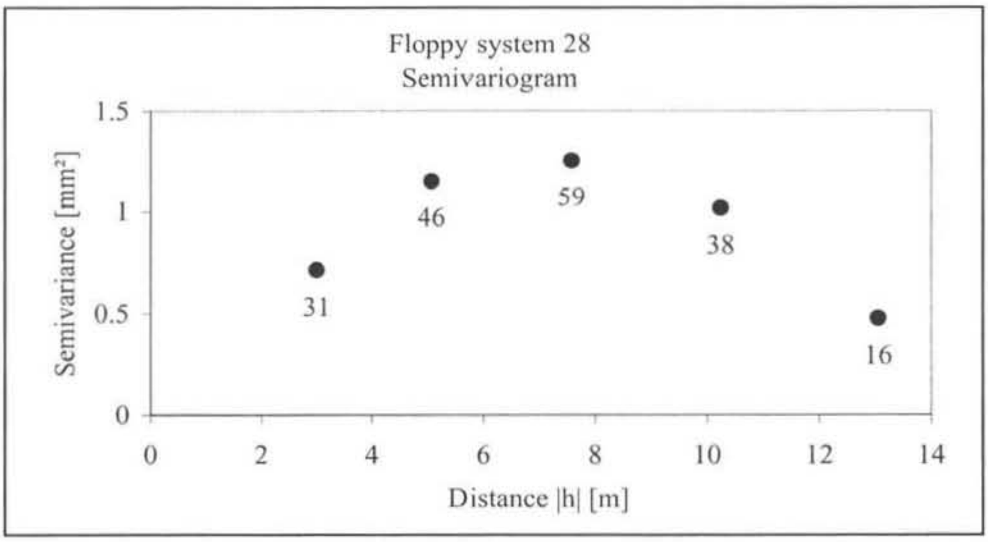

Figure 5.16 Semivariogram for floppy system 28.

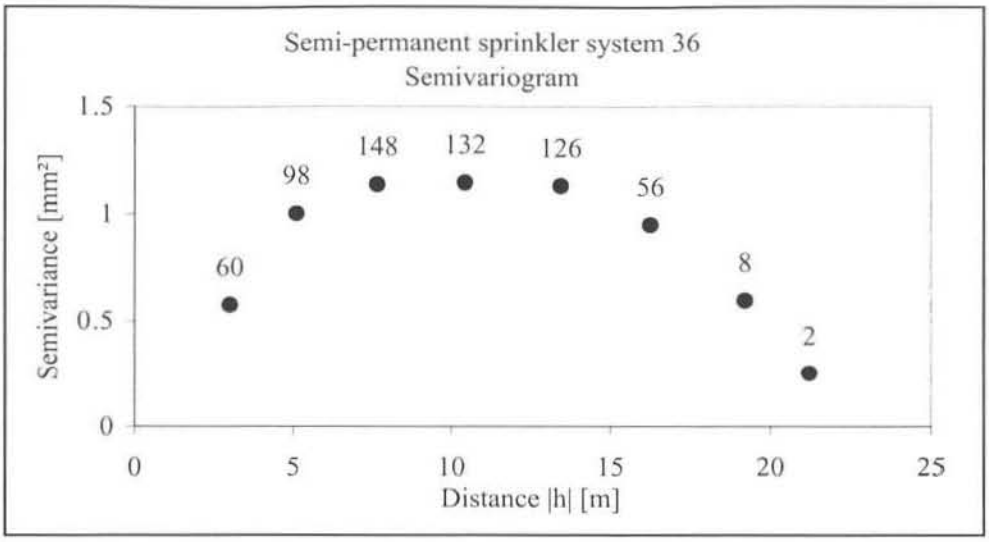

Figure 5.17 Semivariogram for semi-permanent sprinkler system 36.

5.2 Results of the Spatial Analysis of Soil Properties

The physical properties of soil can vary spatially within a field. Some of these properties were measured and the use of geostatistics to characterise this variability was investigated. The results of the soil properties and soil moisture measurements for the Major centre pivot will be discussed in this section. The tension infiltrometer results will be followed by the tensiometer results, and finally the soil property results will be presented.

5.2.1 Tension infiltrometer results

The tension infiltrometer data were used to calculate the final hydraulic conductivity of the soil surface. Table 5.7 shows the average, standard deviation and coefficient of variation of the hydraulic conductivity calculated for tensions of 5, 30 and 60 mm. The individual results for the 35 locations are shown in Appendix G. The high CV values show that there was a large variation in the values calculated for the hydraulic conductivity.

Table 5.7 Summary statistics of the hydraulic conductivity of soil determined at 35 locations at 5, 30 and 60 mm tensions using tension infiltrometer data.

	Tension		
	5 mm	30 mm	60 mm
Mean hydraulic conductivity [cm/s]	3.50E-04	2.54E-04	2.03E-04
Std Dev [cm/s]	1.29E-04	1.09E-04	1.00E-04
CV [%]	36.91	42.79	49.36

The hydraulic conductivities, at each of the three tensions, were analysed for spatial continuity using the semivariogram. The semivariogram for the 5, 30 and 60 mm tensions are shown in Figure 5.18, Figure 5.19 and Figure 5.20, respectively. The semivariograms did not exhibit a shape that could be modelled using an experimental model. A spatial structure was not apparent from the variograms calculated. This could be due to a shortage of sample locations on which to base the semivariogram. The erratic behaviour of the semivariogram could also be due to the variable nature of the hydraulic conductivity over short distances, which could not be characterised by the available data.

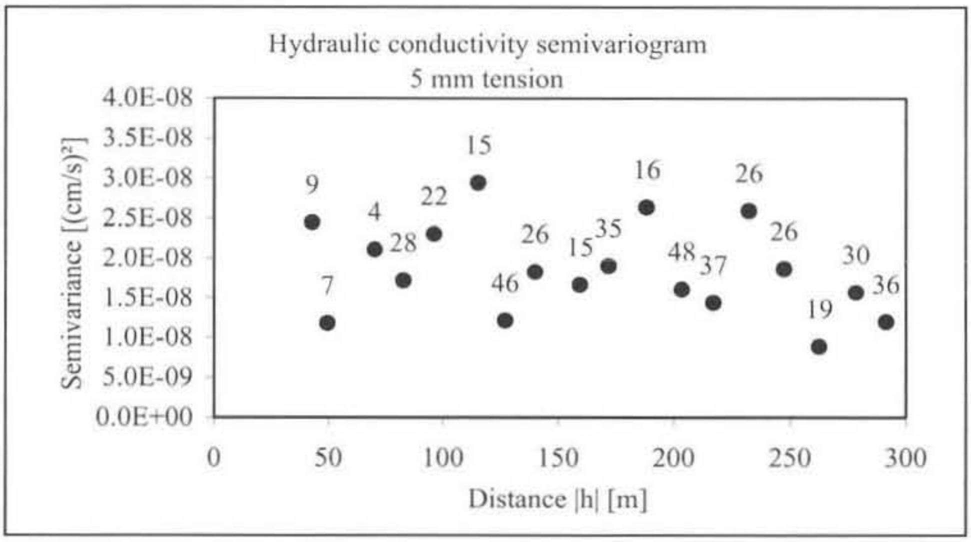

Figure 5.18 Semivariogram of hydraulic conductivity at a tension of 5 mm.

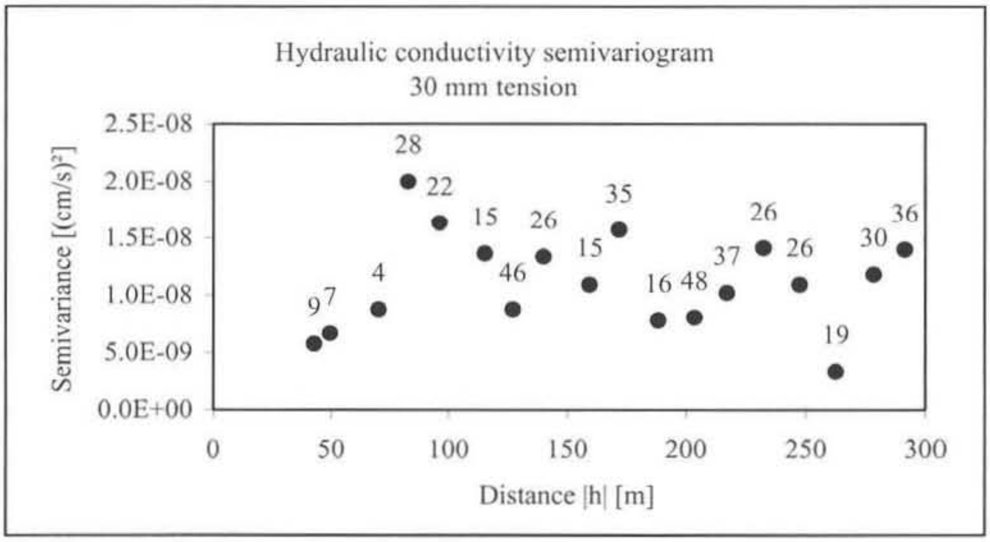

Figure 5.19 Semivariogram of hydraulic conductivity at a tension of 30 mm.

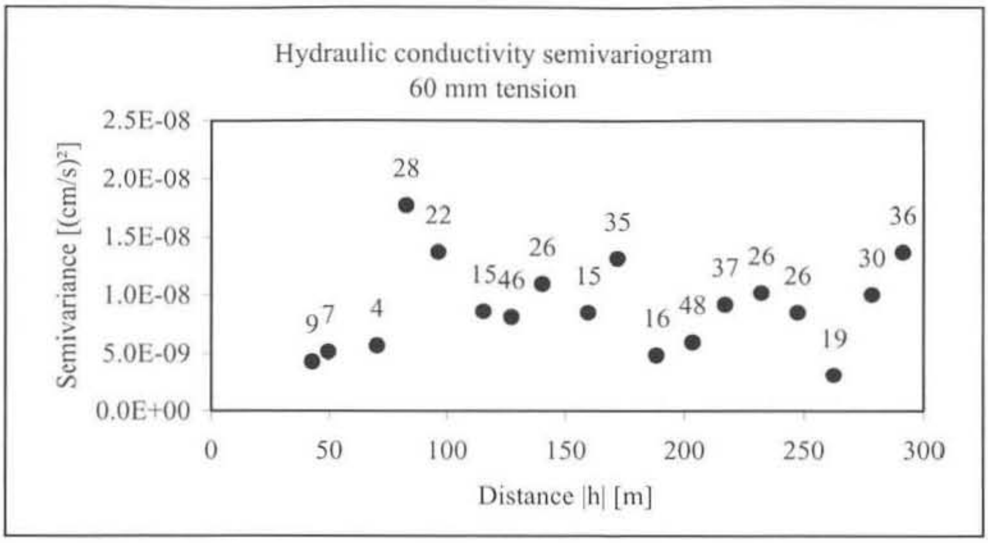

Figure 5.20 Semivariogram of hydraulic conductivity at a tension of 60 mm.

Due to the erratic behaviour of the semivariograms, no maps of hydraulic conductivity could be produced using ordinary kriging or conditional simulation. The poor behaviour of the semivariogram could be due to the lack of sufficient data points at different lag spacings.

5.2.2 Tensiometer results

The data received from most of the tensiometers did not show much activity at the various sites. Some activity was seen at a depth of 250 mm. The most probable causes for the inactivity were the low application depth and a poor interface between the tensiometer and the soil matrix. The most noticeable change was at site Major5, which was situated in the inner two spans with the highest application. The tensiometer data is presented in Figure 5.21 from the date logging started until the tensiometers were removed. The dramatic decrease in tension of the tensiometer at a depth of 1000 mm was possibly due to the intake of air into the hanging column of water in the tensiometer, as opposed to the wetting of the profile. Due to an electronics failure, the site Major6 showed no data. This site was also situated in the inner two spans. The tensiometers placed at a depth of 500 mm and 1000 mm did not show any activity other than small fluctuations caused by the electronics. An exception was the tensiometer at a depth of 1000 mm at site Major3 where the soil tension decreased two and a half days after the first irrigation event. This change in soil tension is shown in Figure 5.22. Another site that showed a discernable change in soil tension at a depth of 250 mm was at tensiometer site Major4, which is shown in Figure 5.23. Here the tension increases before the first irrigation event and then decreases after it. It decreases further after the second irrigation event. The line of tension at a depth of 1000 mm is an example of a tensiometer that showed no activity. The change in the line is caused by a toggling effect of the electronics, which is caused by the recording resolution of the pressure transducer. The soil tension graphs for the tensiometer sites; Major1, Major2, Major7, Major8, Major9, and Major10 are given in Appendix G.

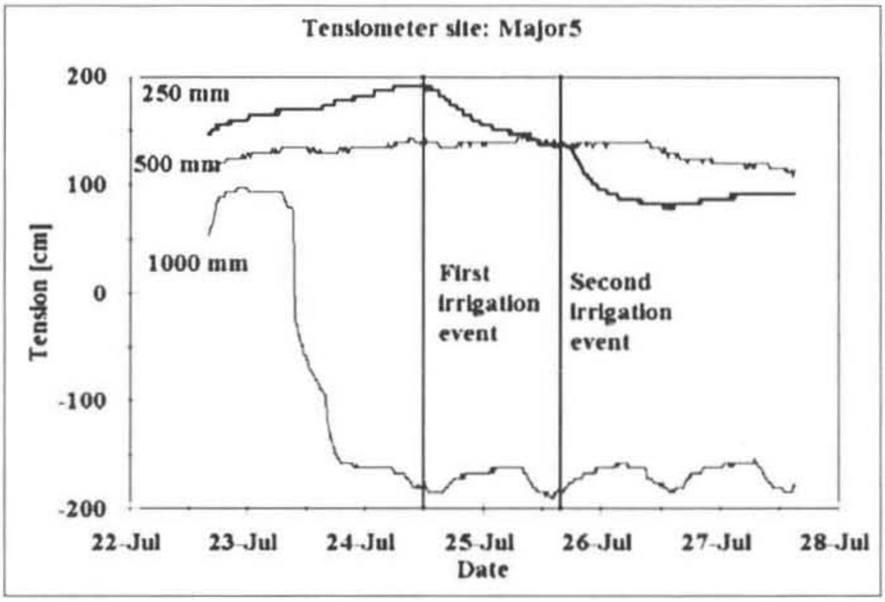

Figure 5.21 Soil tension at site Major5 at depths of 250, 500 and 1000 mm.

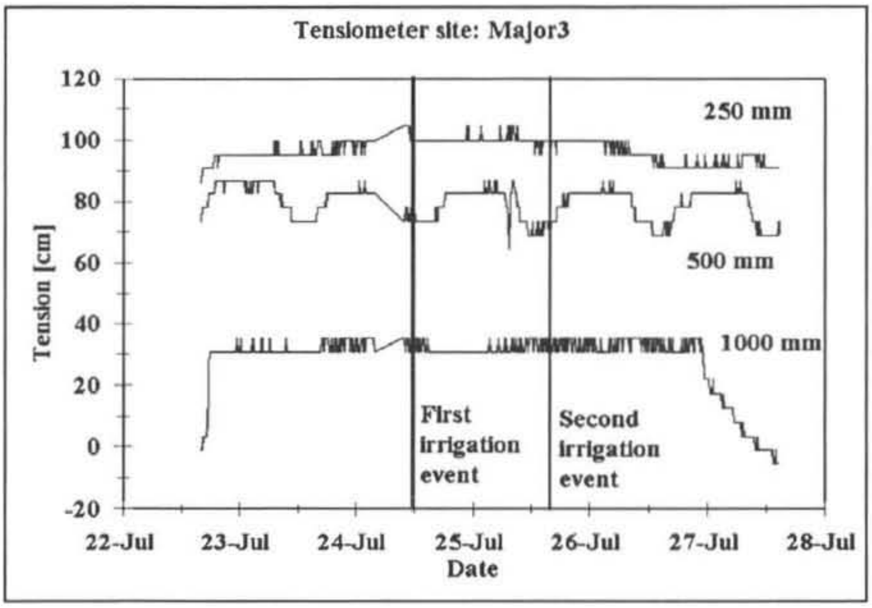

Figure 5.22 Soil tension at site Major3 at depths of 250, 500 and 1000 mm.

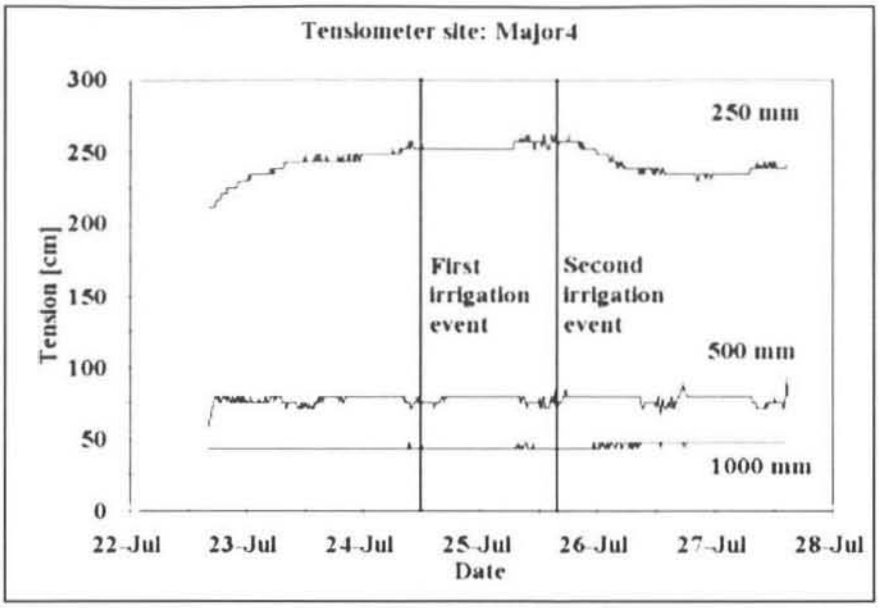

Figure 5.23 Soil tension at site Major4 at depths of 250, 500 and 1000 mm.

The results of the tensiometer data did not indicate that they would prove useful in short-term assessments of irrigation systems. This could be due to the small amount of irrigation water applied to the soil surface and for the short period that they were installed. Tensiometers may be more suited to analysing the seasonal variation in soil moisture tension and for irrigation scheduling purposes.

5.2.3 Soil physical properties

The results of the soil physical properties of the samples taken are shown in Table 5.8. The low CV values of bulk density (BD) and porosity (P) indicate that these properties of each sample were similar. However, the final water holding capacity (WHC) differed by a larger amount. The WHC ranged from 0.054 to 0.162 m/m. The average WHC of the soil samples taken at a depth of 500 mm below the surface was greater than that of the surface samples. The spatial continuity of the soil properties could not be determined from the few samples that were taken at each of the two depths. To characterise the spatial variability of the soil properties would require comprehensive sampling that may be too prohibitive from a cost and time point of view.

Table 5.8 Bulk density (BD), porosity (P) and final water holding capacity (WHC) of soil samples.

	Surface samples								
	Major 1	Major 2	Major 3	Major 4	Major 6	Major 8	Major 10	Average	CV [%]
BD [g/cm^3]	1.376	1.522	1.383	1.610	1.544	1.461	1.450	1.478	5.8
P	0.481	0.425	0.478	0.393	0.418	0.449	0.453	0.442	7.3
WHC [m/m]	0.054	0.147	0.048	0.081	0.121	0.074	0.108	0.090	40.1
	Samples at a depth of 500 mm								
	Major 1	Major 2	Major 3	Major 4	Major 8	Major 10		Average	CV [%]
BD [g/cm^3]	1.763	1.522	1.421	1.392	1.688	1.664		1.575	9.7
P	0.335	0.426	0.464	0.475	0.363	0.372		0.406	14.2
WHC [m/m]	0.162	0.121	0.087	0.067	0.103	0.143		0.114	31.0

5.3 Wind Data Results from the Turner Centre Pivot

The wind speed and wind direction measured during the evaluation period are shown in Figure 5.24 and Figure 5.25, respectively. The wind speed recorded was the average for a 10-minute period and the wind direction was an instantaneous reading every 10 minutes. The curve in Figure 5.25 is shown using a moving average with a period of 6, i.e. an average over the previous hour. The average wind speed was 2.38 m/s (8.57 km/h) and the average wind direction was 97.4°, with 0° being Magnetic North. The wind speed was less than 2 m/s for 47.2% of the duration of the test and the wind speed was less than 5 m/s for 93% of the duration of the test. The wind speed was not excessive for nearly the entire test. This is substantiated by the high value of the CU and DU_{lq} calculated from all the spatial data measured (see Table 5.3). However, there is a difference of 4.7% for CU and 6.3% for DU_{lq} between all the data and the standard line of catch cans. This could be evidence of the influence of changing wind speed and wind direction. However, other factors, such as the change in elevation or the change in travel speed of the centre pivot, could have also contributed to this difference.

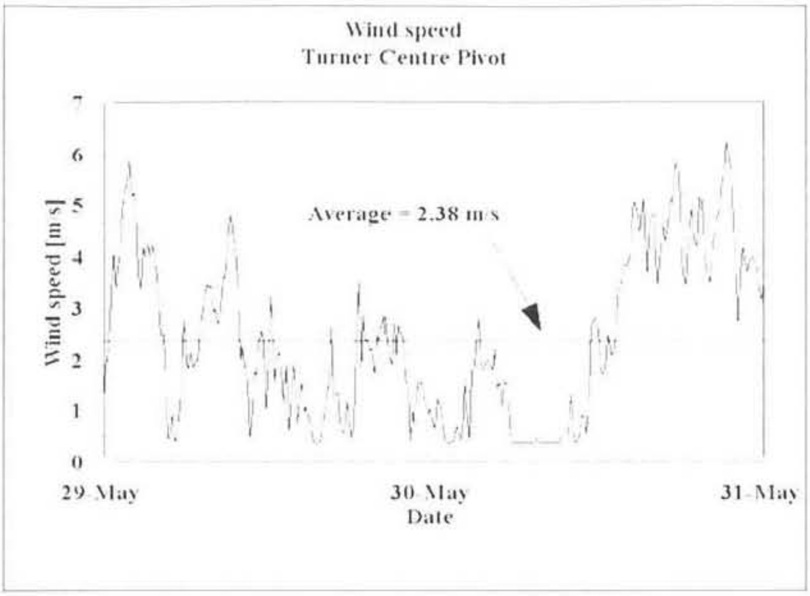

Figure 5.24 Wind speed during evaluation at the Turner centre pivot.

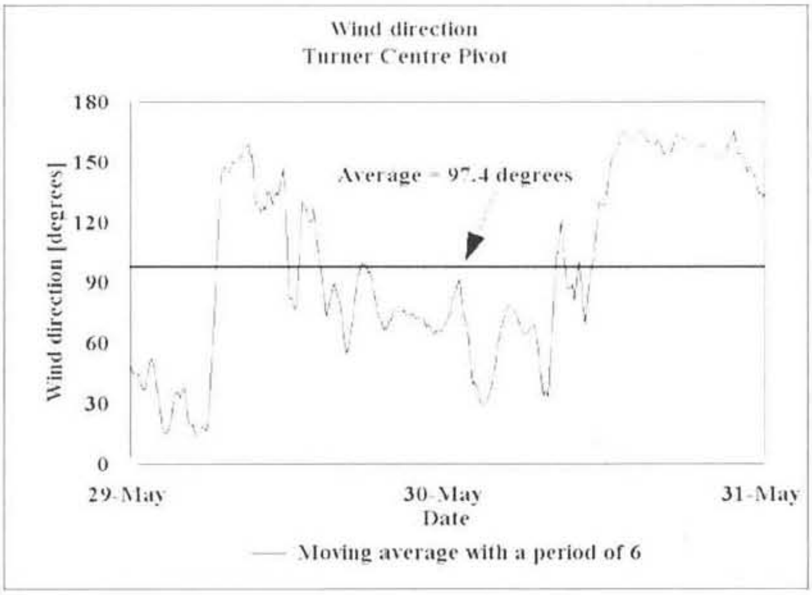

Figure 5.25 Wind direction recorded during Turner Centre pivot evaluation.

5.4 Distribution Uniformity and Application Efficiency Results from Standard Evaluations

The distribution uniformity and application efficiency results will be given in this section. The average wind speed, test pressure at the nozzle, and system pressure variation of the overhead sprinkler systems are shown in Figure 5.26, Figure 5.27, and Figure 5.28, respectively.

The average wind speed recorded during the test was less than 2 m/s for 60.7% of the systems and was less than 5 m/s for 92.9% of the systems tested. The distribution pattern of water in systems that experienced winds of 5 m/s or greater had an observable distortion. In some cases the upwind side of the sprinkler received little or no water at distances greater than 2 m from the sprinkler. In systems where the wind was less than 2 m/s there was little or no distortion of the wetting pattern. The systems that produced small droplets and/or misting showed the largest influence of wind and had more distortion in the distribution pattern.

The emitters in all the centre pivot and floppy systems were pressure compensated. Therefore, the pressures were only measured to ensure that there was sufficient pressure for the compensator to work. The system pressure in all the centre pivot and floppy systems was sufficient for the correct operation of the pressure compensators. The average pressure recorded in the majority of the test blocks were lower than the minimum operating pressure required. Overhead sprinkler systems perform at optimum if the operating pressure is between 60 and 70 times the nozzle diameter in mm (Reinders, 1986). Of the twenty dragline and semi-permanent sprinkler systems evaluated, 14 were operated at a pressure outside these optimal boundaries. The majority of the systems were being operated a pressure that was too low. The coefficient of variation of the system pressure for dragline and semi-permanent sprinkler systems ranged from 1.36% to 37.5%. Two-thirds of the systems had a pressure variation that was greater than the desired maximum of 10%.

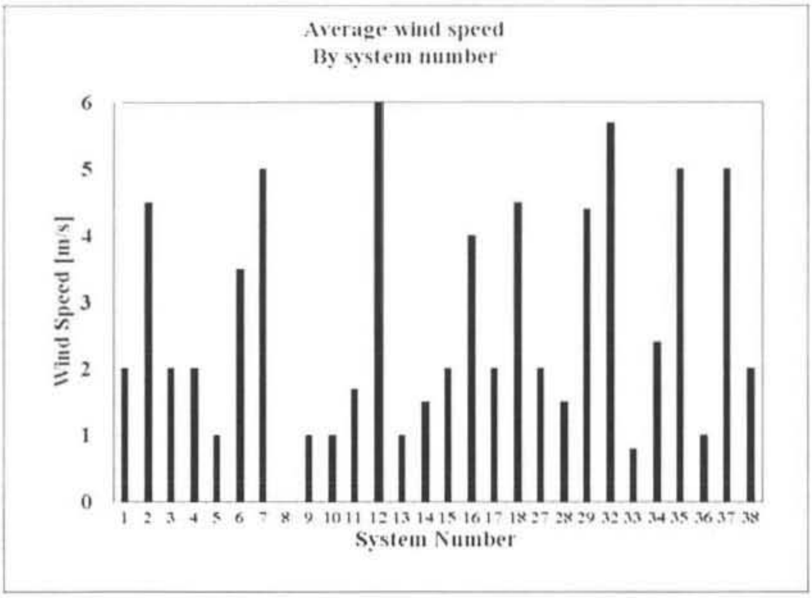

Figure 5.26 Average wind speed of overhead systems evaluated.

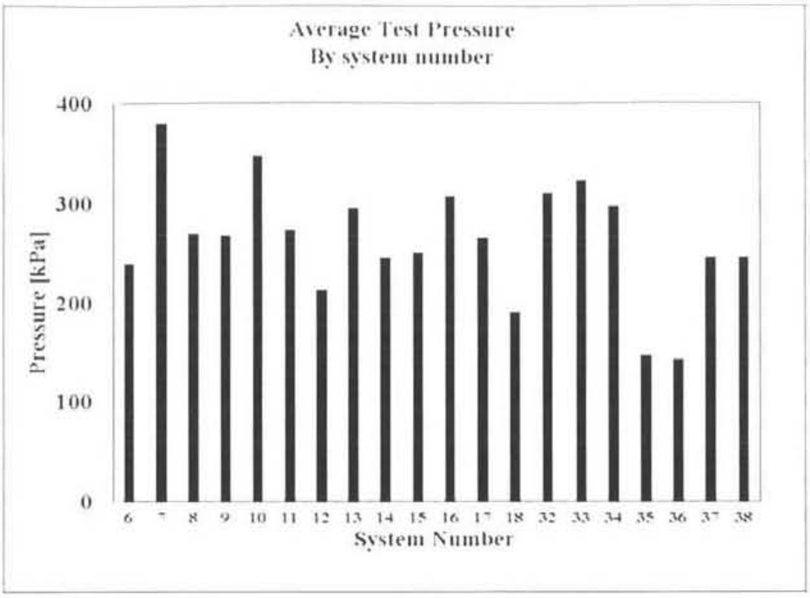

Figure 5.27 Average test pressure of dragline and semi-permanent sprinkler systems.

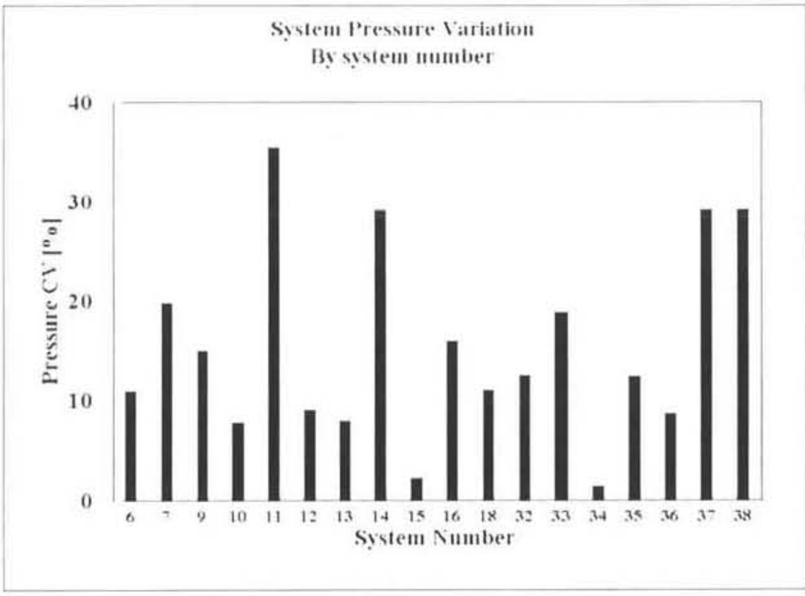

Figure 5.28 System pressure variation at the nozzle for dragline and semi-permanent sprinkler systems.

The average wind speed, coefficient of variation (CV) of the applied depths, the coefficient of uniformity (CU), the low-quarter distribution uniformity (DU_{lq}), the application efficiency (AE), and the emission uniformity (EU) for each system are given in Table H.1 in Appendix H. A summary of the uniformity parameters by irrigation type is given in Table 5.9.

Table 5.9 Summary of uniformity parameters by irrigation type.

	Irrigation system type				
Parameter	Centre Pivot	Dragline	Drip and Micro spray	Floppy	Semi-permanent sprinkler
Average CU [%] (EU [%])	88.0	74.0	81.6 (76.3)	74.5	70.8
Average DU_{lq} [%]	81.4	60.9	72.7	67.4	56.9
Minimum CU [%] (EU [%])	85.7	64.1	17.4 (25.4)	68.5	55.4
Maximum CU [%] (EU [%])	90.6	83.6	95.2 (92.5)	78.2	81.1
Minimum DU_{lq} [%]	77.5	45.9	0	62.9	70.7
Maximum DU_{lq} [%]	84.2	76.6	91.9	70.3	91.1
Standard DU_{lq} [%] (from Pitts *et al.*, 1996)	75	75	85	75	75
Percentage systems with excellent field condition DU_{lq} > Std DU_{lq}	100	15.4	30	0	14.3

The uniformity parameters: CU, DU_{lq} and EU, for centre pivot, dragline, drip and micro spray, floppy and semi-permanent sprinkler systems are shown in Figure 5.29 to Figure 5.33. Pitts *et al.* (1996) conducted a study of the distribution uniformity of 385 irrigation systems and suggested some acceptable standards for DU_{lq} based on best management practices. These standards are included in Table 5.9 for comparison with the calculated DU_{lq}s.

The CU and DU_{lq} of the five centre pivots were high. The average DU_{lq} was 81.4% and the minimum was 77.5%. These are both above the standard DU_{lq} suggested by Pitts *et al.* (1996) indicating that these systems were performing well and had an acceptable DU_{lq}. The uniformity of the dragline, floppy and semi-permanent sprinkler systems were generally poor. Only 15.4% of the dragline systems and 14.3% of the semi-permanent sprinkler systems had a DU_{lq} that was greater than the suggested standard. None of the floppy systems attained this standard. The DU_{lq} of the drip and micro spray systems varied from 0% to 91.9%. Thirty percent of these systems had a DU_{lq} that was above the standard of 85%.

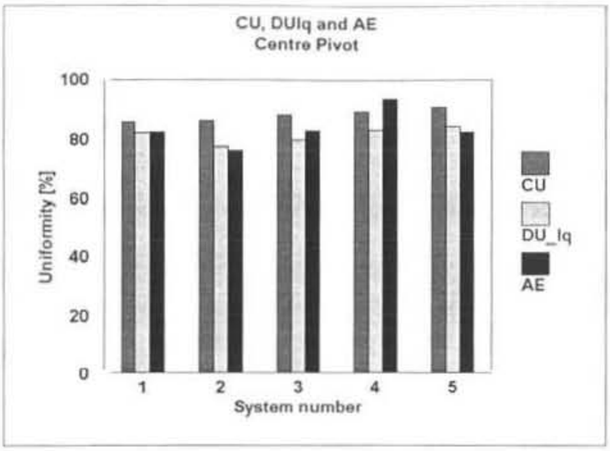

Figure 5.29 CU, DU_{lq} and AE of centre pivots.

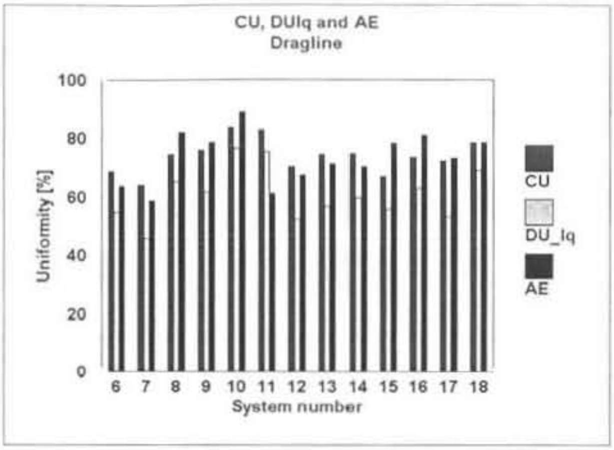

Figure 5.30 CU, DU_{lq} and AE of draglines.

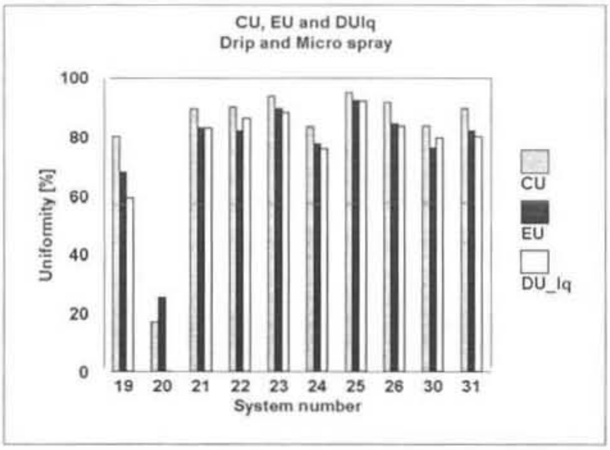

Figure 5.31 CU, EU and DU_{lq} of micro irrigation.

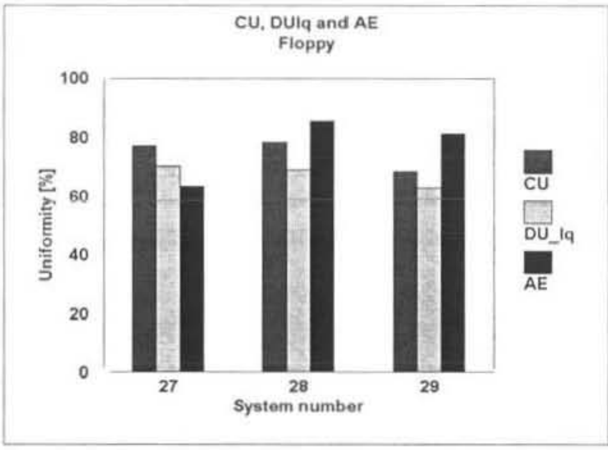

Figure 5.32 CU, DU_{lq} and AE of floppy systems.

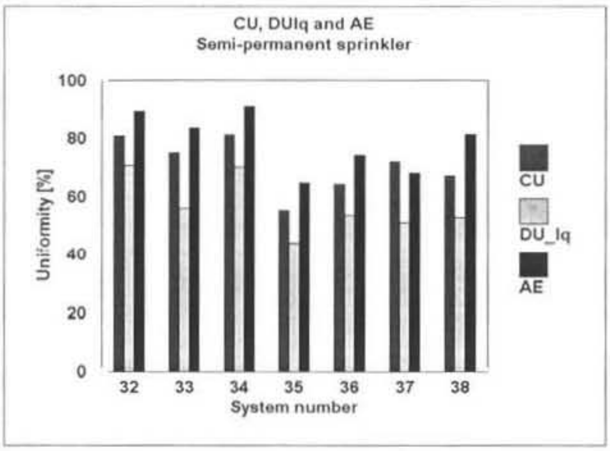

Figure 5.33 CU, DU_{lq} and AE of semi-permanent sprinklers.

The majority of the systems evaluated exhibited poor uniformity of application of irrigation water. The poor uniformities could possibly have been caused by the high wind conditions in some of the tests and the incorrect operating pressure of the overhead sprinkler systems. The drip systems that had poor uniformity was due to emitter clogging and severed lines. In one of the surface drip systems, cane rats had severed a large portion of the lines. The severed lines also contributed to a decrease in the line pressure. Incorrect spacing of sprinklers, malfunctioning sprinkler heads, incorrect hose lengths and diameters, and worn nozzles were observed in systems that had poor uniformity. Some systems were not being operated according to the design. In some systems, the distribution pattern of the sprinkler was being affected due to the operation of additional sprinklers, which decreased the system pressure. These factors, together with the wind and incorrect system pressure, were the probable causes of the poor application uniformity that was measured. It should be emphasised that the uniformity results reported were determined at a specific time and with the ambient climatic conditions at the time of the test. The application uniformity of the same irrigation system can be different with each evaluation. In a study conducted by van der Ryst (1990) on centre pivots over a five-year period, the values calculated for the CU and DU_{lq} varied substantially. The average CU value was 84% with a standard deviation of 5%. The range for the CU value was 64.8 to 93.8% on the same centre pivot. Similarly the DU_{lq} had an average of 73.1% and a standard deviation of 6.5% with a range of 57.4 to 89.5%. The author attributed this to external factors such as the variable climatic conditions, the structural design of the centre pivot, and the available range of emitters.

A summary of the application efficiency obtained for the overhead irrigation systems is shown in Table 5.10. The application efficiency for these evaluations was calculated as the average depth leaving the emitter to the average depth recorded on the ground. This accounts for spray and evaporation losses. The application efficiency of each system evaluated can be seen in Figure 5.29, Figure 5.30, Figure 5.32 and Figure 5.33. From the figures it can seen that the systems that exhibited high uniformities generally had high application efficiencies. It can also be seen that some of the systems that had a poorer DU_{lq} also had high application efficiency. An example of this is System 33 in Figure 5.33, the DU_{lq} was 56% and the AE was 89.4%. This is due to the definition of AE where averages are used. Here the AE was high because the average depth emitted from the sprinkler compared to the average depth recorded on the ground was similar. However, the DU_{lq} shows that the low quarter of the area received only 56% of the average. This means that under-irrigation has occurred in the test area. This may have implications for crop yield and excess deep percolation. The average AE for the irrigation system types are close to the norms suggested by the South African Irrigation

Institute (SABI) (2000). These norms represent the average spray and evaporation losses of the irrigation system.

Table 5.10 Summary of application efficiency by type of irrigation system.

	Type of irrigation system				
	All systems	Centre pivot	Dragline	Floppy	Semi-permanent sprinkler
Average AE [%]	77.0	83.6	73.5	76.7	78.9
Minimum AE [%]	58.9	76.3	58.9	63.5	64.6
Maximum AE [%]	93.8	93.8	89.3	85.4	91.1
SABI AE norms [%] (SABI, 2000)	-	85	75	85	75

The average application, or application rate, that was determined from the evaluations are shown in Figure 5.34 for centre pivot and floppy systems, in Figure 5.35 for drip and micro spray systems, and in Figure 5.36 for dragline and semi-permanent sprinkler systems. A statistical summary of the system delivery by type of system is given in Table 5.11.

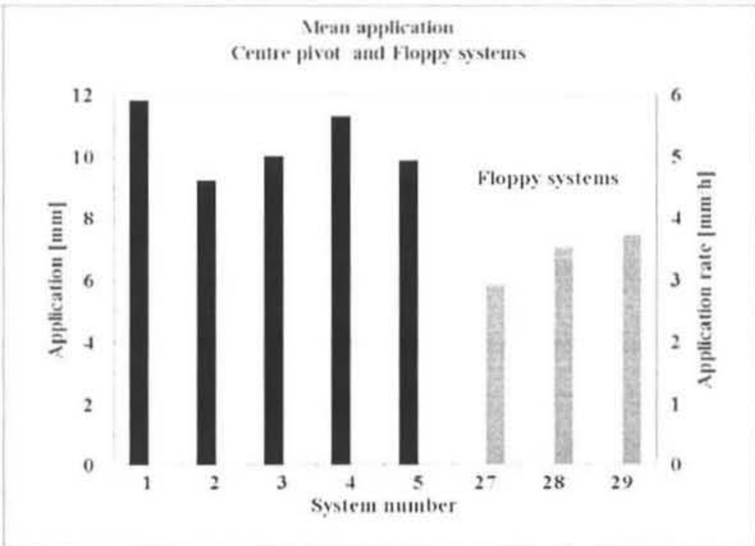

Figure 5.34 Average depth of application for floppy and centre pivot systems.

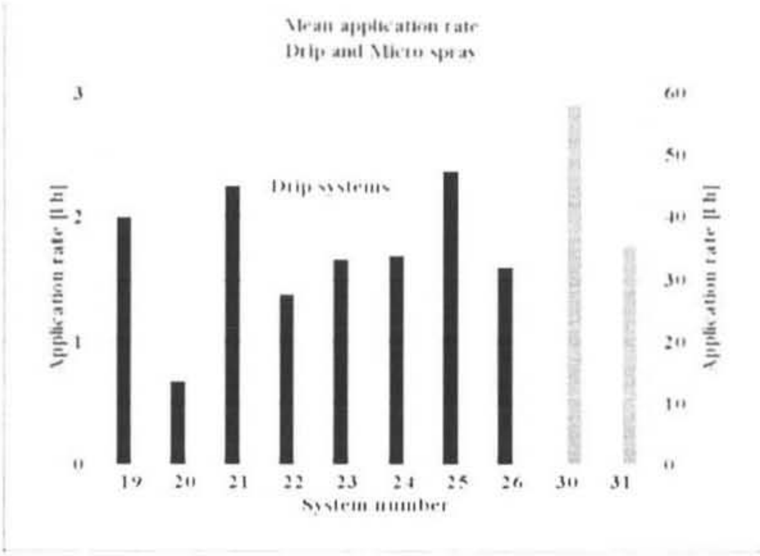

Figure 5.35 Average depth of application for drip and micro spray systems.

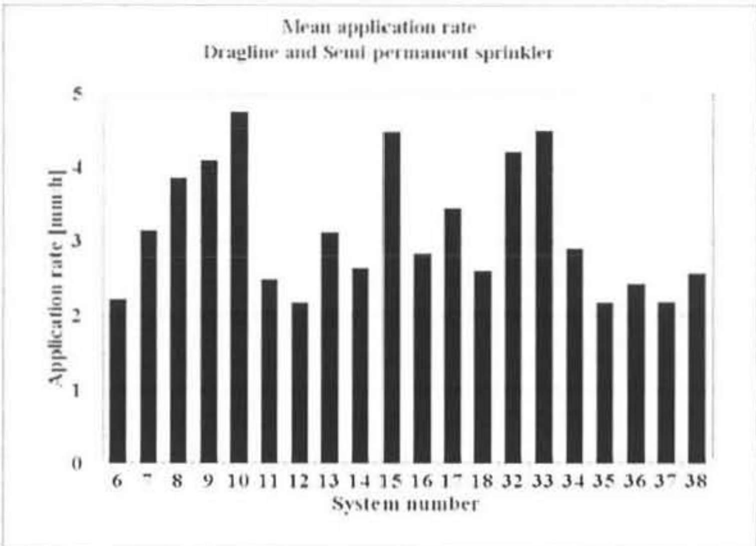

Figure 5.36 Average depth of application for dragline and semi-permanent sprinkler systems.

Table 5.11 Minimum, maximum and average irrigation system delivery by system type.

Statistic	Centre pivot	Dragline and Semi-permanent sprinkler	Drip	Micro spray	Floppy
	[mm]	[mm/h]	[l/h]	[l/h]	[mm/h]
Minimum	9.23	2.17	0.67	35.63	2.93
Maximum	11.82	4.76	2.37	58.23	3.75
Average	10.47	3.14	1.70	46.93	3.41
Standard Deviation	1.08	0.87	0.54	15.98	0.43
CV [%]	10.29	27.86	31.42	34.04	12.49

The delivery of many of the irrigation systems was below the design delivery. In some systems the delivery was as low as half of what the farmer thought they were applying. The lower than expect delivery could have negative results on crop growth if soil moisture monitoring is not part of the scheduling process. The delivery of the centre pivots showed the lowest variation in delivery. The CV for the delivery of dragline and semi-permanent sprinkler systems was high at 27.86%. The majority of these systems were designed with the same spacing and sprinkler and nozzle package. Therefore, this large variation is significant and is probably due to the different climatic conditions and different operational practices. The floppy systems exhibited a lower CV for the delivery of these systems. Inferences about the high variability of the drip and micro spray systems are not possible because of the unique design of each system.

The peak system capacity is shown in Figure 5.37 for each system. The system capacity given is for the irrigation system operated with the performance parameters as determined during the evaluation and at the current scheduling practices. The system capacity could be increased in the systems with a poor uniformity and efficiency by operating the system at the correct pressure and in more favourable wind conditions. There was a large variation in the system capacity of the irrigation systems evaluated. Twenty-three of the systems had a system capacity less than 5 mm/day and 12 of the systems had a system capacity less than 4 mm/day. These systems may not be able to supply the crop water demand during peak periods. The system capacity could not be determined for systems 21, 24 and 31 due to a lack of scheduling information.

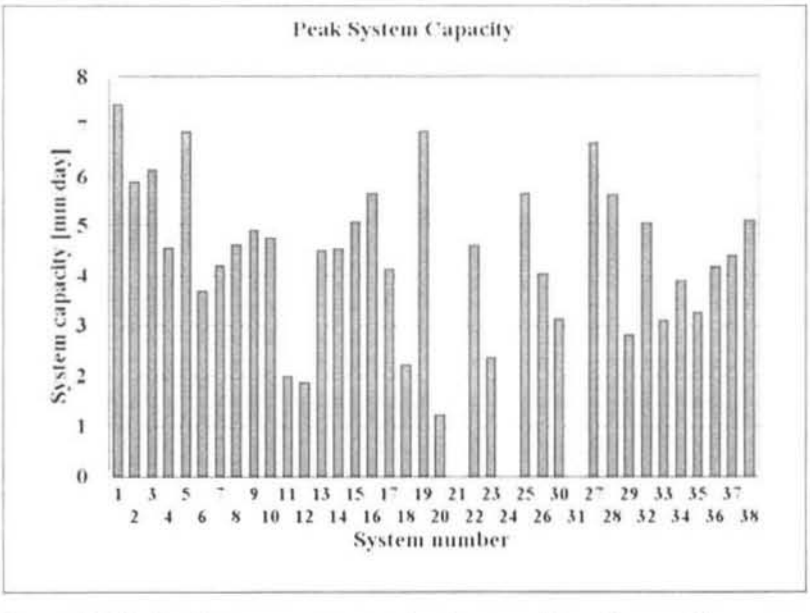

Figure 5.37 Peak system capacity in mm/day for each system.

A statistical summary of the system capacity by type of system is given in Table 5.12. The centre pivots had the highest average system capacity of 6.2 mm/day as well as the lowest CV at 17.7%. The floppy, and drip and micro spray systems showed a large variation in system capacity. The dragline and semi-permanent sprinkler systems were less variable.

Table 5.12 Minimum, maximum and average irrigation system capacity by system type.

System Capacity [mm/day]	Centre Pivot	Dragline and Semi-permanent sprinkler	Drip and Micro spray	Floppy
Minimum	4.57	1.87	1.22	2.81
Maximum	7.46	5.68	6.92	6.70
Average	6.20	4.06	3.99	5.06
Standard Deviation	1.10	1.07	2.29	2.01
CV [%]	17.7	26.4	57.4	39.7

The main results obtained during the study were given in this Chapter. The importance of these findings will be discussed in the following Chapter.

6 DISCUSSION AND CONCLUSIONS

From the literature it is clear that monitoring an irrigation system using performance criteria plays an important role in the economics and efficacy of an irrigation system. In the past there has been great confusion over the use of certain of these criteria. The same term has been given many definitions by different practitioners. This makes the comparison of systems tested at different times, locations, scales, and evaluators difficult. Therefore, a common definition is required to remove any confusion and to allow for comparison. The definitions provided by the ASCE Task Committee should therefore be used as a common basis for the evaluation of irrigation systems or regions. However, there is still the possibility of evaluators having different opinions about what constitutes a reasonable or beneficial use of water. For this reason the reports on irrigation system performance should have clear definitions of the criteria used. To allow for future comparison the scale and elemental area used should also be indicated.

The distribution uniformity of an irrigation system plays an important role in the efficient use of water as well as the realisation of high yields. The distribution uniformity is affected by design, environmental, and managerial factors. For an irrigation system to perform at its optimum, all these factors have to be correctly managed. An irrigation system will only have a good uniformity if it is correctly designed, maintained, and operated. The performance of an irrigation system should be checked using regular maintenance and evaluation.

The use of spatial statistics to describe the performance of an irrigation system gave both positive and negative results. If the spatial continuity of the distribution of water can be determined and modelled, the map produced using the ordinary kriging interpolator provides a useful visual aid to determine areas of over-irrigation or under-irrigation. Since the spatial relationship of the data can be exploited, the map produced by ordinary kriging is more useful than one produced using inverse distance square interpolation. The ordinary kriging technique has a smoothing effect on the predicted data. Therefore the uniformity of the predicted map will be higher than the measured data. For this reason, the data from the predicted map cannot be used to estimate the uniformity of the irrigation system, as it will tend to over estimate the uniformity. To estimate the field-wide uniformity of the irrigation system a single realisation of a conditional simulation could be used. The conditional simulation exploits the spatial dependence of the data and uses the measured data. The results for the uniformity from the conditional simulation resemble the uniformity of the measured data more closely. The cell average over a number of conditional simulations produces a map that closely resembles the ordinary kriging map. The cell variance can also be determined over the number of simulations and can be used to provide cell confidence intervals for the depth applied.

A possible negative result from the study was that the use of spatial statistics greatly increases the amount of data needed compared to the standard evaluations performed. The time required to set up the experiment is increased and the duration of the test can be greater than 36 hours for centre pivots. During this time there are changes in atmospheric and wind conditions. If the changes are dramatic, they may have a large influence on the uniformity results. The Turner centre pivot evaluation showed a difference in the uniformity between the single row of catch cans and the spatial distribution of catch cans. Whether this could be attributed to the varying wind speed and direction or other factors, such as wind and travel speed of the centre pivot, was difficult to quantify. Another possible negative aspect of using spatial statistics to evaluate irrigation systems is that the evaluator would have to be well versed in the theory and application of geostatistics. The process involved with the standard evaluation techniques is relatively simple and less prone to errors than modelling the spatial dependence of the data.

The characterisation of the spatial variance of the soil properties measured was not successful. Since soil properties can vary dramatically over short distances, the parameter being measured will have to be extensively sampled at close distances. This becomes impractical and economically unfeasible at the field scale where large numbers of samples would have to be taken. The number of measurements taken during this study was too few to determine any spatial dependence of the parameter measured. However, other studies using spatial statistics to characterise the spatial variation of soil properties have been successful where sufficient data (at least 150 samples) have been measured.

The use of tensiometers to measure the change in soil tension over short periods of time did not prove to be useful. Firstly, many of the tensiometers did not show any activity. This was possibly due to the tensiometer not making a good connection with the soil matrix, the short time the tensiometers were installed, or low soil moisture at the start of the evaluation. However, tensiometers have been used to monitor changes in soil tension over long periods of time. A tensiometer that was permanently installed could be used for scheduling purposes.

The spatial analysis of the depth data from the standard evaluations showed that the depth of irrigation water applied varies over short distances. Therefore, to characterise a whole field the sampling density would have to be high to include the variation at short lags. This would increase the cost of the evaluation dramatically. The semivariograms from the majority of the systems showed that there was a periodic behaviour in the spatial variation of the depth data. This may indicate that other methods will have to be used to evaluate the spatial dependence of the depth data. The increased sampling density required to accurately map the variation of applied water for these types of systems may make it prohibitively expensive to apply spatial statistical methods to evaluate the spatial distribution.

In general the results from the standard uniformity evaluations performed on the 38 systems considered were poor. The majority of the systems had a uniformity that was less than the standard DU_{lq} suggested by Pitts *et al.* (1996). The centre pivot and drip systems exhibited good application uniformity compared to the dragline and semi-permanent sprinkler systems evaluated. In areas where there are water restrictions, the centre pivot and drip systems may be required since the selection criteria may be the conservation of water resources and not the minimisation of capital costs.

The dragline, semi-permanent sprinkler, and floppy systems appear to be susceptible to strong wind conditions. The distortion of the distribution pattern was greater for these systems than for the centre pivot systems. However, as the results of one of the semi-permanent sprinkler systems show, if the overhead sprinkler is operated at the correct pressure and at the correct spacing in strong wind conditions (6 m/s) the uniformity can still be relatively high. The distribution uniformity of the overhead systems was also greatly affected by the low operating pressure in the system. Without sufficient pressure the sprinkler is not able to achieve the desired radius of throw and break up of the stream. Therefore, to improve the uniformity of these systems they need to be operated within the correct pressure range. Maintenance also plays a crucial role in maintaining good uniformity. The uniformity of systems with worn nozzles, leaking hoses, broken sprinkler heads, or leaking hydromatic couplings were generally poor.

Drip irrigation systems are designed to apply water very uniformly. The drip systems that were tested showed both excellent and poor results. These systems need to be designed with the soil and crop to be grown in mind. It was observed that the subsurface drip systems in clayey soil had emitter clogging that decreased the uniformity. The quality of the water also had an effect on the uniformity. On systems that drew water from a source that contained a high degree of silts and suspended solids the uniformity was low despite an adequately designed filtration system. Therefore, to ensure excellent uniformity in drip systems, the quality of the water and the effectiveness of the filtration system need to be considered.

The irrigation systems that were well maintained and operated according to the design specifications were able to meet or exceed the standard DU_{lq} values suggested. Therefore the standard DU_{lq} values suggested by Pitts *et al.* (1996) could be used as a guideline for the minimum acceptable limit to be used in the calculation of the gross irrigation water requirement. These values could be used as the DU_{lq} used in the potential application efficiency principle given by Burt *et al.* (1997). This method uses the average of the low quarter for scheduling purposes. When the average of the low quarter is at the required depth then there will be minimal under-irrigation and the application efficiency will be a function of the distribution uniformity. Using these principles, the low-quarter potential application efficiency (PAE_{lq}) and the ratio of gross to nett irrigation water requirement for the irrigation systems evaluated are shown in Table 6.1. The norms for application efficiency given by SABI (2000) were used to represent the percent spray and evaporation losses in the PAE_{lq} calculation.

Table 6.1 PAE_{lq} and ratio of gross to nett irrigation water requirement.

System type	SABI Norms for AE [%]	Standard DU_{lq} [%]	PAE_{lq} [%]	Ratio of Gross/Nett irrigation
Centre pivot	85	75	63.8	1.57
Dragline	75	75	56.3	1.78
Floppy	85	75	63.8	1.57
Semi-permanent sprinkler	75	75	56.3	1.78
Drip and Micro spray	95	85	80.8	1.24

The table shows that the efficiency calculated is low for all expect the drip and micro spray systems. These efficiencies mean that the gross amount of water that needs to be applied is 157% of the crop water requirement for centre pivot and floppy systems. This increases to 178% for dragline and semi-permanent sprinkler systems. The drip and micro spray systems would require 124% of the crop water demand. Therefore, in water-stressed areas this technique to calculate the gross amount of irrigation water required may not apply.

For irrigation systems where another level of adequacy is required, the method as given in Chapter 2.4 will have to be followed. Table 6.2 shows the system efficiency (SE) of the irrigation system with an adequacy of 50%. Here, half the field is under-irrigated and half the field is over-irrigated. Since the average depth infiltrated is the average amount that must be applied at the surface, the gross amount of irrigation water required is this mean depth divided by (100 - % losses). The system efficiency is the product of the application efficiency of the infiltrated water (refer to Table 2.7) and (100 - % losses). Here the amount of gross irrigation water that is required is at most 133% of the crop water demand. For example, if the irrigation crop water demand was 1000 mm for the season and a dragline system was used, then the gross amount of water to apply would be 1330 mm. This amount corresponds to the scenario where the field has an adequacy of 50%. For the scenario where the low quarter average is used as the scheduling criteria, the gross amount of water that would be required would be 1780 mm. This is an increase of 450 mm for a 27.5% increase in the area adequately irrigated. These calculations are based on the assumption that the irrigation is correctly scheduled to prevent excess deep percolation.

Table 6.2 System efficiency and ratio of gross to nett irrigation water requirement.

System type	SABI Norms for losses [%]	Standard DU_{lq} [%]	SE [%]	Ratio of Gross/Nett irrigation
Centre pivot	15	75	78.3	1.18
Dragline	25	75	69.1	1.33
Floppy	15	75	78.3	1.18
Semi-permanent sprinkler	25	75	69.1	1.33
Drip and Micro spray	5	85	90.5	1.05

The method described in Chapter 2.4 can also be applied to deficit irrigation scenarios. Here the gross amount of crop water required will be less than the crop water demand. The application efficiency of this type of irrigation will be close to 100% with the only loss of water coming from the spray and evaporation losses. This will probably not be the strategy of commercial farmers who use irrigation to ensure high yields. However, if there are water restrictions, this scenario may become likely when determining water allocations.

One of the objectives of this study was to propose an initial methodology to assess the spatial variability of the application of water in an irrigation system. As already mentioned in this discussion, the increased time and costs will make the spatial evaluation of irrigation systems unattractive. Instead of characterising the variability of the entire field, the standard evaluation test could be performed in a number of places in a field and the results compared. This will not be necessary for drip and micro spray irrigation systems as the standard evaluation procedure is done on an entire irrigation block. For a centre pivot, the test could be repeated along radii in different sectors of the field. However, due to the time it would take for the centre pivot to move round to the new test site, the climatic conditions may be different. This would complicate the comparison of the results from the different tests. The standard evaluation techniques should therefore be used to characterise the application uniformity of irrigation systems, as the results from a spatial evaluation does not indicate that the increased cost and effort is justified.

However, as a recommendation for future research, the use of automated sensor equipment or aerial photography to characterise the distribution of water within a field should be investigated. The use of GPS technology together with automated soil moisture measuring equipment could provide spatial data more quickly and at a lower cost.

More research is required to quantify actual values for distribution uniformity and application efficiency in South Africa. In particular, research into the performance of surface irrigation systems is needed. These values are required to enable actual water allocations to be estimated more accurately. Having more accurate estimates of actual irrigation system performance will allow designers and policy makers to make more informed decisions on which irrigation system to use under certain conditions.

In conclusion, the distribution uniformity of an irrigation system plays an important role in the yield potential of a crop and in the use of limited water resources. The current method of calculating gross irrigation water requirement using spray and evaporation losses should be revised to include the distribution uniformity of an irrigation system. Regular assessment of irrigation systems should occur to ensure that the system is performing correctly. Irrigation systems should also be operated according to the correct design to ensure that there is sufficient operating pressure in the system to give high application uniformity.

7 REFERENCES

Ankeny, MD, Ahmed, M, Kaspar, TC, and Horton, R. 1991. Simple field method for determining unsaturated hydraulic conductivity. *Soil Science Society of America Journal* 55(2):467-470.

ASAE Standards, 40^{th} Ed. 1993a. S436. Test Procedure for Determining the Uniformity of Water Distribution of Center Pivot, Corner Pivot, and moving Lateral Irrigation Machines Equipped with Spray or Sprinkler Nozzles. St. Joseph, Michigan, USA: ASAE.

ASAE Standards, 40^{th} Ed. 1993b. EP458. Field Evaluations of Microirrigation Systems. St. Joseph, Mich., USA: ASAE.

ASAE Standards, 40^{th} Ed. 1993c. S398.1. Procedure for Sprinkler Testing and Performance Reporting. St. Joseph, Mich., USA: ASAE.

ASCE. 1978. Describing irrigation efficiency and uniformity. *Journal of the Irrigation and Drainage Division* 104(1):35-41.

ASCE Task Committee on Geostatistical Techniques in Geohydrology of the Ground Water Hydrology Committee of the ASCE Hydraulics Division (ASCE). 1990a. Review of geostatistics in geohydrology. I: Basic concepts. *Journal of Hydraulic Engineering* 116(5):612-632.

ASCE Task Committee on Geostatistical Techniques in Geohydrology of the Ground Water Hydrology Committee of the ASCE Hydraulics Division (ASCE). 1990b. Review of geostatistics in geohydrology. II: Applications. *Journal of Hydraulic Engineering* 116(5):633-658.

Bogaert, P and Russo, D. 1999. Optimal spatial sampling for the estimation of the variogram based on a least squares approach. *Water Resources Research* 35(4):1275-1289.

Bos, MG and Nugteren, J. 1990. *On Irrigation Efficiencies.* Wageningen, NL: International Institute for Land Reclamation and Improvement (ILRI).

Brus, DJ and de Gruijter, JJ. 1997. Random sampling or geostatistical modelling? Choosing between design-based and model-based sampling strategies for soils (with Discussion). *Geoderma* 80(1-2):1-44.

Burt, CM, Walker, RE and Styles, SW. 1992. *Irrigation System Evaluation Manual.* San Luis Obispo, USA: Irrigation Training Research Centre, California Polytechnic State University.

Burt, CM, Clemmens, AJ, Strelkoff, TS, Solomon, KH, Bliesner, RD, Hardy, LA, Howell, TA and Eisenhauer, DE. 1997. Irrigation performance measures: Efficiency and uniformity. *Journal of Irrigation and Drainage Engineering* 123(6):423-442.

Burt, CM, Clemmens, AJ, Solomon, KH, Howell, TA and Strelkoff, TS. 1999. Irrigation performance measures: Efficiency and uniformity- Closure. *Journal of Irrigation and Drainage Engineering* 125(2):97-99.

Chen, J, Hopmans, JW and Fogg, GE. 1995. Sampling design for soil moisture measurements in large field trials. *Soil Science* 159(3):155-161.

Christiansen, J E. 1942. Irrigation by sprinkling. California Agricultural Experiment Station-Bulletin 670. Berkley, USA: University of California.

Clemmens, AJ. 1991. Irrigation uniformity relationships for irrigation system management. *Journal of Irrigation and Drainage Engineering* 117(5):682-699.

Clemmens, AJ and Solomon, KH. 1997. Estimation of global irrigation distribution uniformity. *Journal of Irrigation and Drainage Engineering* 123(6):454-461.

Cressie, N. 1991. Statistics for Spatial Data. New York, USA: John Wiley & Sons, Inc.

de Juan, JA, Tarjuelo, JM, Valiente, M, and Garcia, P. 1996. Model for optimal cropping patterns within the farm based on crop water production functions and irrigation uniformity: I. Development of decision model. *Agricultural Water Management* 31(1-2):115-143.

Doorenbos, J, and Kassam, AH. 1979. Yield Response to Water. Irrigation and Drainage Paper 33. Rome, IT: Food and Agriculture Organisation (FAO).

Fonteh, MF and Podmore, T. 1994. Application of geostatistics to characterise spatial variability of infiltration in furrow irrigation. *Agricultural Water Management* 25(1-2):153-165.

Goovaerts, P. 1999. Geostatistics in soil science: state-of-the-art and perspectives. *Geoderma* 89(1-2):1-45.

Hansen, VE. 1960. New concepts in irrigation efficiency. *Transactions of the ASAE* 3(1):55-61.

Heermann, DF and Hein, PR. 1968. Performance characteristics of self-propelled center pivot irrigation systems. *Transactions of the ASAE* 11(1):11-15.

Heermann, DF, Duke, HR, Serafim, AM and Dawson, LJ. 1992. Distribution functions to represent center-pivot water distribution. *Transactions of the ASAE* 35(5):1465-1472.

Isaaks, E and Srivastava, RM. 1989. *An introduction to Applied Geostatistics.* New York, USA: Oxford University Press.

Jaynes, DB. 1991. Calculation of distribution and efficiency for nonuniform irrigation. *Journal of Irrigation and Drainage Engineering* 117(5):808-810.

Jensen, ME. 1993. The impact of irrigation and drainage on the environment. In *5th Gulhati Memorial Lecture.* The Hague, NL: International Commission on Irrigation and Drainage.

Journel, AG and Huijbregts, CJ. 1978. *Mining Geostatistics.* London, UK: Academic Press.

Karmeli, D and Keller, J. 1974. *Trickle Irrigation Design.* Glendora, USA: Rain Bird Sprinkler Manufacturing Corporation.

Letey, J. 1985. Irrigation uniformity as related to optimum crop production- Additional research is needed. *Irrigation Science* 6(-):253-263.

Letey, J, Vaux, HJ and Feinerman, E. 1984. Optimum crop water applications as affected by uniformity of water infiltration. *Agronomy Journal* 76(-):435-441.

Li, J. 1998. Modelling crop yield as affected by uniformity of sprinkler irrigation system. *Agricultural Water Management* 38(2):135-146.

Lorentz, S. 2000. Tension Infiltrometer Quick Reference Guide. School of Bioresources Engineering and Environmental Hydrology, University of Natal, Pietermaritzburg, RSA.

Merriam, JL. 1999. Estimation of global irrigation distribution uniformity- Discussion. *Journal of Irrigation and Drainage Engineering* 125(2):100-103.

National Water Act. (1998). RSA Government Gazette No. 36 of 1998: 26 August 1998, No. 19182. Cape Town, RSA.

Olea, R A. 1984. Sampling design optimisation for spatial functions. *Journal of the International Association for Mathematical Geology* 16(-):369-392.

Pebesma, EJ and Wesseling, CG. 1998. GSTAT: A program for geostatistical modelling, prediction and simulation. *Computers and Geosciences* 24(1):17-31.

Pereira, LS. 1999. Higher performance through combined improvements in irrigation methods and scheduling: a discussion. *Agricultural Water Management* 40(2):153-169.

Perrens, SJ. 1984. Numerical analysis of soil water uniformity under sprinkler irrigation. *Journal of Agricultural Engineering Research* 30(-):23-27.

Pitts, D, Peterson, K, Gilbert, G and Fastenau, R. 1996. Field assessment of irrigation system performance. *Applied Engineering in Agriculture* 12(3):307-313.

Reinders, FB. 1986. *Evaluasie van Besproeiingsisteme* (Evaluation of Irrigation Systems). Directorate of Agricultural Engineering and Water Supply, Pretoria, RSA.

Rogers, DH, Lamm, FR, Alam, M, Trooien, TP, Clark, GA, Barnes, PL and Mankin, K. 1997. Efficiencies and Water Losses of Irrigation Systems. [Internet]. Kansas State University, Research and Extension Engineers, Manhattan, USA. Available from: <http://www.oznet.ksu.edu/library/ageng2/mf2243.pdf>. [Accessed 17 March 2000].

SABI. 2000. Design Norms. [Internet]. South African Irrigation Institute (SABI), Strand, RSA. Available from: <http://www.sabi.co.za/html/design_norms.html>.[Accessed 9 September 2000].

Solomon, KH. 1983. Irrigation Uniformity and Yield Theory. PhD thesis, Utah State University, Utah State University, Logan, USA.

Solomon, KH. 1984. Yield related interpretations of irrigation uniformity and efficiency measures. *Irrigation Science* 5(-):161-172.

Solomon, KH. 1990. Sprinkler irrigation uniformity. [Internet]. Centre for Irrigation Technology, California State University, Fresno, USA. Available from: <http://www.wateright.org/site/publications/900803.html>. [Accessed 29 June 2000].

Solomon, KH and Burt, CM. 1999. Irrigation sagacity: a measure of prudent water use. *Irrigation Science* 18 (-):135-140.

Thornton-Dibb, S and Lorentz, S. 2000. Manual for the Operation of Tensiometer Nests Using the HOBO Logger System (v1.2). School of Bioresources Engineering and Environmental Hydrology, University of Natal, Pietermaritzburg, RSA.

van der Ryst, C. 1990. Identifiseting, Kwantifiseering en Beperking van Waterverliese onder Spulpuntbesproeiingstelsels (Identification, Quantification and Limitation of Water Losses under Centre Pivot Irrigation Systems). WRC Report No. 153/1/91. Pretoria, RSA: Water Research Commission.

Warrick, AW. 1983. Interrelationships of irrigation uniformity terms- Discussion. *Journal of Irrigation and Drainage Engineering* 109(3):317-332.

Warrick, AW and Myers, DE. 1987. Optimisation of sampling locations for variogram calculations. *Water Resources Research* 23(3):496-500.

Warrick, AW, Hart, WE and Yitayew, M. 1989. Calculation of distribution and efficiency for nonuniform irrigation. *Journal of Irrigation and Drainage Engineering* 115(4):674-686.

Warrick, AW, Vargas-Guzman, JA, Mayer, S, Restrepo, M and Ellsworth, TR. 1999. Strategies for improving spatial variability assessments. In *Assessment of Non-point Source Pollution in the Vadose Zone*, ed. Corwin, DL, Loague, K and Ellsworth, TR, 93-105. Washington, USA: American Geophysical Union.

Wolters, W. 1992. *Influences on the Efficiency of Irrigation Water Use.* Wageningen, NL: International Institute for Land Reclamation and Improvement (ILRI).

Wopereis, MC, Stein, A, Bouma, J and Woodhead, T. 1992. Sampling number and design for measurements of infiltration rates into puddled rice fields. *Agricultural Water Management* 21(4):281-295.

WRC. 1999. *Technical Report 1998- Water Research Commission.* Pretoria, RSA: Water Research Commission.

Zoldoske, DF and Solomon, KH. 1988. Coefficient of uniformity - what it tells us. [Internet]. Center for Irrigation Technology, California State University, Fresno, USA. Available from: <http://cati.csufresno.edu/cit/rese/88/880106/index.html>. [Accessed 24 August 2000].

Zoldoske, DF, Solomon, KH and Norum, EM. 1994. Uniformity measurements for turfgrass: what's best? [Internet]. Center for Irrigation Technology, California State University, Fresno, USA. Available from: <http://cati.csufresno.edu/cit/rese/94/941102.index.html>. [Accessed 24 August 2000].

APPENDIX A: GPS EQUIPMENT

A.1 TRIMBLE® GPS Pathfinder System

A TRIMBLE® GPS Pathfinder Pro XRS System was used to fix the positions of the catch cans for the spatial analyses. This GPS was also used to fix the position of the centre and towers of the centre pivots tested. The specifications of the GPS receiver are given in Table A.1.

Table A.1 GPS receiver specifications.

GPS Pathfinder Pro XRS	
General	12-channel L1/CA code tracking with carrier phase filtered measurements and multi-bit digitiser
	Integrated GPS/Beacon/Satellite receiver with EVEREST™ multipath rejection technology WAAS differential ready.
Update rate	1 Hz
Accuracy (RMS):	
Differential Correction	50 cm + 1 ppm on a second-by-second basis (horizontal) Sub meter + 2 ppm on a second-by-second basis (vertical)
Data logger	Trimble® TSC1

APPENDIX B: TENSION INFILTROMETER EQUIPMENT

B.1 Tension Infiltrometer Equipment Description

The components of the tension infiltrometer are detailed in Figure B.1. The bubble column is used to control the tension experienced at the soil surface. The supply column is used to supply the water that infiltrates the soil. The change in height of water of the supply column versus time is recorded to determine the rate at which water is entering the soil surface. The tension at the soil surface is controlled by placing the tip of the bubble rod at a depth below the water surface in the bubble column. The required depth of the bubble rod can be calculated from:

$$\text{Bubble rod depth} = \text{desired tension} + h_1 \quad (B.1)$$

where h_1 is the height indicated in Figure B.1. At the interface between the tension infiltrometer and soil there is a porous nylon mesh.

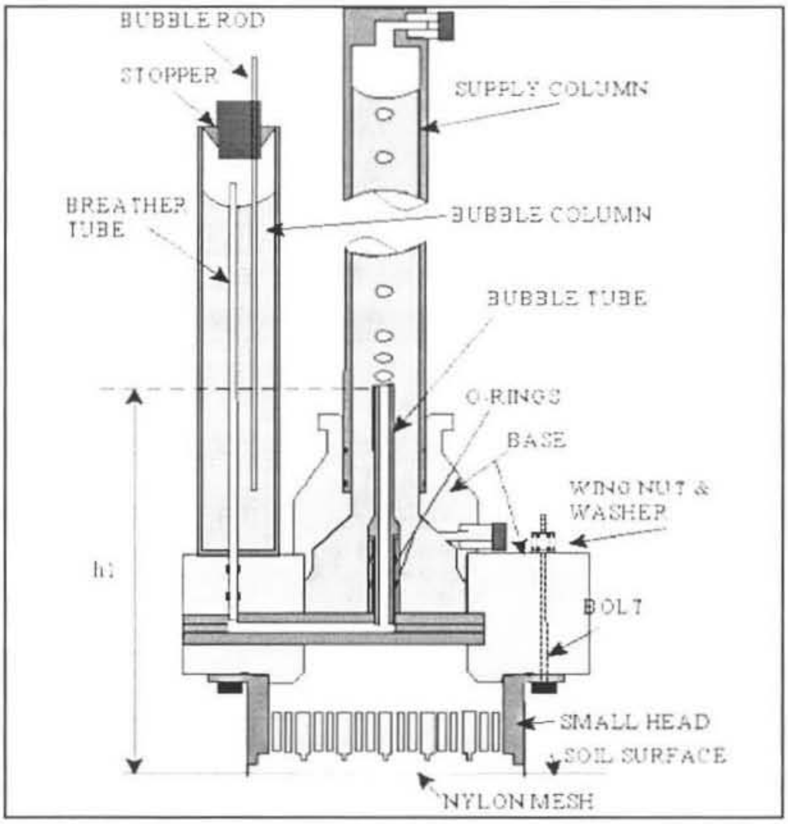

Figure B.1 Tension infiltrometer components (after Lorentz, 2000).

B.2 Operation

A layer of contact sand is spread over the soil and levelled. This is to ensure good contact between the mesh and the soil so that no air enters into the supply column through the mesh. The height of the bubble rod is set to the desired tension according to Equation B.1. The height of water in the supply column is recorded versus time. Either the height is recorded at regular time intervals, or the time for a specific decrease in height is recorded. The test is stopped at a given tension when steady state conditions are reached. The bubble tube is then lowered to the next tension and the readings taken. Readings are taken at a minimum of three different tensions.

B.3 Equations for Calculations

To calculate the hydraulic conductivity of the soil at different tensions, the following equations are used (Ankeny *et al.*, 1991):

$$Q(\varphi_1) = \pi r^2 K(\varphi_1) + 4 r \phi(\varphi_1) \qquad B.2$$

$$Q(\varphi_2) = \pi r^2 K(\varphi_2) + 4 r \phi(\varphi_2) \qquad B.3$$

where $Q(\varphi_i)$ is steady infiltrating flux [cm^3/s] at a tension of φ_i [cm],

$K(\varphi_i)$ is the field saturated hydraulic conductivity [cm/s],

$\phi(\varphi_i)$ is the matric flux potential [cm^2/s].

The ratio $K(\varphi_i)/\phi(\varphi_i)$ is assumed to be constant and is given the symbol A [cm^{-1}]. Dividing Equations B.2 and B.3 by $\phi(\varphi_i)$ and substituting for the ratio $K(\varphi_i)/\phi(\varphi_i)$ gives (Ankeny *et al.*, 1991):

$$Q(\varphi_1) = [\pi r^2 + 4 r/A] K(\varphi_1) \qquad B.4$$

$$Q(\varphi_2) = [\pi r^2 + 4 r/A] K(\varphi_2) \qquad B.5$$

To solve for the third unknown, an approximation for the difference between the matric flux potential at two tensions. This is expressed as:

$$\phi(\varphi_1) - \phi(\varphi_2) = (\varphi_1 - \varphi_2)[K(\varphi_1) + K(\varphi_2)]/2 \qquad B.6$$

Replacing $\phi(\varphi_i)$ with $K(\varphi_i)/A$ gives the following relationship:

$$[K(\varphi_1) - K(\varphi_2)]/A = (\varphi_1 - \varphi_2)[K(\varphi_1) + K(\varphi_2)]/2 \quad \text{B.7}$$

Solving Equations B.4, B.5 and B.7 simultaneously for A yields the following relationship:

$$A = \frac{(Q_i - Q_{i+1})}{(Q_i - Q_{i+1})} \cdot \frac{2}{(\varphi_i - \varphi_{i+1})} \quad \text{B.8}$$

The method for estimating the field saturated hydraulic conductivity at the different tensions (0, 0.5, 3, and 6 cm) for the tension pairs (φ_1,φ_2) is as follows:

$$K(0) = K(0)_{0,\,0.5} \quad \text{B.9}$$

$$K(0.5) = [K(0.5)_{0,\,0.5} + K(0.5)_{0.5,\,3}]/2 \quad \text{B.10}$$

$$K(3) = [K(3)_{0.5,\,3} + K(3)_{3,\,6}]/2 \quad \text{B.11}$$

$$K(6) = K(6)_{3,\,6} \quad \text{B.12}$$

The steady state volume flux (Q) is the slope of the line fitted to the volume versus time line for the steady state conditions. The volume leaving the supply column is calculated from:

$$\Delta\text{Volume} = \frac{\pi \cdot d^2}{4} \cdot \Delta\text{depth} \quad \text{B.13}$$

where ΔVolume = the change in volume [cm^3],

Δdepth = change in height of supply column between time i and i+1 [cm],

d = diameter of supply column [cm].

APPENDIX C: TENSIOMETER EQUIPMENT

C.1 Tensiometer Equipment Description

The tensiometer is used to measure the soil moisture tension. From these tensions, the amount of moisture in the soil can be determined from a soil moisture retention curve. The components of typical tensiometers are shown in Figure C.1. The tensiometer is connected to a HOBO 4 channel data logger that records the output of the pressure transducer every twelve minutes. The pressure transducer measures the tension created by the soil by means of a ceramic cup that is in contact with the soil. The tube between the pressure transducer and the ceramic cup is filled with water. The soil tension is measured relative to atmospheric pressure. Each pressure transducer is calibrated and the millivolts (mV) recorded by the data logger are converted to tensions using a simple linear regression equation.

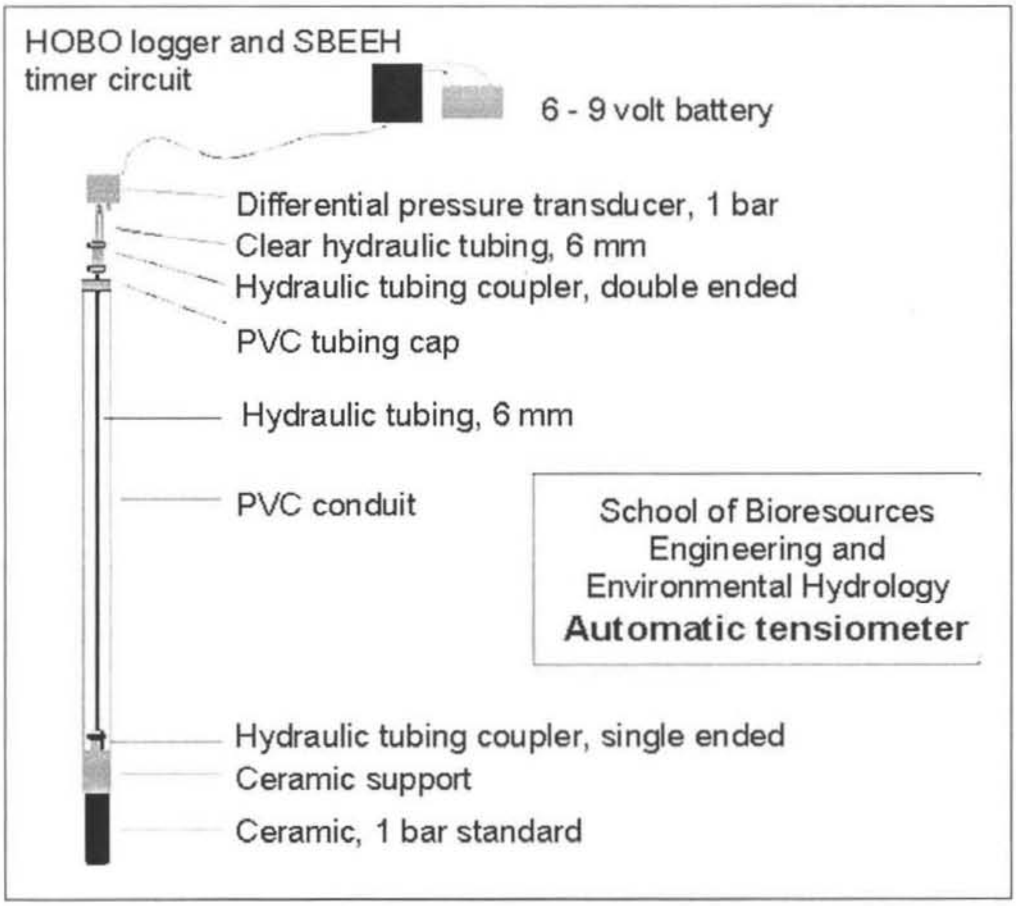

Figure C.1 Automatic tensiometer components (after Thornton-Dibb and Lorentz, 2000).

APPENDIX D: *GSTAT* FILE FORMATS

D.1 Example of *GSTAT* Data Input File

Major Centre Pivot - Cycle 1&2 - All Spans {File description}

5 {Number of co-ordinates and variables}

X, m {X co-ordinate}

Y, m {Y co-ordinate}

Volume, cm^3 {Variable 1}

Depth, mm {Variable 2}

Radius, m {Variable 3}

-176465.082	-2875960.685	5.5	0.94684	250.746
-176474.447	-2876033.878	6	1.03291	253.685
-176068.418	-2875798.88	7.5	1.29114	267.912
-176210.432	-2876136.067	9	1.54937	117.603
.				
.				
.				
.				
.				
.				
.				
.				
-176093.825	-2876268.718	10.8	1.85925	280.365
-176011.152	-2876151.746	11	1.89368	248.502

D.2 Example of GSTAT Command File

```
#
# gstat command file, Win32/Cygwin version 2.1.0 (August 1999)
# Tue Nov 28 14:55:49 2000
#
data(depth): 'maj12ind.txt', x=1, y=2, v=3, average;  {data input file parameters}
```

```
variogram(depth): 0.51 Nug(0) + 1.02 Sph(200); {fitted variogram model}

set cutoff = 300; {maximum lag separation}
set fit = 1; {fitting method – weighted least squares}
set width = 30; {lag separation}

mask: 'maj10map'; {locations to perform interpolations at}
predictions(depth): 'depth.asc'; {output file for predictions}
variances(depth): 'vardepth.asc'; {output file for estimation variances}
```

D.3 Example of ASCII Grid File

```
NCOLS 5        {number of columns of data}
NROWS 5        {number of rows of data}
XLLCENTER  -107335.04  {X co-ordinate of lower left block}
YLLCENTER  -3258394.56 {Y co-ordinate of lower left block}
CELLSIZE     10.00 {Grid size}
NODATA_VALUE  -9999 {No data value}
-9999 -9999 1 1 1      {data in 5 columns and 5 rows}
-9999 1 1 1 1
1 1 1 1 1
1 -9999 -9999 1 1
1 1 1 -9999 –9999
```

APPENDIX E: ADDITIONAL MAPS FOR MAJOR SITE

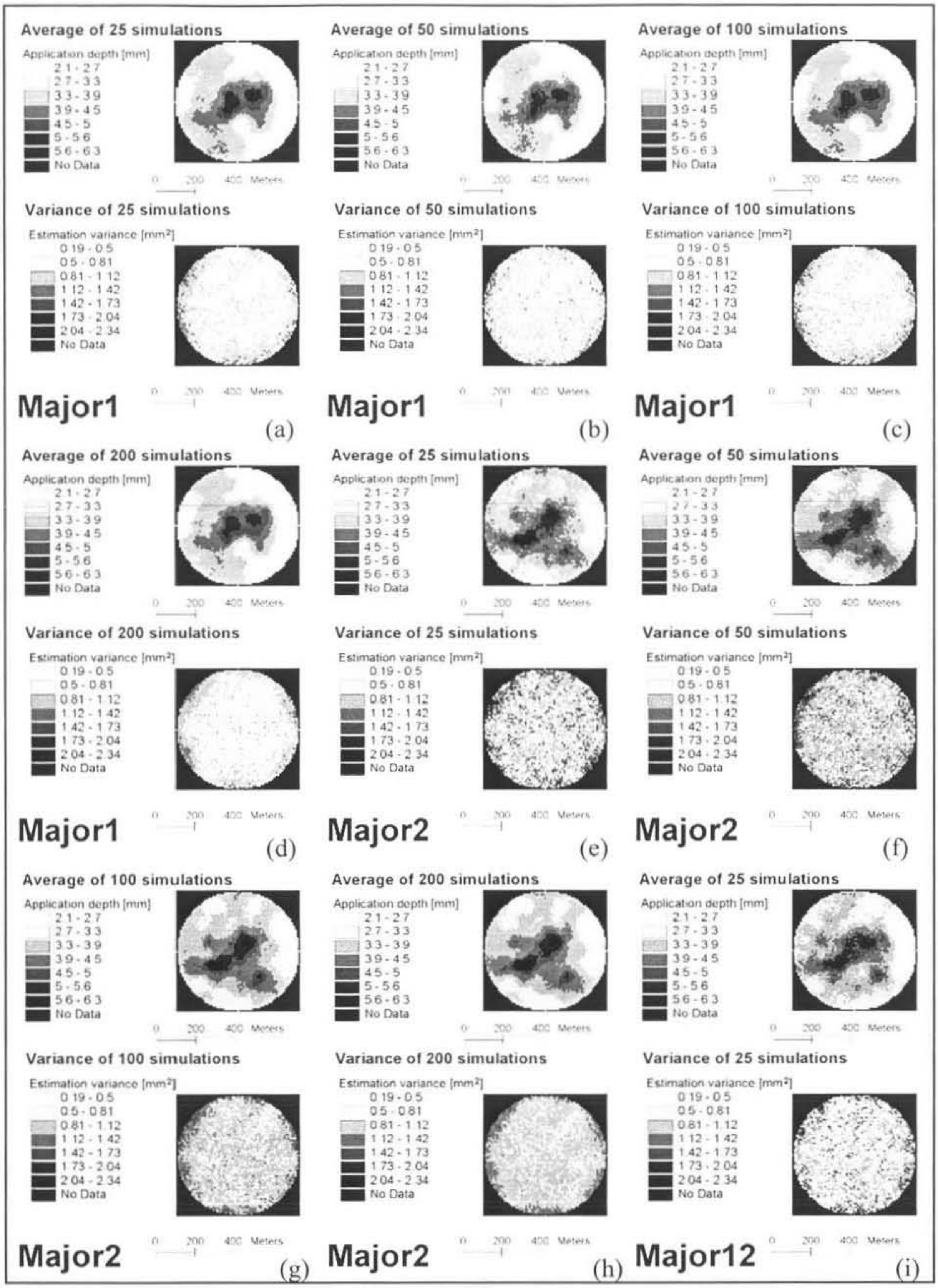

Figure E.1 (a) to (i) Maps produced using conditional simulation for the Major data sets.

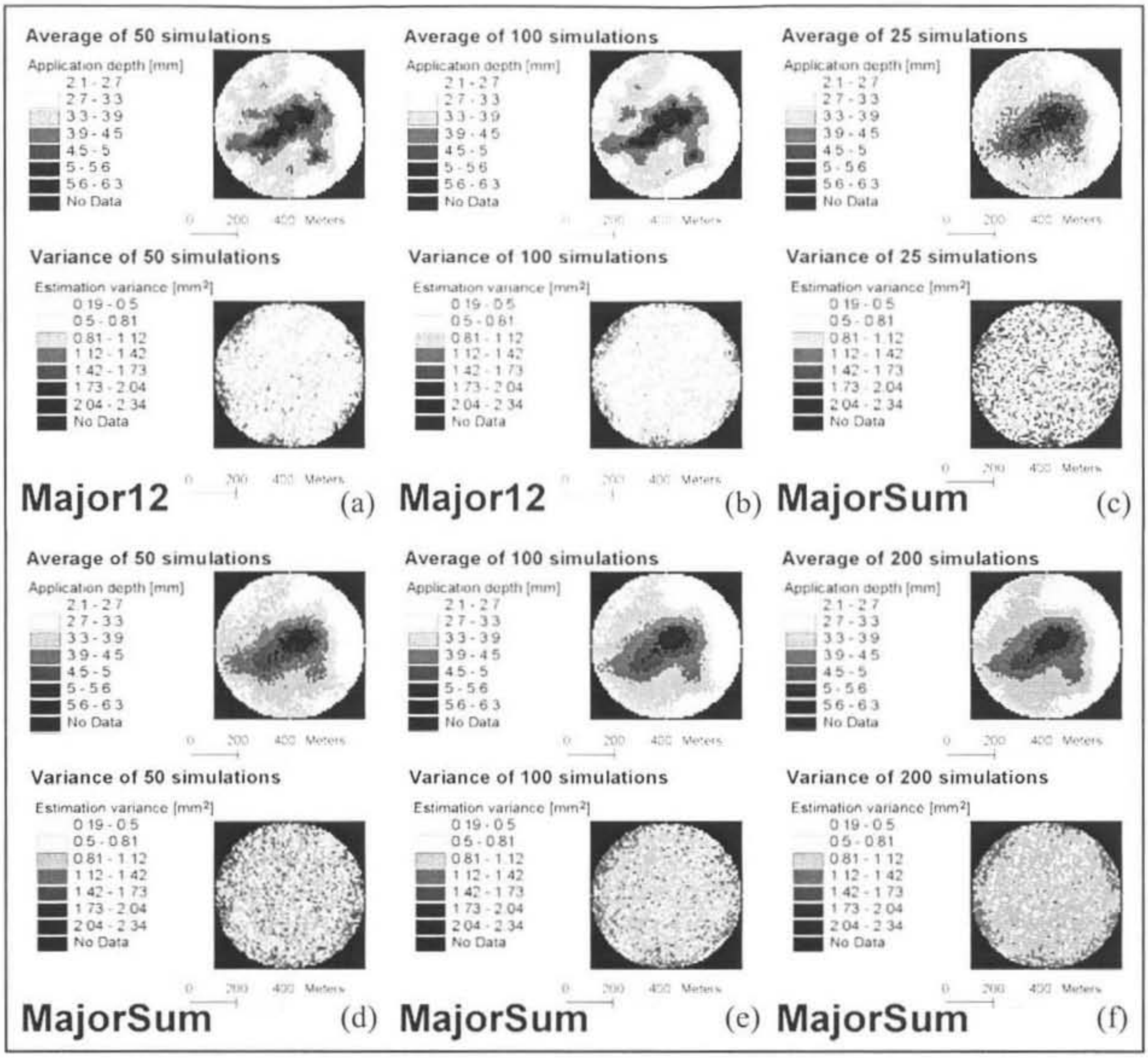

Figure E.2 (a) to (f) Maps produced using conditional simulation for the Major data sets.

APPENDIX F: SEMIVARIOGRAMS FOR STANDARD EVALUATION SITES

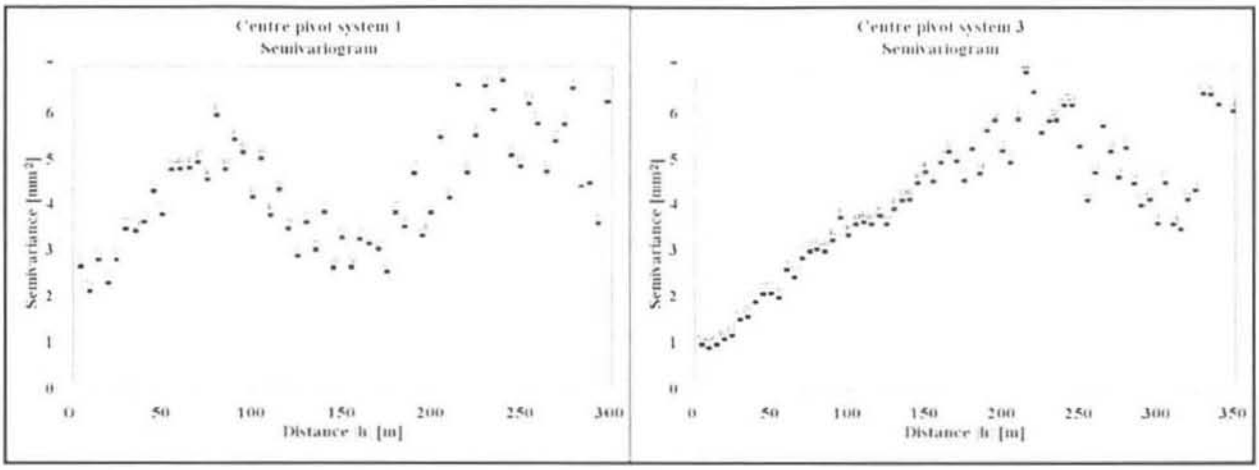

Figure F.1 Semivariogram for centre pivot systems 1 and 3.

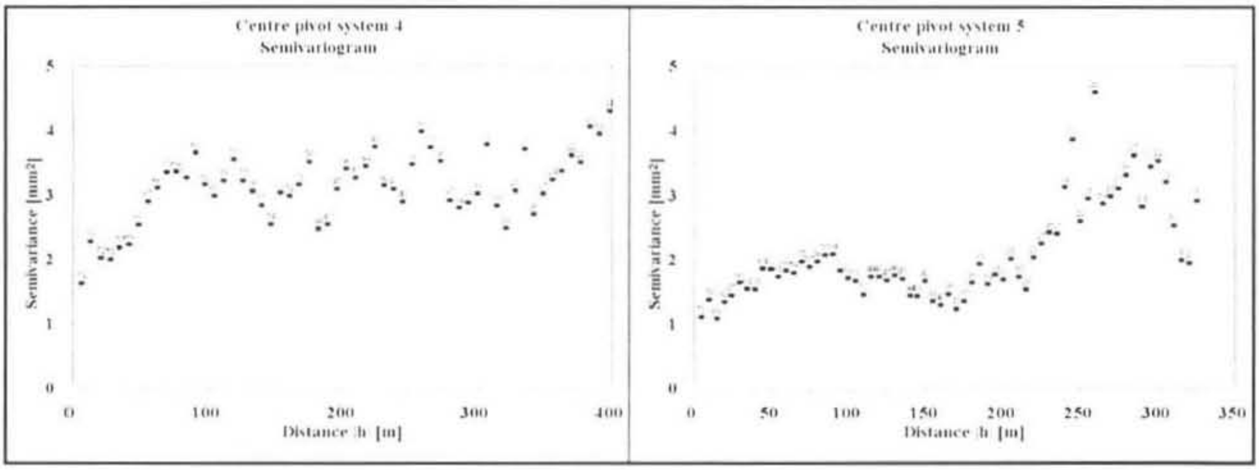

Figure F.2 Semivariogram for centre pivot systems 4 and 5.

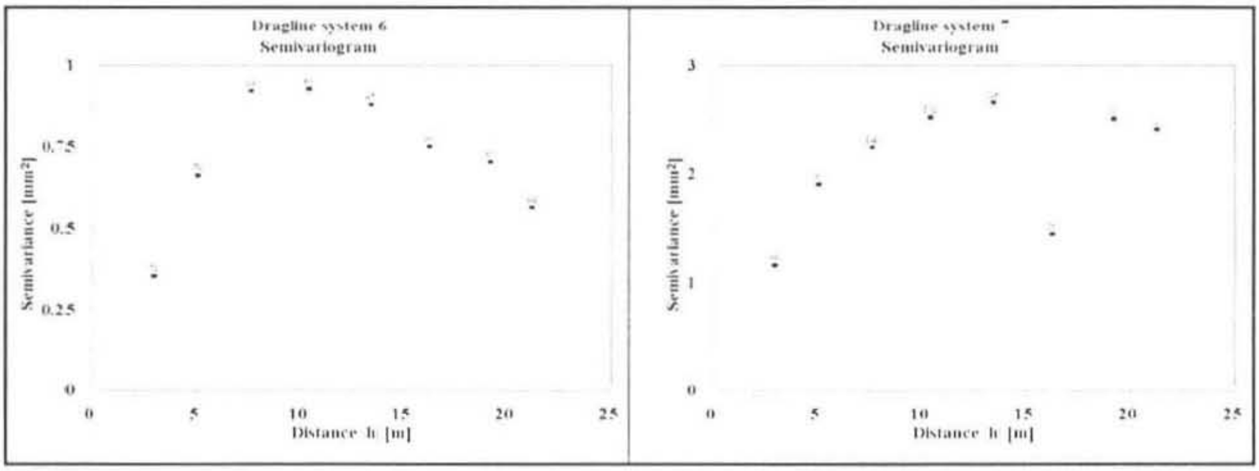

Figure F.3 Semivariogram for dragline systems 6 and 7.

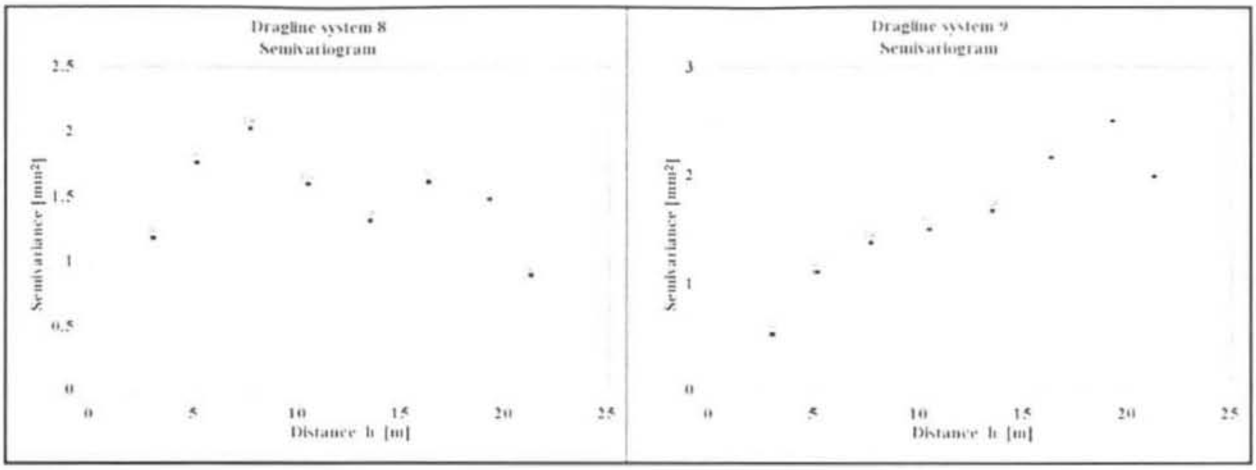

Figure F.4 Semivariogram for dragline systems 8 and 9.

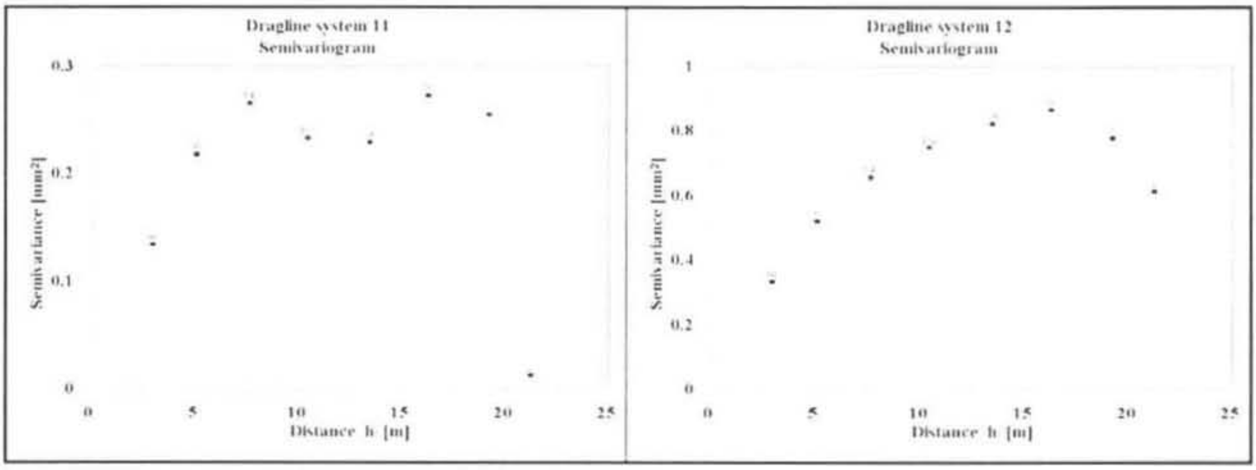

Figure F.5 Semivariogram for dragline systems 11 and 12.

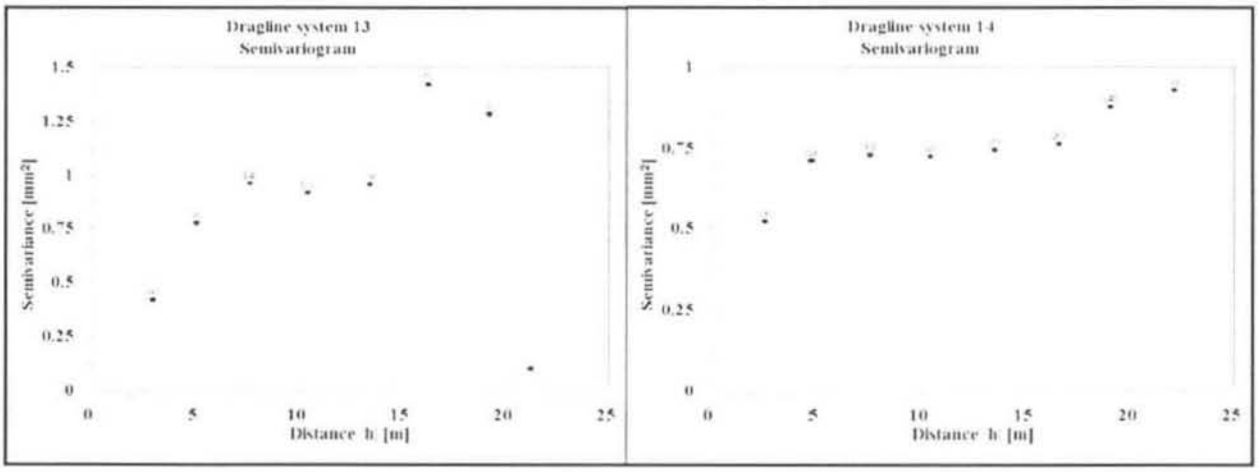

Figure F.6 Semivariogram for dragline systems 13 and 14.

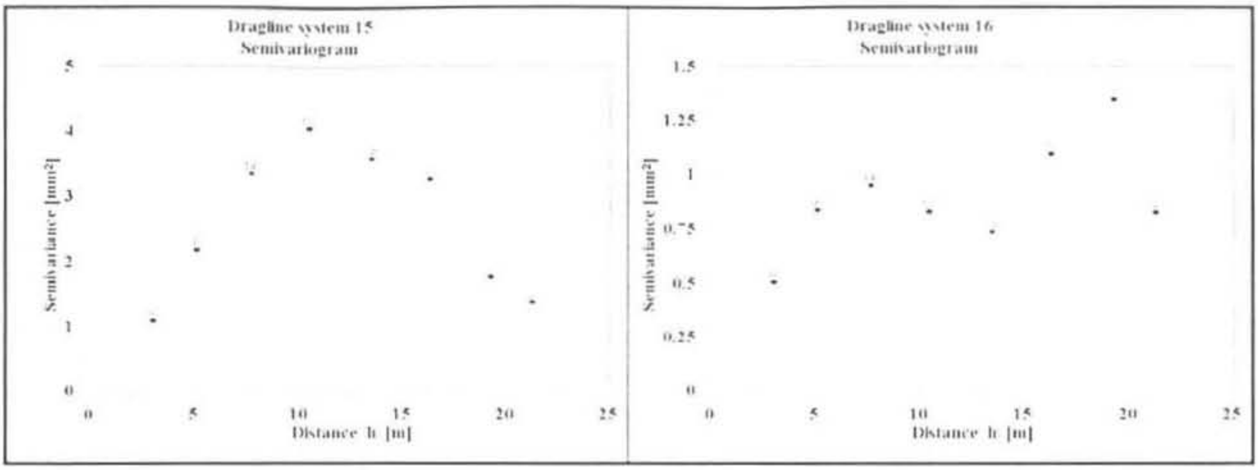

Figure F.7 Semivariogram for dragline systems 15 and 16.

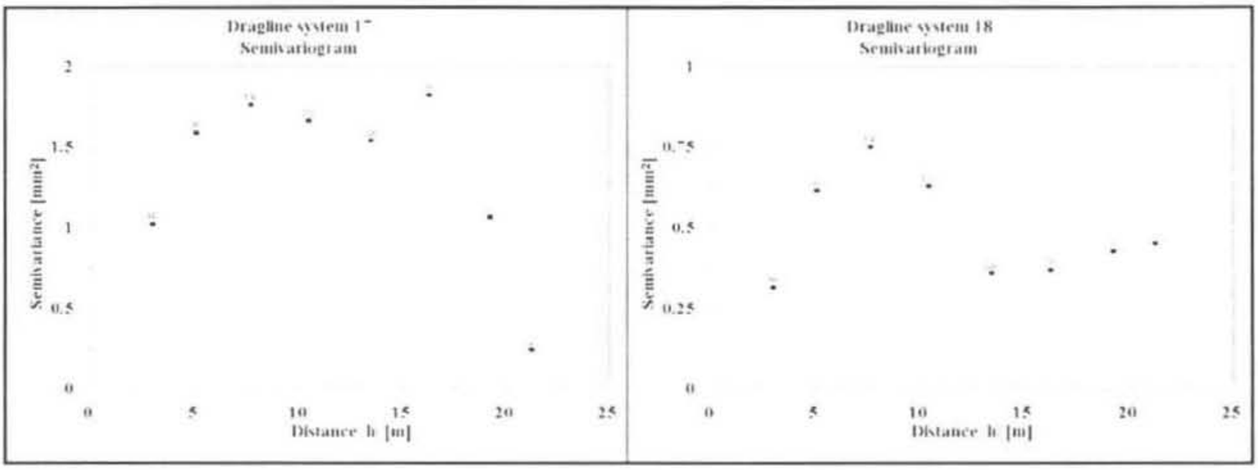

Figure F.8 Semivariogram for dragline systems 17 and 18.

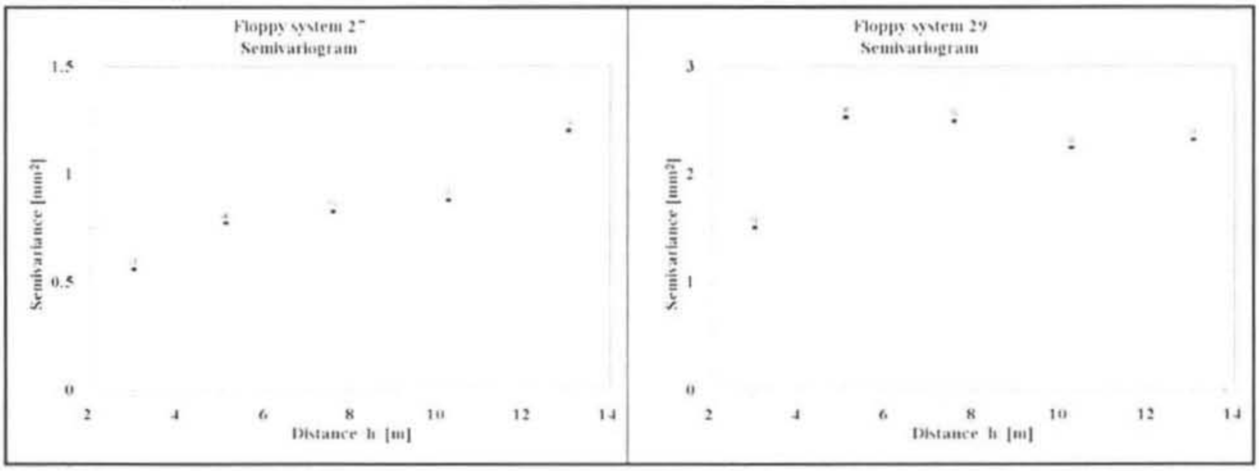

Figure F.9 Semivariogram for floppy systems 27 and 29.

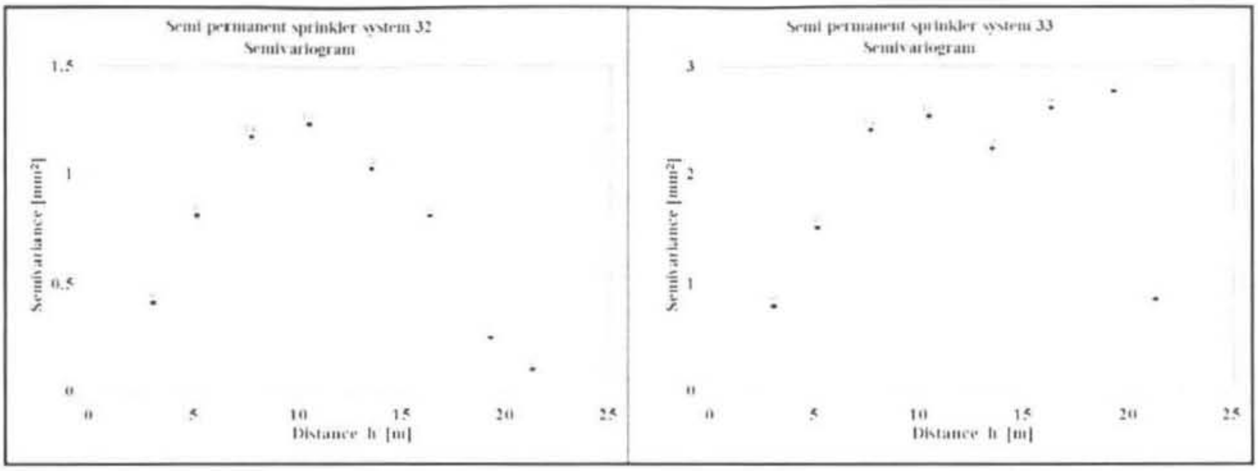

Figure F.10 Semivariogram for semi-permanent sprinkler systems 32 and 33.

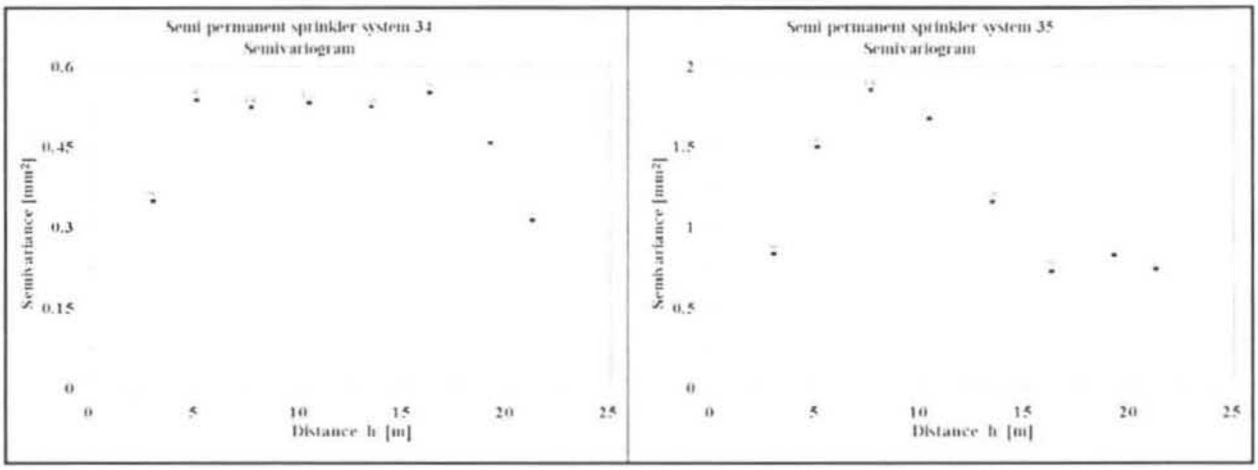

Figure F.11 Semivariogram for semi-permanent sprinkler systems 34 and 35.

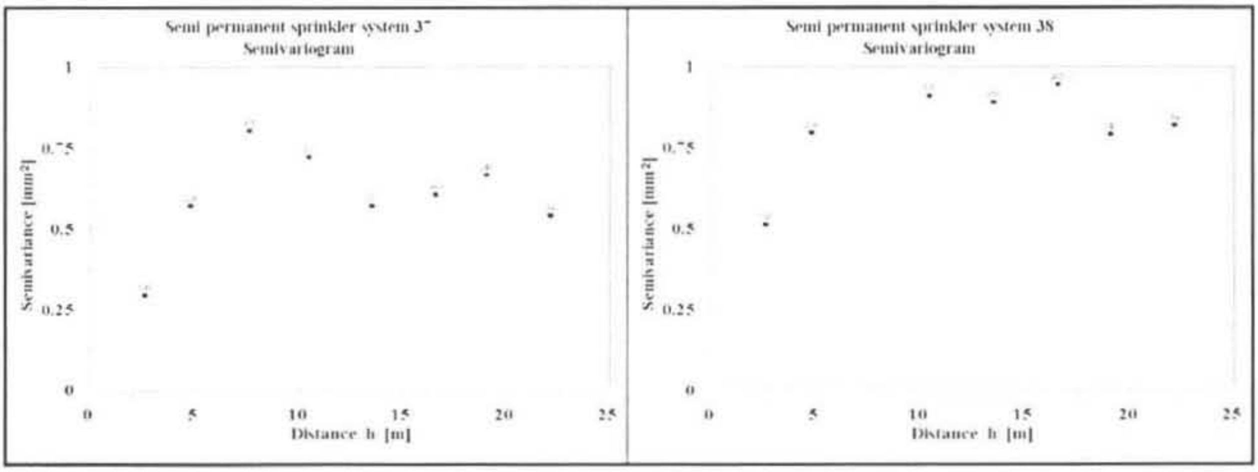

Figure F.12 Semivariogram for semi-permanent sprinkler systems 37 and 38.

APPENDIX G: HYDRAULIC CONDUCTIVITIES AND TENSIOMETER DATA FOR MAJOR SITE

Table G.1 Hydraulic conductivity of soil at 35 locations at 5, 30 and 60 mm tensions.

	Tension				Tension		
	5 mm	30 mm	60 mm		5 mm	30 mm	60 mm
Location	Hydraulic conductivity [cm/s]			Location	Hydraulic conductivity [cm/s]		
Major1	2.49E-04	2.14E-04	1.93E-04	Major19	3.15E-04	2.14E-04	1.67E-04
Major2	2.30E-04	9.74E-05	2.49E-05	Major20	4.71E-04	3.66E-04	2.43E-04
Major3	2.47E-04	1.92E-04	1.64E-04	Major21	3.36E-04	2.26E-04	1.78E-04
Major4	2.33E-04	1.86E-04	1.63E-04	Major22	3.68E-04	2.23E-04	1.62E-04
Major5	4.94E-04	3.14E-04	2.41E-04	Major23	1.79E-04	1.76E-04	1.74E-04
Major6	2.04E-04	2.31E-04	2.05E-04	Major24	3.19E-04	1.84E-04	1.27E-04
Major7	3.72E-04	2.55E-04	1.97E-04	Major25	3.21E-04	2.11E-04	1.55E-04
Major8	5.10E-04	3.85E-04	3.22E-04	Major26	2.44E-04	1.52E-04	1.05E-04
Major9	2.18E-04	1.41E-04	1.09E-04	Major27	4.56E-04	2.82E-04	2.06E-04
Major10	1.86E-04	1.27E-04	1.01E-04	Major28	2.70E-04	1.87E-04	1.50E-04
Major11	3.27E-04	2.52E-04	2.13E-04	Major29	4.90E-04	6.47E-04	5.76E-04
Major12	3.56E-04	3.42E-04	3.33E-04	Major30	4.18E-04	2.97E-04	2.41E-04
Major13	3.68E-04	2.68E-04	2.21E-04	Major31	5.43E-04	4.51E-04	4.06E-04
Major14	1.96E-04	1.53E-04	1.30E-04	Major32	2.48E-04	1.52E-04	1.14E-04
Major15	4.47E-04	3.40E-04	2.88E-04	Major33	2.54E-04	1.79E-04	1.46E-04
Major16	5.76E-04	3.13E-04	2.02E-04	Major34	4.76E-04	2.63E-04	1.78E-04
Major17	6.21E-04	3.73E-04	2.77E-04	Major35	5.54E-04	3.54E-04	2.71E-04
Major18	1.66E-04	1.57E-04	1.53E-04				

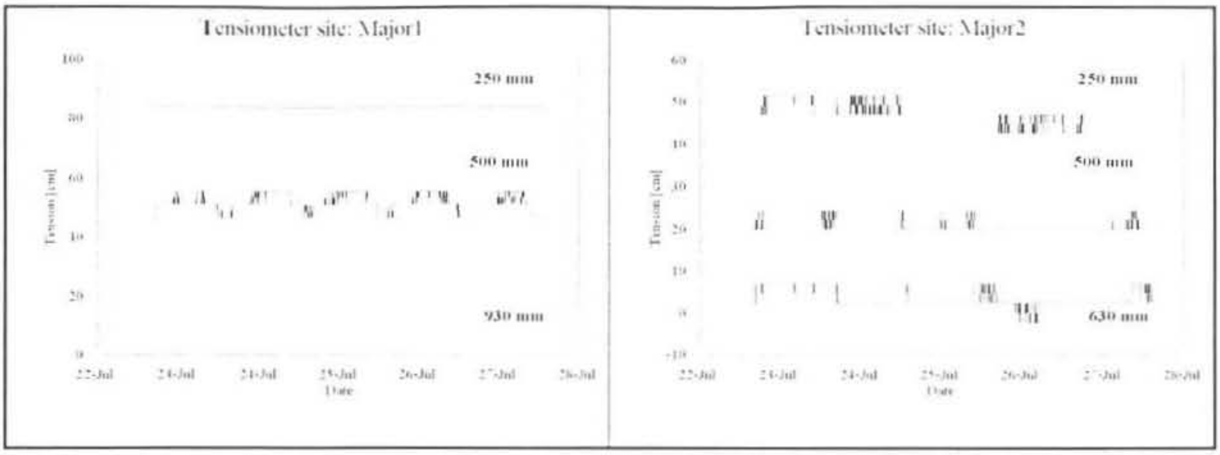

Figure G.1 Soil tension data at tensiometer sites Major1 and Major2.

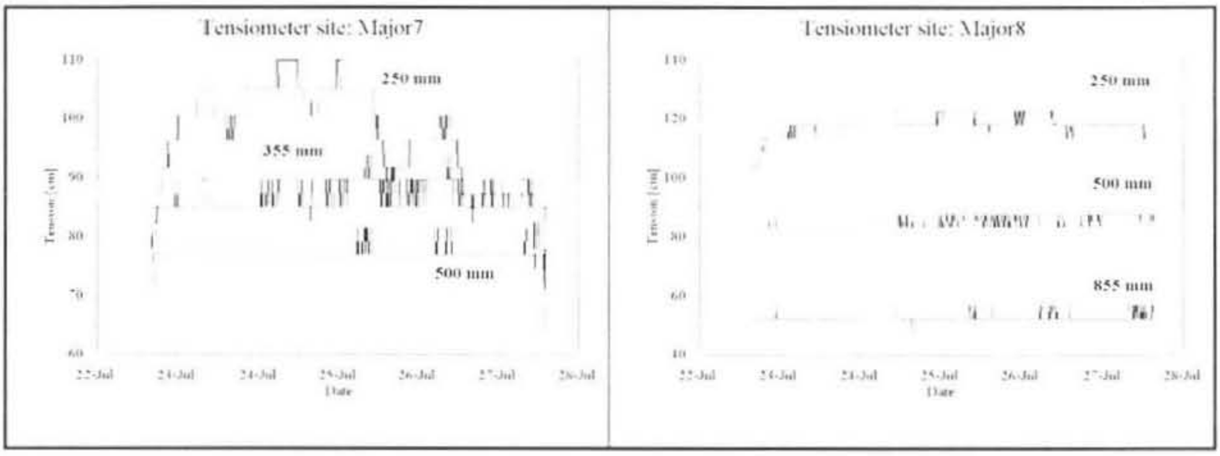

Figure G.2 Soil tension data at tensiometer sites Major7 and Major8.

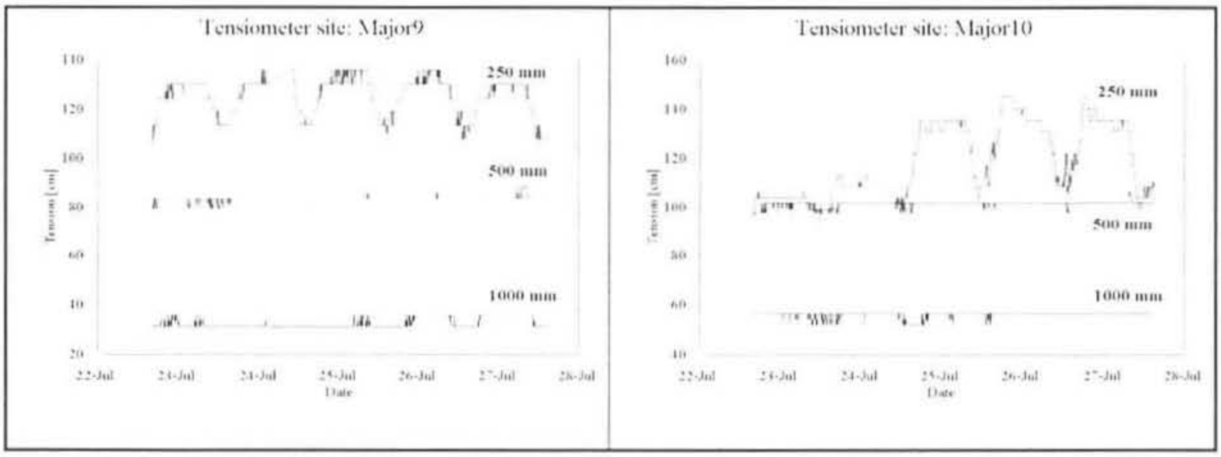

Figure G.3 Soil tensiometer data at tensiometer sites Major9 and Major10.

APPENDIX H: STANDARD EVALUATION DATA

Table H.1 Average wind speed, CV of depth applied, CU, DU_{lq}, application efficiency (AE).

System Number	System Type	Wind [m/s]	CV [%]	CU [%]	DU_{lq} [%]	AE [%]	EU [%]
1	Centre Pivot	2.0	12.6	85.7	82.3	82.5	
2	Centre Pivot	4.5	22.4	86.3	77.5	76.2	
3	Centre Pivot	2.0	18.8	88.1	79.8	83.0	
4	Centre Pivot	2.0	16.1	89.5	83.2	93.8	
5	Centre Pivot	1.0	13.9	90.6	84.2	82.5	
6	Dragline	3.5	42.1	69.0	55.1	63.8	
7	Dragline	5.0	46.8	64.1	45.9	58.9	
8	Dragline	0.0	33.1	74.8	65.4	82.2	
9	Dragline	1.0	29.1	76.3	61.9	78.6	
10	Dragline	1.0	20.1	83.6	76.6	89.3	
11	Dragline	1.7	19.3	83.0	75.5	61.2	
12	Dragline	6.0	37.8	70.4	52.6	67.7	
13	Dragline	1.0	30.7	74.6	57.1	71.4	
14	Dragline	1.5	30.6	74.9	59.8	70.3	
15	Dragline	2.0	39.3	67.1	56.0	78.4	
16	Dragline	4.0	32.2	73.6	63.0	81.2	
17	Dragline	2.0	36.6	72.4	53.5	73.5	
18	Dragline	4.5	28.4	78.7	69.3	78.6	
19	Drip		32.6	80.1	59.1		68.4
20	Drip		87.6	17.4	0.0		25.4
21	Drip		13.1	89.7	83.0		83.3
22	Drip		13.4	90.3	86.2		82.3
23	Drip		9.2	94.0	88.2		89.8
24	Drip		18.8	83.5	76.1		77.8
25	Sub-surface drip		6.3	95.2	91.9		92.5
26	Sub-surface drip		11.4	91.8	83.5		84.6
30	Micro-sprayer		20.0	83.8	79.4		76.6
31	Micro-sprayer		15.6	89.8	79.9		82.1
27	Floppy	2.0	30.7	76.9	70.3	63.5	
28	Floppy	1.5	28.7	78.2	69.0	85.4	
29	Floppy	4.4	40.2	68.5	62.9	81.3	
32	Semi-permanent	5.7	23.5	81.0	70.7	89.4	
33	Semi-permanent	0.8	32.3	75.2	56.0	83.3	
34	Semi-permanent	2.4	24.7	81.1	70.0	91.1	
35	Semi-permanent	5.0	54.6	55.4	44.0	64.6	
36	Semi-permanent	1.0	41.9	64.2	53.5	74.2	
37	Semi-permanent	5.0	37.3	71.8	51.0	68.0	
38	Semi-permanent	2.0	39.8	67.1	52.8	81.4	